


國立交通大學

電信工程學系

博士論文

混合型分碼多工蜂巢網路中  
下行鏈路軟性遞移機制及細胞重組規劃之研究



Downlink Soft Handoff Mechanisms and  
Cell Reconfiguration Planning in  
Mixed-Size CDMA Cellular Networks

研究生：廖青毓

指導教授：張仲儒 博士

中華民國九十三年十二月

混合型分碼多工蜂巢網路中  
下行鏈路軟性遞移機制及細胞重組規劃之研究

Downlink Soft Handoff Mechanisms and  
Cell Reconfiguration Planning in  
Mixed-Size CDMA Cellular Networks

研究生：廖青毓

Student: Ching-Yu Liao

指導教授：張仲儒 博士

Advisor: Chung-Ju Chang

國立交通大學

電信工程學系

博士論文



A Dissertation

Submitted to Institute of Communication Engineering  
College of Electrical Engineering and Computer Science  
National Chiao Tung University  
in Partial Fulfillment of the Requirements  
for the Degree of Doctor of Philosophy  
in Communication Engineering  
Hsinchu, Taiwan

2004, December

中華民國九十三年十二月

# 混合型分碼多工蜂巢網路中 下行鏈路軟性遞移機制及細胞重組規劃之研究

研究生：廖青毓

指導教授：張仲儒

國立交通大學電信工程學系

## 摘要

考慮分碼多工無線行動通訊系統，為了在負載非平均分佈的細胞中有效率的利用無線頻譜資源，利用不同大小細胞來建構混合型蜂巢網路是一可行架構。在此種混合型蜂巢網路中，系統容量與細胞服務涵蓋範圍兩者間的互相消長特性，是系統設計中配置無線頻譜所面臨的嚴峻挑戰。此外，由於多媒體訊務的非對稱特性，下行鏈路成為系統容量的限制鏈路。因此，在本論文中，我們特別針對混合型分碼多工蜂巢網路之下行鏈路，設計軟性遞移機制的功率與速率配置方法，以及重新規劃細胞結構，來達成細胞間負載平衡的目標，並抑制系統容量與細胞服務涵蓋範圍的互相消長問題。

首先，我們探討軟性遞移機制對混合型分碼多工蜂巢網路的影響。根據具有不同細胞大小的雙細胞簡化模型，我們分析計算細胞近似容量。分析結果發現，在混合型分碼多工蜂巢系統中，傳統軟性遞移機制的『等量式功率配置法』會導致微細胞功率耗盡的問題，造成系統容量降低。對此，我們提出軟性遞移機制的『連線品質等比例式功率配置法』。我們利用具有多個巨細胞與微細胞的混合型蜂巢網路模擬模型來檢驗系統容量效能。相較於其他軟性遞移機制之功率配置法，模擬結果顯示，『連線品質等比例式功率配置法』可有效達成細胞間功率負載平衡，進而提供較佳的系統容量。此外，若在選擇連線組合時發生量測錯誤，相較於單方傳輸的遞移機制，多方傳輸的軟性遞移機制配合『連線品質等比例式功率配置法』較不易因較差的連線組合而浪費功率而造成大量干擾，系統容量的增益將更加顯著。

接著，我們考慮能提供多速率傳輸的混合型寬頻分碼多工蜂巢網路。由於在細胞邊緣活動的軟性遞移使用者相較於一般使用者通常必須配置較多的功率資源，因此針對多速率軟性遞移之資源配置問題，我們提出了一功率與速率配置法的最佳化機制。設計上，我們將此配置問題定義為一有限制條件的離散整數的最佳化問題，並且提出『結合功率與速率配置機制』。此機制包含了前述所提的『連線品質等比例式功率配置法』及『演進計算之速率配置法』。此配置方式能夠有效簡化計算複雜度過高問題，因此，在真實系統中是可實現的機制。我們利用具有多個巨細胞與微細胞的混合型蜂巢網路模擬模型來檢驗系統容量效能。相較於傳統的功率與速率配置法，此『結合功率與速率配置機制』確實能夠有效

降低遞移失敗率，達成較佳的細胞涵蓋率，並且改善系統容量。

此外，由於多樣化多媒體服務活動率與使用者隨機移動的特性，訊務分佈將具有高度的時變特性，下一代蜂巢系統將必須能夠適應此高度時變訊務特性所造成的不均勻細胞負載，且能依據細胞負載狀態重組細胞涵蓋範圍，來動態的建構混合型蜂巢網路，以容納多媒體服務所需的系統容量；然而，若僅藉由調整導向訊號功率來改變細胞涵蓋範圍會有造成系統效能降低的問題。因此我們設計一新型『動態細胞重組配合無線頻譜資源管理』機制來解決此問題，包括：導向訊號功率配置，最大連線功率配置，軟性遞移機制與訊務允諾機制。我們首先將導向訊號功率配置問題模型化約為一馬可夫決策鍊過程，最大化系統容量，並運用『強化學習技術』的『乏析 Q-learning』演算法，提出『乏析 Q-learning 式動態細胞重組機制』，精確估算各個細胞的導向訊號功率準位，並配合連線功率預算分析來動態調整無線頻譜資源管理參數。模擬結果顯示，與固定細胞結構相比，此『動態細胞重組配合無線頻譜資源管理』機制可提供較高的系統容量與細胞涵蓋率。

針對本論文所提出在混合型分碼多工蜂巢網路中的軟性遞移及細胞重組規劃機制，模擬結果顯示『動態細胞重組配合無線頻譜資源管理』機制配合軟性遞移機制的『連線品質等比例式功率配置法』，將可在系統具有高度不均勻細胞負載狀態時達成最佳的功率負載平衡和系統效能。



# Downlink Soft Handoff Mechanisms and Cell Reconfiguration Planning in Mixed-Size CDMA Cellular Networks

Student: Ching-Yu Liao

Advisor: Dr. Chung-Ju Chang

Institute of Communication Engineering  
National Chiao Tung University

## Abstract

To utilize radio resources efficiently, the cellular system may deploy mixed-size cells in cellular systems when there exist non-uniform traffic loads among cells. This mixed-size cellular architecture raises some challenging and crucial issues about the radio resource management, in which the system design faces the dilemma between system capacity and service coverage, especially in CDMA cellular networks. Because of abundance multimedia traffics in the downlink, the downlink transmission is generally the capacity-limited direction. In this dissertation, we specialize in the downlink soft handoff mechanisms and cell reconfiguration planning in terms of *power balance characteristics* to tackle tradeoffs between coverage and capacity in mixed-size CDMA cellular systems.

We first investigate impacts of the soft handoff in the CDMA system with mixed-size cells because the soft handoff mechanism directly affects the system capacity and coverage via multi-site transmission. Based on a simple analytic approximation for user capacity in a simplified model of two mixed-size cells, results show that unequal power allocation and maximum link power constraint for each active connection of soft handoff in mixed-size CDMA cellular systems are necessary, otherwise the *power exhausting problem* may occur in congested microcells, in which the microcell has stringent power budget. To tackle this problem, a downlink power allocation mechanism for soft handoff in mixed-size CDMA cellular systems is proposed. It is based on the concept of *power balance* by unequal power allocation for active links in proportional to the link qualities, which is link proportional power

allocation (LPPA) scheme. A simulation model of mixed-size CDMA cellular environment is adopted, and simulation results show that the LPPA scheme outperforms existing schemes because of its excellent capability of power balance. Besides, it shows that the LPPA scheme offers better resistance to occurrences of measurement errors during active set selection.

Next, a soft handoff mechanism in multirate mixed-size WCDMA cellular systems is proposed. Most of previous studies focus on joint power and rate allocation for all users in the homogeneous system with the same-size cells, whereas the possible combinatorial numbers of the solutions are too large to be tractable for optimal allocations. To make system implementation feasible, we emphasize the optimization for multirate soft handoffs by a joint power and rate assignment (JPRA) algorithm to accomplish *power balance* among cells. The JPRA algorithm contains a LPPA scheme and an evolutionary computing rate assignment (ECRA) method. Compared to existing power allocation schemes with best-effort rate allocation, simulation results show that the JPRA algorithm can reduce the handoff forced termination probability and improve the total throughput, resulting in better cell coverage and higher system capacity.

Finally, to balance traffic loads over cells when there are time-varying traffic load distributions among cells, it is crucial for future multimedia cellular networks to be aware of system situations and to configure mixed-size cells dynamically. The problem of dynamic cell configuration is addressed by observing that dynamically adjusting pilot power alone while not changing other radio resource management algorithms can result in performance degradation. We then propose a novel dynamic cell configuration (DCC) scheme with radio resource management for multimedia CDMA networks via reinforcement-learning technologies. The DCC scheme takes into account pilot allocation, maximum link power allocation, call admission control as well as soft handoff mechanisms. Simulation results demonstrate that the DCC scheme is effective in next-generation situation-aware CDMA networks.

# Acknowledgements

Along the long journey to accomplish this dissertation, there are profound appreciations springing up from the bottom of my heart.

My first and sincerely gratitude go to my advisor, Dr. Chung-Ju Chang, for his professional guidance and patient advising. Also, special thanks to Dr. Victor Leung, Dr. Li-Chun Wang, Dr. Fei Yu, and Dr. Yih-Shen Chen for the fruitful collaboration and as co-authors. Moreover, many thanks to the committee of my dissertation defense. Their insightful suggestions greatly contribute to the presentation of this dissertation.

Next, I would undoubtedly express my heartfelt thanks to my considerate colleagues of Broadband Network Lab. in NCTU and all my dear friends, who accompany me through thousands of days with a mixture of laughs and tears. Were not their friendship, it would be tough for me to wind up this program. Furthermore, I especially would like to thank my friends at St. John's College in UBC, for their encouragements mustering my courage to get over the last year of the PhD program. This is going to be a memorial year in my life definitely.

At last but not the least, I am deeply indebted to my dearest parents and family for their wholehearted love, care, and understanding. Without their full inspiration and support, it's impossible for me to accomplish this work and explore my life freely.

**This dissertation is dedicated to my dearest parents and  
in memory of this bittersweet and worthwhile journey.**

# Contents

Mandarin Abstract	i
English Abstract	iii
Acknowledgements	v
Contents	vi
List of Figures	ix
List of Tables	xiii
Notation Table	xiv
<b>1 Introduction</b>	<b>1</b>
1.1 <i>Motivation</i> . . . . .	2
1.2 <i>Paper Survey</i> . . . . .	5
1.3 <i>Dissertation Organization</i> . . . . .	9
<b>2 A Downlink Power Allocation Mechanism for Soft Handoff in Mixed-Size CDMA Cellular Systems</b>	<b>11</b>
2.1 <i>Introduction</i> . . . . .	12
2.2 <i>System Model</i> . . . . .	15
2.2.1 <i>Signal Model</i> . . . . .	15
2.2.2 <i>A Simplified Capacity Approximation for Two Mix-Sized Cells</i> . . . .	17
2.2.3 <i>The Power Exhausting Problem</i> . . . . .	19





2.3	<i>The Problem of the Mixed-Size Cellular System</i>	21
2.3.1	<i>Related Works for Soft Handoff Power Allocations</i>	21
2.3.2	<i>The Problem of Soft Handoff Power Allocation Mechanisms</i>	23
2.4	<i>Downlink Power Resource Allocation Mechanisms</i>	25
2.4.1	<i>Soft Handoff Algorithm</i>	26
2.4.2	<i>The Downlink Power Allocation Algorithm for Soft Handoff Users</i>	27
2.4.3	<i>The Downlink Power Allocation Algorithm for Non-Handoff Users</i>	30
2.4.4	<i>Removal Algorithm</i>	33
2.5	<i>Simulation Results and Discussions</i>	33
2.5.1	<i>The Same-Size Cellular Case</i>	35
2.5.2	<i>The Mixed-Size Cellular Case</i>	37
2.6	<i>Concluding Remarks</i>	41
<b>3</b>	<b>A Joint Power And Rate Allocation mechanism for Multirate Soft Handoff in Mixed-Size WCDMA Cellular Systems</b>	<b>43</b>
3.1	<i>Introduction</i>	44
3.2	<i>System Operation</i>	48
3.2.1	<i>System Model</i>	48
3.2.2	<i>The MQBPA algorithm</i>	49
3.2.3	<i>The MRV algorithm</i>	51
3.3	<i>The JPRA Algorithm</i>	52
3.3.1	<i>The LPPA Scheme</i>	52
3.3.2	<i>The ECRA Method</i>	53
3.4	<i>Simulation Results and Discussion</i>	56
3.4.1	<i>Simulation Model</i>	56
3.4.2	<i>Results and Discussion</i>	59
3.5	<i>Conclusions</i>	65
<b>4</b>	<b>Dynamic Cell Configuration with Radio Resource Management in Next-</b>	

<b>Generation Situation-Aware Mobile Networks</b>	<b>66</b>
4.1 <i>Introduction</i> . . . . .	67
4.2 <i>Dynamic Cell Configuration (DCC) Issues</i> . . . . .	70
4.2.1 <i>Effects of Pilot Power Allocation Schemes</i> . . . . .	70
4.2.2 <i>Effects of Soft Handoff Power Allocation Schemes</i> . . . . .	71
4.2.3 <i>Simulation Examples of Adjusting Pilot Power Only</i> . . . . .	72
4.2.4 <i>Our Approach</i> . . . . .	74
4.3 <i>System Model</i> . . . . .	74
4.3.1 <i>Signal Model</i> . . . . .	74
4.3.2 <i>Handoff Power Allocation Schemes</i> . . . . .	76
4.3.3 <i>Link Budget Analysis</i> . . . . .	78
4.3.4 <i>DCC Problems</i> . . . . .	80
4.3.5 <i>Solving DCC Problems by Reinforcement-Learning</i> . . . . .	81
4.4 <i>DCC Design</i> . . . . .	82
4.4.1 <i>Problem Formulation as a Markov Decision Process (MDP)</i> . . . . .	83
4.4.2 <i>Reinforcement-Learning-Based Solutions</i> . . . . .	84
4.4.3 <i>FQ-DCC Scheme</i> . . . . .	85
4.4.4 <i>Dynamic Maximum Link Power Constraint Design</i> . . . . .	90
4.4.5 <i>Call Admission Controller</i> . . . . .	91
4.5 <i>Simulation Results and Discussions</i> . . . . .	92
4.5.1 <i>Simulation Model</i> . . . . .	92
4.5.2 <i>Performance Measurements and Discussions</i> . . . . .	94
4.6 <i>Concluding Remarks</i> . . . . .	101
<b>5 Conclusions and Future Works</b>	<b>103</b>
<b>Bibliography</b>	<b>106</b>
<b>Vita</b>	<b>114</b>

# List of Figures

1.1	The mixed-size cellular model . . . . .	3
2.1	A simplified mixed-size cellular model with two mixed-size cells . . . . .	15
2.2	The capacity of (a) the equal power allocation (EPA) and (b) the unequal power allocation (UPA) for soft handoff against the cell radius size ratio $\rho$ . . . . .	20
2.3	Total capacity of the equal power allocation (EPA) and the unequal power allocation (UPA) schemes for soft handoff with and without power constraint. . . . .	21
2.4	Examples for different soft handoff downlink power allocation schemes. (a) The same-size cellular system and (b) the mixed-size cellular system. . . . .	23
2.5	The flowchart of a downlink power resource allocation mechanism integrating four key techniques: 1) the soft handoff algorithm, 2) the downlink power allocation for handoff users, 3) the downlink power allocation for non-handoff users, and 4) the removal algorithm. . . . .	26
2.6	Simulation models of the CDMA mixed-size cellular network with (a) $\rho = 1/2$ , (b) $\rho = 1/3$ . . . . .	34
2.7	Averaged outage probability of the same-size cellular systems with $\rho = 1.0$ for EPA, QBPA, SSDT, LPPA-RV1 and LPPA-RV2 schemes. . . . .	36
2.8	Averaged outage probability of the same-size cellular systems with $\rho = 1.0$ subject to measurement errors for EPA, QBPA, SSDT, LPPA-RV1 and LPPA-RV2 schemes. . . . .	37
2.9	Averaged outage probability of the mixed-size cellular systems with $\rho = 1/2$ for EPA, QBPA, SSDT, LPPA-RV1 and LPPA-RV2 schemes. . . . .	38

2.10	Averaged outage probability of the mixed-size cellular systems with $\rho = 1/2$ subject to measurement errors for EPA, QBPA, SSDT, LPPA-RV1 and LPPA-RV2 schemes. . . . .	39
2.11	Averaged outage probability of the mixed-size cellular systems with $\rho = 1/3$ for EPA, QBPA, SSDT, LPPA-RV1 and LPPA-RV2 schemes. . . . .	40
2.12	Averaged outage probability of the mixed-size cellular systems with $\rho = 1/3$ subject to measurement errors for EPA, QBPA, SSDT, LPPA-RV1 and LPPA-RV2 schemes. . . . .	41
2.13	Total capacity with and without measurement errors for EPA, QBPA, SSDT, LPPA-RV1 and LPPA-RV2 schemes of (a) the same-size cellular system, (b) the mixed-size cellular system with $\rho = 1/2$ , (c) the mixed-size cellular system with $\rho = 1/3$ . . . . .	42
3.1	The system operation of downlink power and rate assignment . . . . .	47
3.2	The flowchart of the MRV algorithm . . . . .	51
3.3	The mixed-size cellular model ( $\rho = 1/2$ ) with an example of mobility trajectory. . . . .	56
3.4	Averaged handoff forced termination probability without measurement errors (ME) and with 1.5 dB measurement errors (ME). . . . .	59
3.5	Total handoff throughput versus the number of data users per cell without measurement errors (ME) and with 1.5 dB measurement errors (ME). . . . .	61
3.6	The average call dropping probability versus the number of data users per cell without measurement errors (ME) and with 1.5 dB measurement errors (ME). . . . .	62
3.7	The total throughput gain, which is referred to SSDT, versus the number of data users per cell without measurement errors (ME) and with 1.5 dB measurement errors (ME). . . . .	63
3.8	The user satisfaction index (USI) versus the number of data users per cell for (a) USI of voice users ( $USI_v$ ) and (b) USI of data users ( $USI_d$ ), respectively. . . . .	64
4.1	Diagram of total power allocation of the base station in downlink CDMA systems with (a) fixed pilot and (b) dynamic pilot schemes. . . . .	70

4.2	Diagram of the soft handoff power allocation in downlink CDMA systems with (a) soft handoff in two mixed-size cell model, (b) before soft handoff, and (c) during soft handoff. . . . .	71
4.3	Capacity results of the fixed pilot power design by applying SSDT and LPPA schemes under cases with (a) uniform ( $\rho = 1$ ) and (b) non-uniform ( $\rho = 4$ ) cell loads. . . . .	73
4.4	System block diagram of the proposed dynamic cell configuration (DCC) scheme with radio resource management. . . . .	75
4.5	Service coverage with different service rates. . . . .	80
4.6	Fuzzy Q-learning-based dynamic cell configuration (FQ-DCC) scheme. . . . .	86
4.7	The structure of the fuzzy inference system (FIS). . . . .	87
4.8	For fixed pilot power design, capacity results by applying SSDT and LPPA schemes in terms of different referenced service coverage under uniform ( $\rho = 1$ ) and non-uniform ( $\rho = 4$ ) cell load cases. . . . .	95
4.9	The average pilot power of hotspot, 1st-tier, and 2nd-tier cells for the fixed pilot (FIX) with SSDT (FIX-SSDT) and LPPA (FIX-LPPA), and pilot power allocation for dynamic cell configuration (DCC) with SSDT (DCC-SSDT) and LPPA (DCC-LPPA) schemes. . . . .	96
4.10	The average blocking probability of (a) real-time and (b) non-real-time services for FIX-SSDT, FIX-LPPA, DCC-SSDT, and DCC-LPPA schemes, respectively. . . . .	97
4.11	The average handoff forced termination probability for FIX-SSDT, FIX-LPPA, DCC-SSDT, and DCC-LPPA schemes. . . . .	98
4.12	The average total throughput of systems for FIX-SSDT, FIX-LPPA, DCC-SSDT, and DCC-LPPA schemes. . . . .	99
4.13	The average frame error probability for FIX-SSDT, FIX-LPPA, DCC-SSDT, and DCC-LPPA schemes. . . . .	99

4.14 The average size of the active set for FIX-SSDT, FIX-LPPA, DCC-SSDT, and  
DCC-LPPA schemes. . . . . 100



# List of Tables

2.1	SYSTEM PARAMETERS OF THE SIMULATION MODEL FOR THE MIXED-SIZE CDMA CELLULAR SYSTEM . . . . .	35
3.1	SERVICE CLASSES . . . . .	58
4.1	LINK BUDGET IN THE MULTIMEDIA WCDMA SYSTEM . . . . .	93
4.2	AVERAGE COVERAGE FAILURE PROBABILITY . . . . .	101



# Notation Table

$W$ : bandwidth

$P_b^I$ : pilot power of base station  $b$  for the pilot channel

$P_b^T$ : total transmission power of base station  $b$  for the traffic channel

$\tilde{P}_b$ : maximum transmission power of base station  $b$

$\tilde{p}_b$ : maximum link power constraint of the mobile station in base station  $b$

$p_{b,m}$ : transmission power from base station  $b$  to mobile station  $m$

$p_{b,m}(r)$ : transmission power from base station  $b$  to mobile station  $m$  with service rate  $r$

$p_h^*$ : required transmission power for handoff user  $h$

$L_{b,m}$ : link quality between base station  $b$  and mobile station  $m$

$f_\alpha$ : orthogonality factor

$d_{b,m}$ : distance between base station  $b$  and mobile station  $m$

$d_{corr}$ : decorrelation distance

$z_b$ : breaking point of base station  $b$

$C_L$ : constant of the channel model

$\xi_b$ : shadowing effect of base station  $b$

$\sigma_1, \sigma_2$ : standard deviation of the 2-step shadowing model

$\lambda$ : wavelength

$h_m$ : antenna height of the mobile station

$h_b$ : antenna height of the base station

$\alpha_b, \beta_b$ : pathloss exponent of base station  $b$

$I_{b,m}$ : received total interference for user  $m$  in cell  $b$

$G_P$ : processing gain (single service)



$G_P(r)$ : processing gain of service rate  $r$

$G_P^I$ : processing gain of the pilot signal

$\gamma_{b,m}$ : received signal quality of mobile station  $m$  from base station  $b$

$\gamma_{b,m}(r)$ : received signal quality of mobile station  $m$  with service rate  $r$  from base station  $b$

$\gamma^*$ : required signal quality of bit-energy-to-noise ratio ( $E_b/I_o$ ) for single service

$\gamma^*(r)$ : required signal quality of bit-energy-to-noise ratio ( $E_b/I_o$ ) for service rate  $r$

$\gamma_h$ : received signal quality of handoff user  $h$

$\gamma_h(r)$ : received signal quality of handoff user  $h$  with service rate  $r$

$\nu_{b,m}$ : received chip-energy-to-interference ratio ( $E_c/I_o$ )

$\eta_o$ : background noise

$r$ : service rate

$r_{min}$ : minimum service rate

$r_{max}$ : maximum service rate

$r^*$ : referenced service rate

$D_h$ : active set of user  $h$

$\rho$ : cell radius size ratio between the macrocell and the microcell;

traffic load ratio between the hotspot cell and the adjacent cell

$A_b$ : total transmission power of non-handoff users of base station  $b$

$B_b$ : total transmission power of handoff users of base station  $b$

$\tilde{B}_b$ : maximum transmission power constraint base station  $b$  for all handoff users

$J_m(r)$ : removal index for user  $m$  with service rate  $r$

$J_m$ : removal index for user  $m$  (single service)

$f_{min}$ : minimum pilot power fraction of the maximum transmission power

$f_{max}$ : maximum pilot power fraction of the maximum transmission power

$\phi_m$ : allocated power ratio of the traffic channel power for mobile station  $m$

$U_b$ : set of all mobile stations served by base station  $b$ .

$\omega_{b,m}$ : weighting factor of the power allocation algorithm

$\psi_b$ : tuning factor of base station  $b$ 's total power by Modified-QBPA or MQBPA algorithm



$\varphi_h$ : tuning factor of required power for handoff user  $h$  by the LPPA algorithm

$\eta$ : threshold of the soft handoff algorithm

$O(\mathbf{x})$ : objective function of the allocation rate vector  $\mathbf{x}$  in the ECRA algorithm

$s(\mathbf{x})$ : decoder function of the allocation rate vector  $\mathbf{x}$  in the ECRA algorithm

$X(\mathbf{x})$ : violation function of the allocation rate vector  $\mathbf{x}$  in the ECRA algorithm

$p_c$ : crossover rate

$p_u$ : mutation rate

$T$ : maximum number of generations

$K_P$ : number of populations

$N_S$ : number of service class

$N_v$ : number of handoff voice users in each cell

$N_d$ : number of handoff data users in each cell

$N_b$ : number of base stations in the system

$E_P$ : equivalent isotropic radiated power (EIRP)

$G_B$ : antenna gain of the base station

$L_C$ : cable loss

$G_S$ : soft handoff gain

$G_M$ : antenna gain of the mobile station

$L_D$ : body loss of the downlink receiver

$E_T$ : total EIRP

$\Omega_I$ : interference margin

$H_S(r)$ : required signal-to-interference ratio (SIR) of service rate  $r$

$H_R(r)$ : receiver sensitivity of the mobile station with service rate  $r$

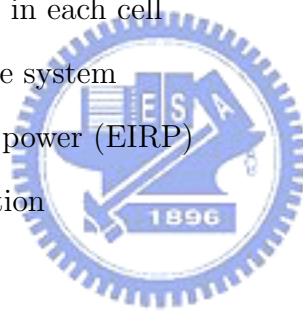
$\Omega_L$ : log-normal fading margin

$PL(r)$ : maximum allowable pathloss of service rate  $r$

$R(r)$ : cell radius of service rate  $r$

$L_C$ : cable loss

$R(r)$ : cell radius of service rate  $r$



$\Upsilon$ : received chip-energy-to-interference ratio ( $E_c/I_o$ )  
 $s$ : system state for the DCC scheme  
 $\varpi_M, \varpi_V$ : state vector includes sample mean and sample variance  
 $a(s)$ : action of state  $s$  for the DCC scheme  
 $\mathbf{A}$ : action set  
 $\mathbf{S}$ : system state set  
 $\mu(s, a(s))$ : reward function with state-action pair  $\{s, a(s)\}$   
 $r_m$ : service rate of user  $m$   
 $V^\pi(s)$ : value function of state  $s$  with policy  $\pi$   
 $Q^\pi(s, a(s))$ : Q-function of state-action pair  $\{s, a(s)\}$  with policy  $\pi$   
 $Q^*(s, a(s))$ : optimal Q-function of state-action pair  $\{s, a(s)\}$   
 $\Delta Q$ : temporal difference error of Q-function  
 $U(s, \pi(s))$ : mean reward function  
 $\Pr(s'|s, a(s))$ : transition probability from state  $s$  to state  $s'$   
 $\gamma_d$ : discount factor  
 $\lambda_L$ : learning rate of the Q-function  
 $S_k$ : state of rule  $k$   
 $a_k(j)$ : action value of rule  $k$  with rule action  $j$   
 $\pi^*$ : optimal policy  
 $e_k(j)$ : replace eligibility of possible action  $a_k(j)$  in rule  $k$   
 $q_k(j)$ : q-value of rule action  $j$  in rule  $k$   
 $\alpha_k(\mathbf{x})$ : truth value of each rule for the input vector  $\mathbf{x}$   
 $\varphi_{S_{k,i}}(x_i)$ : membership degree to the different fuzzy sets  
 $T(\mathbf{x}), T(\mathbf{y})$ : input/output linguistic terms  
 $S_{k,z}$ : fuzzy label for  $z$ -th input variable in rule  $k$   
 $\mathbf{A}_s$ : feasible action set  
 $f_\Theta$ : cutting value of the action set  
 $\Theta$ : threshold of the mean power as the quality-of-service constraint



$K$ : total number of elementary rules

$J$ : overall action set

$Z$ : size of the input vector

$\Lambda_b$ : call admission threshold of signal-to-interference-ratio (SIR) for cell  $b$



# Chapter 1

## Introduction

---

In recent years, the evolution of wireless mobile communication systems have experienced tremendous growth. To utilize the radio spectrum efficiently, the cellular architecture is used in wireless mobile networks, and code division multiple access (CDMA) has been a promising technique for the third or beyond third generation wireless mobile cellular systems. In the CDMA cellular networks, base stations density and the associated cell configuration are primarily determined by the service coverage and system capacity objectives. Generally, in interference-limited CDMA cellular systems, system designs of the service coverage and system capacity are deemed to be challenging issues.

In CDMA cellular networks, capacity and coverage can be limited by the uplink and downlink interference which comes from other mobile stations and from adjacent base stations, respectively. It is generally regarded that service coverage is uplink-limited because of transmission power constraint of mobile equipments. On the other hand, the system capacity may be either uplink or downlink limited depending upon the cell configuration or traffic profile. The uplink capacity-limited scenario may occur in a rural environment where the service coverage of the network is planned with lower uplink cell load and interference margin. Besides, the downlink capacity-limited scenario may occur in suburban or urban environments where the service coverage of the network is planned with a higher uplink load. Therefore, a cell is uplink or downlink capacity limited when it exceeds the predefined interference margin or when it reaches its maximum total transmission power, respectively. For the initial systems deployment, to afford capacity upgrades without extra efforts and investments, it is necessary to take into account the present and future coverage and capac-

ity requirements, i.e. by including additional carriers, adding new base stations or adding additional sectorization [1].

## 1.1 Motivation

Nowadays, the enormous demands of internet services drive multimedia services becoming necessary for future cellular networks. The versatile multimedia traffic activity makes the interrelation between the service coverage and system capacity bond closer because service coverage have to be reduced to offer higher capacity for multimedia traffics with higher service rates. Moreover, because the multimedia traffic is generally asymmetric with a greater amount of traffic on the downlink, the cellular network tends to the downlink capacity-limited scenario, in which improving service coverage will lead to a loss in system capacity, and vice versa. Therefore, system designs of the service coverage and cell capacity turn into a thorny problem.

Due to random user mobility and diverse multimedia activity, cell loads will distribute non-uniformly. Since the system capacity depends on the amount of interference, the CDMA system work best when the traffic patterns are uniform [2]-[4]. There are many techniques developed for improving system capacity. For example, setting up hierarchical cellular structure by adding more carriers can upgrade more than double the system capacity. However, because of scarce frequency resource, there may be no available carriers. Other techniques should be further considered such as transmitting diversity, beamforming, and adding sectorization or microcells.

Assume the same carrier frequency is used at different layers of the cellular network, to enhance system capacity for the cellular network with non-uniform cell loads, a mixed-size cellular network with mixed-size cells may be deployed as shown in Fig. 1.1. First, to maintain service coverage, a small microcell may be installed at the boundary of surrounding macrocells. Second, to increase the system capacity, a macrocell may be split up into a cluster of microcells. However, in the cellular system with mixed-size cells, a macrocell easily blocks a nearby microcell due to near-far effect. This is because higher transmission

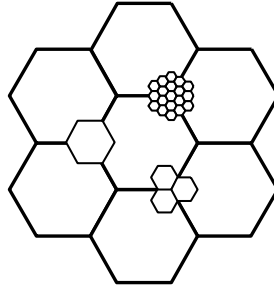


Figure 1.1: The mixed-size cellular model

power is needed to compensate higher pathloss to macrocell whereas more interference is induced to interfere the adjacent microcell. Moreover, since a microcell's base station usually owns capability of low transmission power, the stringent power budget on the downlink results in downlink capacity-limited scenarios. As aforementioned, in view of the system capacity, the CDMA cellular system works best when cell loads are uniformly distributed. Therefore, *power balance* becomes a vital characteristic to tackle the problem of downlink radio resource management arisen by the CDMA mixed-size cellular system. To afford the necessity for future capacity upgrades, in this dissertation, we consider CDMA mixed-size cellular systems with mixed-size cells and specialize in downlink soft handoff mechanisms and cell reconfiguration planning in terms of *power balance characteristics* to tackle problems between service coverage and system capacity.

In CDMA cellular systems, soft handoff is one of the most important techniques to balance traffic loads between cells. When mobile users move from one cell to another cell, the soft handoff technique applies multi-site transmission mechanism to support seamless connections and better signal qualities for users near cell boundaries. However, base stations often have to consume more power to serve soft handoff users than that to serve non-handoff users. Therefore, congested microcells, which are with stringent power budget for maximum total transmission power, may easily exhaust their total transmission power because of serving soft handoff users in the downlink, and then there is no extra power resource to serve other users in the system. This raises the issue of tradeoffs between the service coverage and system capacity. For example, if a base station fails to serve handoff users near cell boundaries,

the cell's service coverage is shrunk whereas there are more power applicable to non-handoff users. Therefore, soft handoff technique plays an important role for downlink radio resource management, and it will make a significant impact on system performance. However, most of conventional radio resource management techniques of soft handoff are designed for the homogeneous cellular system, which is assumed as uniform traffic loads and with the same-size cells. Therefore, in future CDMA heterogeneous cellular networks, the advanced soft handoff techniques for radio resource management are necessary .

For the narrowband CDMA system supporting voice service only, system performance will be determined by power allocation algorithms. To achieve power balance among cells, multi-site transmission mechanism is adopted to satisfy a handoff user's quality of service (QoS) by distributing required transmission power among active links in its active set. Furthermore, consider the wideband CDMA (WCDMA) system supporting multirate services, power and rate allocations impact on system capacity and cell's service coverage dramatically. Most of previous studies focus on joint power and rate allocations for all users in the CDMA system. However, the possible combinatorial numbers of the solutions are too huge to be tractable for global optimal allocations. To make system implementation feasible, we propose an effective idea providing optimal joint power and rate allocations for soft handoffs. This way can not only reduce computation complexity but also specialize in the characteristic of the *power balance* through optimizing radio resource for soft handoffs. However, when system loads is heavy or handoff rate is high, the computation complexity will be increased. To further scale down the computation complexity, applying statistical optimization techniques are necessary, such as genetic algorithm, evolutionary algorithm, simulated annealing algorithm, etc.

Currently, in CDMA cellular networks, the cell coverage and capacity of a network are planned in the pre-deployment stage according to pre-defined traffic patterns. That is, the pilot power allocation is fixed. In practice, however, traffic patterns are changing with time due to random user mobility and versatile service activity. The planned cellular mobile networks may not utilize radio resources optimally under the varying traffic patterns. In next-generation CDMA cellular networks, this problem becomes more severe. The sophisticated



techniques of radio resource management are necessary for future multimedia cellular systems to be adaptive to the emerging multimedia services.

Dynamic cell configuration is an advanced technique to balance traffic load by controlling pilot power dynamically. Since each base station has finite power resource, the pilot channel and traffic channels have to share the total power resource. This explains the interdependence of coverage and capacity in CDMA systems. Pilot power can be adjusted between them based on various traffic situations. When the required traffic power is low, the pilot power can be increased to extend cell coverage so as to accommodate more users around the adjacent cells. On the other hand, when the required traffic power is too high to have risks of degrading system performance, the pilot power can be decreased to shrink cell coverage. Therefore, to utilize radio resources efficiently, it is crucial for next-generation CDMA cellular networks to be aware of system situations and configures cell coverage and system capacity dynamically to balance traffic loads over all cells. That is, the mixed-size cell configuration can be formed dynamically by being aware and adaptive to system situations. Tradeoffs between the coverage and capacity motives us that pilot power allocation and other radio resource management schemes, such as soft handoff power and maximum link power allocations as well as call admission control mechanisms, should be highly coupled in situation awareness CDMA cellular networks.

In this dissertation, to accomplish power balance features for future CDMA mixed-size cellular systems, we are motivated to design soft handoff mechanisms and to plan cell configurations.

## 1.2 *Paper Survey*

Due to non-uniform traffic load distribution, using the same frequency band and mixed-size cells has been a necessary network architecture to form CDMA mixed-size cellular systems. References [5]-[7] considered capacity issues in mixed-size cellular systems with mixed-size cells. Both [5] and [6] only focused on the reverse link. On the other hand, Kishore, et al, [7] concluded that uplink and downlink directions are equivalent in mixed-size mixed-

size cellular systems. However, it does not consider soft handoff mechanisms and multirate services which are both regarded as highly resource-exhausting traffics.

The major challenge of the CDMA mixed-size cellular system is that link qualities from a macrocell and a microcell to the handoff user are quite unequal, so most of handoff users near cell boundaries easily choose the microcell with less pathloss for the target cell to handoff. Under the downlink capacity-limited scenario, a microcell with low pilot power (small coverage) and high traffic loads (high capacity) may thus exhaust its stringent power resource, which is addressed as *power exhausting problem*. This problem makes the power allocation for soft handoff with multirate services becoming a more critical issue because most of previous studies of radio resource management focus on homogeneous cellular systems only [1], [8].

Moreover, the previous works about downlink power allocation for soft handoff in CDMA systems can be summarized as follows. Viterbi et. al. [9] examined the impact of soft handoff on downlink capacity of the CDMA system in a homogeneous cellular structure with the same-size cells, in which all the serving base stations in the active set allocate the same amount of power to a user, it is called equal power allocation (EPA) scheme. However, [10]–[12] showed that EPA-based downlink power allocation of soft handoff may decrease system capacity due to unequal path gains from a handoff user to the serving base stations. Moreover, Kim [13] proposed a simple quality balancing algorithm by adjusting cell-site transmitter power to balance quality to a common level so that all users can receive equal signal quality. However, the quality balancing power allocation (QBPA) strategy is suitable for non-handoff but not handoff users because more power will be wasted. Furthermore, Furukawa et al. [14] proposed a site selection diversity transmission (SSDT) scheme for CDMA downlink transmissions, in which transmission diversity is provided by dynamically selecting one base station with best link quality in the active set. However, due to the maximum link power constraint, SSDT sometimes could not afford enough power to multirate soft handoff users. Moreover, since SSDT is a single-site transmission mechanism at one time, it may select the wrong link resulting in wasting more power for handoffs when suffering measure-

ment errors during active set selection. The advantage of the power saving characteristic for SSDT would disappear. To combat the occurrence of the measurement errors, the authors in [15] suggested multi-site transmission mechanism to enhance conventional SSDT scheme. The multi-site transmission schemes are also proposed to balance power loads in reference [16] and [17]. The former presented a a cost-function-based differentiated power control scheme to determine different power levels of each radio link from two base stations to the handoff user. Also, the latter proposed two proportional power allocation methods for soft handoff in terms of transmission power and target signal quality. However, none of the aforementioned downlink power allocation for soft handoff have been evaluated in a mixed-size cellular system.

Furthermore, consider multirate CDMA cellular systems, many literatures discussed the topic of joint power and rate allocation for *all users* in the sense of global optimization problem [18], [19]. However, they focused on the reverse link. References [20] and [21] proposed joint power and rate allocation algorithms in the downlink WCDMA homogeneous cellular systems. The former proposed two sub-optimal algorithms based on fairness consideration, and the latter adopted dynamic programming technique to optimize total throughput. Moreover, Kim [22] dealt with rate-regulated power control in the reverse link without concerning handoff. Reference [23] discussed radio resource management in multiple-chip-rate direct sequence CDMA systems supporting multiclass services, in which inter-system or inter-frequency handoff had been taken into account. Kim and Sung [24] proposed a handoff management scheme for multirate services using guard channels and reservation on demand queue control. All the aforementioned joint power and rate allocation schemes considered homogeneous CDMA cellular systems without soft handoff mechanisms.

To obtain an overall evaluation, in addition to radio resource management of soft handoff, there are two important algorithms considered for the downlink radio resource management, including downlink power allocation for non-handoff users and removal algorithm. Zander [25] proposed quality balancing power allocation techniques for downlink power allocation, in which all users in the same cell can obtain the same quality level. Based on the concept

of quality balancing in [25], Kim [13] further proposed a simple scheme to balance signal quality to the same required level for each user in each cell by adjusting total power of each base station. Both [25] and [13] were studied only for a single service rate with unique required signal quality, and both took all users into quality balancing procedures of power allocation. Furthermore, in order to find a convergent solution for downlink power allocation, the removal algorithm is designed to remove some users who owns weaker link quality for transmission [26], [27]. However, the link-based and received signal-strength based removal algorithms were only suitable for single service. Besides, the prioritized removal algorithm in [28], based on predefined service priority, did not consider service rate tuning for users in the reverse link of a multiservice cellular system.

The preceding previous works all focus on the fixed cell configuration by fix pilot power allocation. In order to make pilot power adaptive to the traffic load variation due to random mobility and diverse multimedia services, it is crucial for next-generation CDMA cellular networks to be aware of system situations and configures cell coverage and capacity dynamically to balance traffic loads over all cells [29], [30]. Several schemes have recently been proposed for dynamic cell configuration in cellular networks [31]–[37]. In [31], the optimization of pilot power and the planning procedures of downlink capacity and cell coverage were proposed. In [32], authors used analytical methods to study the competitive characteristics of network coverage and capacity in a simple network. Only one class of service was considered in [31] and [32], and it may be difficult to extend these schemes to a network with multi-classes of services. There are also some heuristic-rule-based techniques in the literature for dynamic pilot control to balance downlink traffic load while assuring service coverage [33]–[35]. However, these schemes may cause some “coverage failure regions” between cells where all the received pilot signals are too weak to serve a mobile station [36], [37]. The common shortcomings of the previous work [31]–[37] are that only pilot power is adjusted and other radio resource management schemes are not taken into account in the time-varying environment.

As a matter of fact, pilot power allocation and other radio resource management schemes

are highly coupled. For example, [4] was showed that signal quality degradation can be prevented by configuring cell areas adaptively and setting transmission power levels appropriately. Also, authors in [38] and [39] showed that soft handoff has significant impacts on the system capacity and service coverage.

### 1.3 *Dissertation Organization*

In this dissertation, we specialize in the downlink soft handoff mechanisms and cell re-configuration planning in terms of *power balance characteristics* to tackle tradeoffs between service coverage and system capacity in CDMA mixed-size cellular systems.

In Chapter 2, we explore impacts of soft handoff mechanism in the mixed-size cellular system. A power exhausting problem is addressed by a simple analytic approximation of user capacity based on a simplified two cell model. To deal with this problem, a novel link proportional power allocation (LPPA) scheme for soft handoff is proposed, which is a multi-site transmission mechanism. The LPPA scheme distributes the required power in proportion to the link qualities between a soft handoff user and all base stations in its active set. The proof of the convergence of the LPPA is also provided. In simulations, the LPPA scheme is compared with several existing power allocation schemes of soft handoff in the narrowband CDMA mixed-size cellular system with multiple mixed-size cells supporting voice service only. It is shown that LPPA can alleviate the power exhausting power for the CDMA mixed-size cellular system with or without measurement errors during active set selection.

In Chapter 3, based on the power allocation of soft handoff in Chapter 2, consider mutlirate WCDMA mixed-size cellular systems, we propose a joint power and rate allocations (JPRA) for soft handoff, which accomplishes power balance among cells by multi-site transmission mechanisms using LPPA and evolutionary computing rate assignment (ECRA) method. Both of them can aid in distributing the required power of the soft handoff user to all base stations in its active set. The optimization of the soft handoff can be formulated by an integer and discrete optimization problem under a predefined total power constraint

for soft handoffs in each cell. It is well known that conventional optimization methods can hardly cope with problems with integer and discrete variables, whereas evolutionary computing methods are very efficient for these problems to reduce the searching complexity [40], in which evolutionary computing is known for the efficiency of the optimization problem. In simulations, the JPRA scheme is compared with the existing power allocation schemes with best-effort rate allocation in the multirate mixed-size cellular system with multiple mixed-size cells. As a result, JPRA can dynamically adapt to changes of non-uniform load situations in the mixed-size cellular environment.

Furthermore, in order to specialize radio resource management of handoff, we differentiate handoff users from all users, and propose a modified quality balancing power allocation only for non-handoff users in Chapter 2. Besides, in Chapter 3, a new multi-quality balancing power allocation (MQBPA) algorithm for non-handoff users for multiple service rates with multiple quality requirements is developed. Also, the multirate removal (MRV) algorithm is proposed to pick out a user who consumes system resource most and to reduce its service rate or even block it when the system resource is insufficient.

In Chapter 4, we further consider pilot power control to form dynamic cell configuration for the cellular system with non-uniform traffic load distribution. The dynamic cell configuration (DCC) scheme can form mixed-size cellular networks with irregular mixed-size cells automatically. We address the problem of dynamic cell configuration by observing that dynamically adjusting pilot power alone while not changing other radio resource management algorithms can result in performance degradation. We then propose a novel DCC scheme with radio resource management in multimedia CDMA networks via a reinforcement-learning technique, which takes into account pilot, soft handoff, and maximum link power allocations as well as call admission control mechanisms. Simulation results demonstrate the effectiveness of the proposed scheme in situation-aware CDMA networks.

Finally, concluding remarks and future research topics are addressed in Chapter 5.

## Chapter 2

# A Downlink Power Allocation Mechanism for Soft Handoff in Mixed-Size CDMA Cellular Systems

---

*In this Chapter, we investigate impacts of soft handoff in CDMA system with mixed-size cells because soft handoff mechanism directly affects system capacity and coverage. Based on a simple analytic approximation of user capacity for a simplified model of two mixed-size cells, it is found that a power exhausting problem may occur in microcells of mixed-size cellular systems. This is because a congested microcell has more stringent constraints of the maximum total power and link power than a macrocell. To tackle the problem, we develop a novel link proportional power allocation (LPPA) scheme, which is based on the concept of unequal power allocation for active links in proportional to the link quality. Many existing power allocation schemes for soft handoff, including site-selection diversity transmission (SSDT), quality balancing power allocation (QBPA), and equal power allocation (EPA) schemes, have been taken into comparison. Simulation results show that the LPPA scheme outperforms all existing schemes because of its excellent capability of power balance. Besides, it shows that the LPPA scheme offers better resistant to occurrences of measurement errors during active set selection.*

## 2.1 Introduction

Soft handoff is an important technique for the code division multiple access (CDMA) cellular system. Traditional soft handoff algorithms are mainly developed for the same-size cellular system which has same-size cells. Although soft handoff technique has been extensively discussed in the literature, fewer works have concentrated on the design for the soft handoff technique in mixed-size cellular systems. As mentioned in Chapter 1, the major challenge of the mixed-size cells is that link qualities from a macrocell and a microcell to the soft handoff user are quite unequal, so most of handoff users near cell boundaries add the microcell with better link quality of the connection into their active set for transmission. The microcell with stringent power budget of total power may thus exhaust its stringent power resources. We address this issue as a “power exhausting problem”. This problem also illustrate the importance of the soft handoff power allocation in the mixed-size cellular system because soft handoff users generally need more power than non-handoff users. To specializing in the radio resource management of soft handoff for mixed-size cellular system, the key concept to enhance system performance is to achieve power balance among macrocells and microcells. Therefore, the ultimate goal of this chapter is to design a novel power allocation algorithm for soft handoff to achieve *power balance* among cells, which is suitable for using in the mixed-size cellular system.

The previous works about power allocation for soft handoff in downlink CDMA systems can be summarized as follows. In [9], authors examined the impact of soft handoff on downlink capacity of the CDMA system in a same-size cellular structure. It was mentioned that soft handoff can maximize the diversity gain when the involved serving base stations allocate the same amount of power to a user. In this chapter, if the serving base stations allocate the same amount of power to the handoff user, we call it the equal power allocation (EPA) method. In [12], it was shown that EPA-based downlink soft handoff may decrease system capacity due to unequal path gains from a handoff user to the two serving base stations. In [13], a simple quality balancing algorithm was proposed to adjust cell-site transmitter power for non-handoff and handoff users in the downlink. We call the power



allocation method of [13] as the quality balancing power allocation (QBPA) method in this chapter. Furukawa [14] proposed a site selection diversity transmission (SSDT) technique for CDMA downlink transmissions to select a serving base station with the best link quality among the active set. In [15], the author proposed an enhanced SSDT technique to allow more than one base station to transmit signals to the handoff user. Reference [16] presented a cost-function based differentiated power control technique to determine different power levels of each radio link from two base stations to the handoff user. Reference [17] proposed two proportional power allocation methods in terms of the transmission power and the target signal quality.

With respect to the performance of mixed-size CDMA cellular systems, some works have been reported in the literature [41]–[42]. In [41], it was concluded that the capacity of a hierarchical cellular system can be improved by integrating downlink power control of microcells and uplink power control of a macrocell. In [5] it was found that for a CDMA system with mixed-size cells, the interference from adjacent macrocell may decrease the uplink capacity improvements resulting from cell splitting. In [6] the authors suggested tier selection algorithms to improve the uplink capacity of a microcell/macrocell overlaying system. In [42], a macrodiversity scheme was proposed to enable a hierarchical CDMA system to share the same spectrum between the macrocell and the microcell by adopting the SSDT technique in the downlink and the maximal ratio combining technique in the uplink. To our knowledge, in an environment with a cluster of microcells surrounded by macrocells, the downlink capacity of such a CDMA system considering both handoff and power control has not been fully addressed in the literature.

Aiming to resolve the power exhausting problem for the CDMA mixed-size system, we propose a novel link proportional power allocation (LPPA) scheme. The LPPA scheme adopts multi-site transmission mechanism to distribute transmission power in proportional to link qualities between the user and the base stations under the constrain of maximum link power. Furthermore, to obtain an overall evaluation for system performance, in addition to radio resource management of soft handoff, there are two important algorithms consid-

ered for the downlink radio resource management, including downlink power allocation for non-handoff users and removal algorithm. Zander [25] proposed quality balancing power allocation techniques for downlink power allocation, in which all users in the same cell can obtain the same quality level. Based on the concept of quality balancing in [25], Kim [13] further proposed a simple scheme to balance signal quality to the same required level for each user in each cell by adjusting total power of each base station. In this chapter, in order to specialize radio resource management of handoff, we differentiate handoff users from all users, and propose a modified quality balancing power allocation only for non-handoff users. Also, to achieve convergent solution for downlink power allocation, [26], [27] proposed removal algorithms to remove some users who owns weaker link quality for transmission. In this chapter, we further design two removal schemes to provide priority for soft handoff users who need seamless transmission.

Consider CDMA heterogenous cellular systems with mixed-size cells supporting voice service only, our simulation compares LPPA with many existing soft handoff power allocation scheme, such as SSDT, QBPA, and EPA schemes. The simulation results show that our proposed LPPA scheme can alleviate the power exhausting problem and deliver higher system capacity in a CDMA system with mixed-size cells than other existing schemes. Besides, it shows that the LPPA scheme offers better resistant to occurrences of measurement errors during active set selection.

The rest of this chapter is organized as follows. section 2.2 describes the system model for a simplified case of two mixed-size cells. Also, the power exhausting problem is addressed by a simple analytic approximation of user capacity based on a simplified two cell model. Section 2.3 discusses the related handoff power allocation algorithms. Section 2.4 propose a novel LPPA scheme for soft handoff power allocation and prove its convergence characteristic. Also, this section illustrates details the designs of the CDMA mixed-size cellular system integrating soft handoff and non-handoff power allocations as well as removal procedures. Simulation model and results are discussed in section 2.5. Section 2.6 provides concluding remarks.

## 2.2 System Model

In this section, we demonstrate a simplified model with two mixed-size cells and then address the power exhausting problem that is arisen by the soft handoff power allocation analytically.

### 2.2.1 Signal Model

Consider a simplified mixed-size cellular model with a single microcell adjacent to a macrocell as shown in Fig. 2.1. Denote  $R_M$  and  $R_\mu$  as the radii of the macrocell  $M$  and the microcell  $\mu$ , respectively. Assume a handoff user is located at  $H$ .

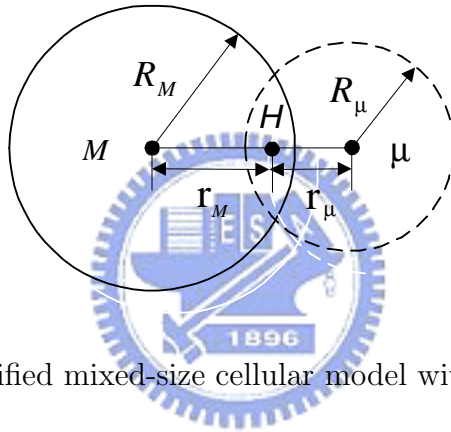


Figure 2.1: A simplified mixed-size cellular model with two mixed-size cells

Denote  $p_{b,m}$  as the transmission power from base station  $b$  to user  $m$ . The received interference,  $I_{b,m}$ , of user  $m$  served by base station  $b$  is

$$I_{b,m} = (1 - f_\alpha)(P_b^T - p_{b,m})L_{b,m} + \sum_{k \neq b} P_k^T L_{k,m} + \eta_o, \quad (2.1)$$

where  $f_\alpha$  is the orthogonality factor;  $P_k^T = \sum_m p_{k,m}$  is the downlink total transmission power of the traffic channel in cell  $k$ ;  $L_{b,m}$  is the link quality from cell  $b$  to user  $m$ ;  $\eta_o$  is the background noise. Note that the first and second terms in (2.1) mean intra-cell and inter-cell interferences, respectively, in which the first term is caused by imperfect orthogonality of channel codes.

Let  $\gamma_{b,m}$  be the downlink received bit energy-to-noise density ratio ( $E_b/N_o$ ). Then  $\gamma_{b,m}$  can be written by

$$\gamma_{b,m} = \frac{p_{b,m} \cdot L_{b,m} \cdot G_P}{I_{b,m}} \geq \gamma^*, \quad (2.2)$$

where  $G_P$  is the processing gain, and  $\gamma^*$  is the required  $E_b/N_o$ . By including effects of both pathloss and shadowing,  $L_{b,m}$  can be expressed by [43], [44]

$$L_{b,m} = \frac{C_L}{d_{b,m}^{\alpha_b} (1 + (\frac{d_{b,m}}{z_b})^{\beta_b})} \times 10^{\xi_b/10} , \quad (2.3)$$

where  $\alpha_b$  and  $\beta_b$  are the pathloss exponents of base station  $b$ ,  $d_{b,m}$  is the distance from user  $m$  to the base station  $b$ ,  $z_b$  is the break point in cell  $b$ , and  $C_L$  is a constant of the channel model. In (2.3), the standard deviation of the shadowing  $\xi_b$  is described by a distance dependent variable [45], i.e.,

$$\sigma_b(d_{b,m}) = \begin{cases} \sigma_1 & , d_{b,m} \leq z_b \\ \sigma_2 & , d_{b,m} > z_b \end{cases} . \quad (2.4)$$

Also, the breakpoint  $z_b$  is given by

$$z_b = \frac{4 h_b h_m}{\lambda} , \quad (2.5)$$

where  $h_b$  is the antenna height of base station  $b$ ,  $h_m$  the antenna height at the user side, and  $\lambda$  the wavelength. We define the cell boundary as the point at which user  $m$  receives the same signal strength from both adjacent cells  $M$  and  $\mu$  first [44]. Then at the cell boundary, we have

$$P_M^I \times L_{M,m} = P_\mu^I \times L_{\mu,m} , \quad (2.6)$$

where  $P_M^I$  and  $P_\mu^I$  represent pilot power emitting from the base stations of the macrocell and the microcell, respectively. For simplicity, we only consider the effect of pathloss in (2.6) first. Then, combining (2.3) and (2.6), we have

$$\begin{aligned} \frac{P_M^I}{P_\mu^I} &= \frac{L_{\mu,m}}{L_{M,m}} = \frac{R_M^{\alpha_b} (1 + (\frac{R_M}{z_M})^{\beta_b})}{R_\mu^{\alpha_b} (1 + (\frac{R_\mu}{z_\mu})^{\beta_b})} \\ &\propto \left(\frac{R_M}{R_\mu}\right)^{\alpha_b + \beta_b} \times \left(\frac{h_\mu}{h_M}\right)^{\beta_b} . \end{aligned} \quad (2.7)$$

Note that (2.7) is valid only when the microcell radius is larger than the break point distance.

When considering only the microcell interference in (1), we have

$$\begin{aligned}
p_{b,m} &\geq \frac{\gamma^* \cdot (P_M^T \cdot L_{M,m} + P_\mu^T L_{\mu,m})}{(G_P + \gamma^*) \cdot L_{M,m}}, \\
&= \frac{\gamma^*}{(G_P + \gamma^*)} \cdot (P_M^T + P_\mu^T \frac{L_{\mu,m}}{L_{M,m}}), \\
&= \frac{\gamma^*}{(G_P + \gamma^*)} \cdot \{P_M^T + P_\mu^T X_m 10^{(\xi_\mu - \xi_M)/10}\},
\end{aligned} \tag{2.8}$$

where

$$X_m = \frac{d_\mu^{-\alpha_\mu} (1 + \frac{d_\mu}{z_\mu})^{-\beta_\mu}}{d_M^{-\alpha_M} (1 + \frac{d_M}{z_M})^{-\beta_M}}. \tag{2.9}$$

To make macrocell users receive required  $E_b/N_o$ , the maximum link power  $\tilde{p}_M$  can be obtained by substituting the maximum total power  $\tilde{P}_M$  and  $\tilde{P}_\mu$  in (2.8). Then, we have the maximum link power of macrocell  $M$

$$\tilde{p}_M = \frac{\gamma^*}{(G_P + \gamma^*)} (\tilde{P}_M + \tilde{P}_\mu \cdot X_m), \tag{2.10}$$

where  $X_m$  is given in (2.9). For simplicity, we only consider the effect of pathloss in (2.6). Note that the total power of the base station is dependent on the summation of the allocated power for each user. From (2.7) and (2.10), the maximum link power of microcell  $\mu$  can be obtained as

$$\tilde{p}_\mu = \tilde{p}_M \cdot \frac{L_{M,m}}{L_{\mu,m}}. \tag{2.11}$$

As for the soft handoff users, the maximum ratio combining (MRC) method is adopted to combine received signal from each active link for the soft handoff [46]. Thus, the received  $E_b/N_o$  for soft handoff user  $h$ , denoted as  $\gamma_h$ , is given by

$$\gamma_h = \sum_{b \in D_h} \gamma_{b,h}, \tag{2.12}$$

where  $D_h$  is the action set of user  $h$ , in which  $|D_h| > 1$  means the user is in the soft handoff mode.

### 2.2.2 A Simplified Capacity Approximation for Two Mix-Sized Cells

In this section, to address the power exhausting problem analytically, we evaluate the capacity for the CDMA mixed-size cellular system with two mixed-size cells case, as shown

in Fig. 2.1. Consider user  $h$  at location  $H$ . Let  $M \rightarrow \mu$  represent the event of soft handoff when user  $h$  moves from the originally serving macrocell  $M$  to adjacent microcell  $\mu$ . Assume soft handoff is initiated for a user when the following condition is satisfied:

$$P_M^I \cdot L_{M,m} - P_\mu^I \cdot L_{\mu,m} \leq \eta , \quad (2.13)$$

where  $L_{M,m}$  and  $L_{\mu,m}$  are the link qualities from user  $m$  to base stations  $M$  and  $\mu$ , respectively;  $\eta$  is the handoff threshold.

In this section, we consider two strategies of soft handoff power allocation, including equal power allocation (EPA) and unequal power allocation (UPA) schemes. According to the EPA scheme, base stations in the active set transmit the same power level. Thus, the serving base station  $M$  will allocate power for user  $h$  according to (2.8) with an upper constraint defined in (2.10). Denote  $p'_{\mu,h}$  and  $p'_{M,h}$  as the transmission power for handoff user  $h$  from macrocell  $M$  and microcell  $\mu$ , respectively. Then,  $p'_{\mu,h}$  and  $p'_{M,h}$  can be written as

$$p'_{M,h} = p'_{\mu,h} = \frac{1}{2} \min ( p_{M,h}, \tilde{p}_M ), \quad \text{for } M \rightarrow \mu. \quad (2.14)$$

Note that  $p_{M,h}$  and  $p'_{M,h}$  indicate the allocated power before and during soft handoff mode, respectively. The factor of  $\frac{1}{2}$  in (2.14) is related to the number of base stations involved in soft handoff, i.e. two base stations in this case.

If the UPA scheme is used, the two serving base stations will allocate power at different levels according to (2.8) and (2.10). That is,

$$\begin{aligned} p'_{M,h} &= \frac{1}{2} \min( p_{M,h}, \tilde{p}_M ) & \text{for } M \rightarrow \mu \\ p'_{\mu,h} &= \frac{1}{2} \min( p_{\mu,h}, \tilde{p}_\mu ) & \text{for } M \rightarrow \mu \end{aligned} \quad (2.15)$$

For a microcell user moving into a macrocell, i.e.  $\mu \rightarrow M$ , we can simply swap  $M$  and  $\mu$  in (2.14) and (2.15) to obtain the allocated power from the macrocell and the microcell during soft handoff mode.

In [9], the downlink outage probability is defined as the probability of transmitted total power of a base station exceeding its constraint of maximum total power. That is,

$$P_{otg}^{(M)} = \text{Prob}\{ P_M^T > \tilde{P}_M \} . \quad (2.16)$$

Denote  $N_M$  and  $N_\mu$  as the number of users in the macrocell and microcell, respectively. Let  $N_M^H$  and  $N_\mu^H$  be the number of soft handoff users in the macrocell  $M$  and microcell  $\mu$ , respectively. Thus, the total transmission power of macrocell  $M$  in (2.16) can be calculated as

$$P_M^T = \sum_{m=1}^{N_M - N_M^H} p_{M,j} + \sum_{m=1}^{N_M^H} p'_{M,h} + \sum_{m=1}^{N_\mu^H} p'_{\mu,h} , \quad (2.17)$$

where the sum of the second and the third terms (denoted as  $P_M^H$ ) is equal to the total transmission power for soft handoff users. From (2.14) and (2.15) we can obtain  $P_M^H$ . We further substitute (2.8) for  $p_{M,m}$  in (2.17), and obtain

$$Y_M = \sum_{m=1}^{N_M - N_M^H} X_m \cdot 10^{(\xi_\mu - \xi_M)/10} , \quad (2.18)$$

where  $D_m$  is defined in (2.9). Let

$$\chi = \frac{\tilde{P}_M - K_C \cdot P_M^T \cdot (N_M - N_M^H) - P_M^H}{K_C \cdot P_\mu^T} , \quad (2.19)$$

where  $K_C = \gamma^*/(G_P + \gamma^*)$ . Then  $P_{otg}^{(M)}$  in (2.16) becomes

$$P_{otg}^{(M)} = \text{Prob} \left( Y_M > \frac{\tilde{P}_M - K_C P_M^T (N_M - N_M^H) - P_M^H}{K P_\mu} \right) , \quad (2.20)$$

$$= Q \left( \frac{\chi - m_Y}{\sigma_Y} \right) , \quad (2.21)$$

where  $Q(x) = \frac{1}{2} \int_x^\infty e^{-t^2/2} dt$ . Note that since  $Y_M$  is a sum of independent log-normal random variables, it can be approximated by a new log-normal random variable  $Y_M$  with mean  $m_Y$  and standard deviation  $\sigma_Y$  by using the Yeh's approximation method in [47]. The outage probability for the microcell users in the downlink can be also obtained by using the same method.

### 2.2.3 The Power Exhausting Problem

Assume that mobile stations are uniformly distributed in both macrocell and microcell. The system capacity is defined as the maximal number of users subject to the constraint of outage probability less than a certain value, say  $P_{otg}^{(M)} < 0.05$ . Thus we can obtain the capacity of macrocell and microcell. The analysis results of the user capacity for the two mixed-size cell model are presented.

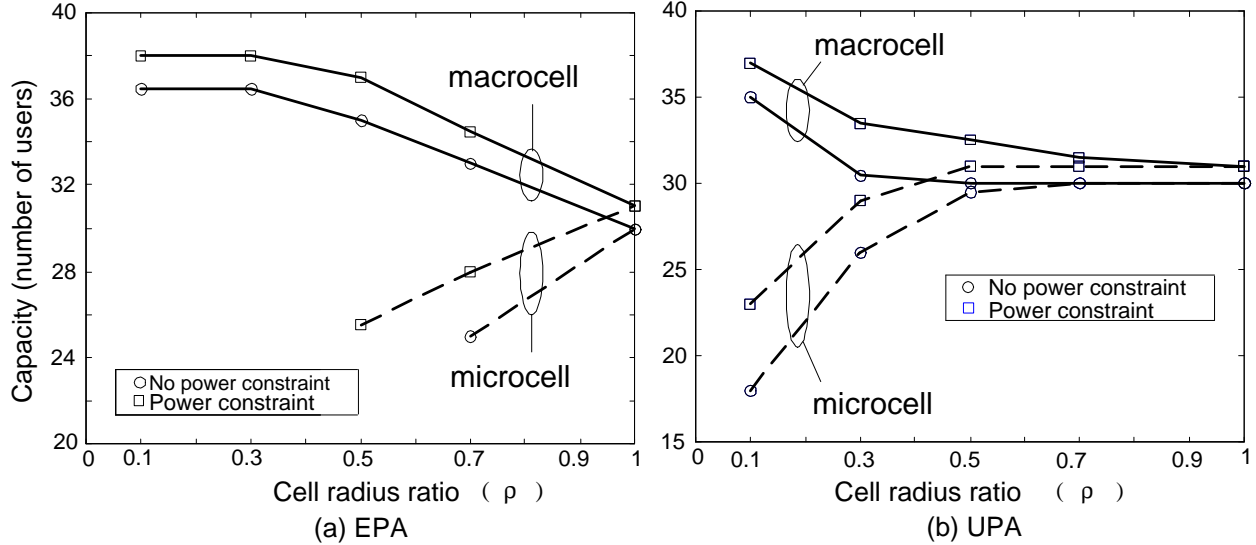


Figure 2.2: The capacity of (a) the equal power allocation (EPA) and (b) the unequal power allocation (UPA) for soft handoff against the cell radius size ratio  $\rho$ .

Figure 2.2(a) shows the capacity by using EPA for soft handoff against the cell radius ratio  $\rho$ . In the figure, the capacity is defined as the maximum number of users subject to the constraint of outage probability less than 0.05. To get some insights through analysis, we consider a simplified two cell model in Fig. 2.1 and apply (2.20) to calculate the system capacity. We observe that the power exhausting problem occurs in the microcell when  $\rho < 0.7$  without constraint of maximum link power and when  $\rho < 0.5$  with the constraint of maximum link power. One can see that the smaller the value of  $\rho$ , the higher the macrocell capacity will be. The increase of the macrocell capacity as the value of  $\rho$  decreases is mainly because interference from the microcell is reduced. Constraining the maximum link power can relieve the power exhausting problem in the microcell slightly although the improvement is not significant. Fig. 2.2(b) demonstrates the capacity of a system using the UPA scheme for soft handoff against the cell radius ratio. Unlike the EPA scheme, the UPA scheme can maintain a good capacity for both microcell and macrocell from  $\rho = 0.5 - 1.0$ . The power exhausting problem does not occur even with  $\rho = 0.1$ . It is also noted that the power constraint can improve the capacity, especially when  $\rho$  is small. For  $\rho = 0.1$ , the capacity for the constrained UPA scheme increases microcell capacity about 30%.



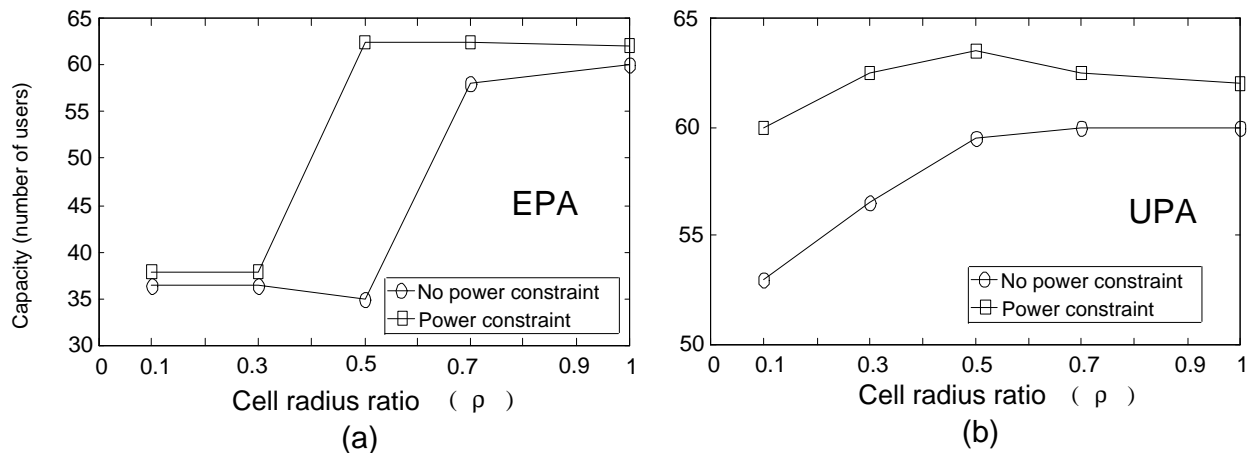


Figure 2.3: Total capacity of the equal power allocation (EPA) and the unequal power allocation (UPA) schemes for soft handoff with and without power constraint.

Furthermore, Fig. 2.3 shows the total capacity of EPA and UPA methods. The total capacity here is the summation of a macrocell capacity and a microcell capacity in Figure 2.2. The above analytical results demonstrate that the constrained UPA scheme for soft handoff can ease power exhausting problem [48]. In next section, we discuss related work and propose an effective power allocation of soft handoff for the CDMA mixed-size cellular system.

## 2.3 The Problem of the Mixed-Size Cellular System

Consider single service transmission, to manage resources for soft handoff is actually the issue of allocating power from multiple cells to a user in the CDMA system [49]. Many previous works about techniques of handoff power allocation have been proposed, such as EPA [9], QBPA [13], and SSDT [14]. Moreover, we propose a novel link proportional power allocation (LPPA) scheme. In the following, represent  $|D_h|$  as the size of the active set  $D_h$  of handoff user  $h$  and  $\gamma^*$  as the required signal quality for a handoff user.

### 2.3.1 Related Works for Soft Handoff Power Allocations

- Equal Power Allocation (EPA): Based on the EPA scheme, base stations allocate power to a handoff user according to the following principle: All the base stations in active

set  $D_h$  allocate power  $\frac{p_h^*}{|D_h|}$  to the handoff user, where  $p_h^*$  is the required transmission power for handoff user  $h$  to obtain its required signal quality.

- Quality Balancing Power Allocation (QBPA): The QBPA scheme was introduced in [13] based on a quality balance perspective for all users in each cell. The basic idea of QBPA is to allocate more power to a user with poor link quality, while assigning less power to a user with better link quality. However, when this concept is applied for multi-site transmission mechanism, it turns out that more power may be wasted for soft handoff users. Assume  $p_{b,h}$ ,  $b \in |D_h|$ , is the required power from base station  $b$  to achieve the required signal quality  $\gamma^*$  for handoff user  $h$ , the QBPA scheme allocates power to a handoff user according to the following principle:

$$p_{1,h} : p_{2,h} : \cdots : p_{|D_h|,h} = \frac{1}{L_{1,h}} : \frac{1}{L_{2,h}} : \cdots : \frac{1}{L_{|D_h|,h}} . \quad (2.22)$$

- Site Selection Diversity Transmission (SSDT): The SSDT scheme always selects the base station with the best link in the active set to serve handoff users. Because of this, it can transmit the least power, thereby decreasing the downlink interference. The SSDT scheme allocates power to a handoff user according to the following principle:

if

$$\kappa_s = \arg_b \min \{p_{b,h}, b \in |D_h|\} , \quad (2.23)$$

then

$$p_{b,h} = \begin{cases} p_{\kappa_s,h} & \text{if } b = \kappa_s \\ 0 , & \text{if } b \neq \kappa_s \end{cases} \quad (2.24)$$

- Link Proportional Power Allocation (LPPA): We propose a novel LPPA scheme to balance power load among cells through proper soft handoff power allocation. According to LPPA, the allocated power from a base station should be in proportional to the link quality between the handoff user and its serving base stations. In other words, LPPA aims to find a set of  $p_{b,h}$ ,  $b \in |D_h|$ , such that  $\sum_b \gamma_{b,h} \geq \gamma^*$  and

$$p_{1,h} : p_{2,h} : \cdots : p_{|D_h|,h} = L_{1,h} : L_{2,h} : \cdots : L_{|D_h|,h} . \quad (2.25)$$

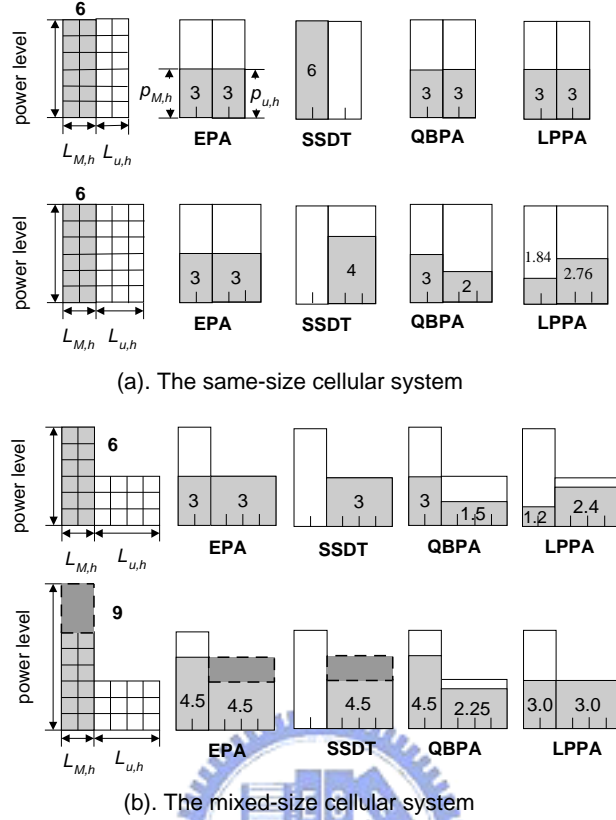


Figure 2.4: Examples for different soft handoff downlink power allocation schemes. (a) The same-size cellular system and (b) the mixed-size cellular system.

### 2.3.2 The Problem of Soft Handoff Power Allocation Mechanisms

In this subsection, we illustrate the power exhausting problem of a CDMA system with mixed-size cells, as shown in Fig. 2.4. We assume that a macrocell  $M$  and a microcell  $\mu$  simultaneously serve user  $h$  at the cell boundary. In the figure, the height of the blocks is defined as the maximum link power of the cell and the width of the blocks is proportional to the link quality, where  $L_{M,h}$  ( $L_{\mu,h}$ ) represents link quality from user  $h$  to macrocell (microcell) base station  $M$  ( $\mu$ ). We represent the equivalent received signal quality of user  $h$  by the product of multiplying the allocation power and the link quality. For example, for the same-size cellular systems case as shown in Fig. 2.4(a), the required received signal quality equals 12 ( $6 \times 2$ ) units before handoff. Here, we compare the following power allocation techniques: (1) EPA, (2) QBPA, (3) SSDT, and (4) LPPA.

For the same-size cellular system as in Fig. 2.4(a), assume that user  $h$  has equal link quality between macrocell and microcell, and it receives the same signal strength from macrocell and microcell, respectively. In this case, all the three power allocation methods will be the same.

Consider the mixed-size cellular system as shown in Fig. 2.4(b). Let the link quality to the microcell be two times of that to the macrocell, i.e.  $L_{\mu,h} = 2L_{M,h}$ , and the maximum link power in the macrocell be two times of that in the microcell. Then the distributions of power allocation from the two serving base stations based on different schemes are discussed as follows.

- Equal power allocation (EPA):

$$p_{M,h} = p_{\mu,h} = 3,$$

$$\Rightarrow \gamma_h = 18,$$

where  $p_{M,h}$  and  $p_{\mu,h}$  are the allocated power from the macrocell and that from the microcell, respectively; and  $\gamma_h$  is the received signal quality.

- Quality balancing power allocation (QBPA)[13]:

$$p_{M,h} = \frac{(12/2)}{L_{M,h}} = 3, p_{\mu,h} = \frac{(12/2)}{L_{\mu,h}} = 1.5,$$

$$\Rightarrow \gamma_h = 12.$$

- Site Selection Diversity Transmission (SSDT):

$$p_{M,h} = 0, p_{\mu,h} = 3,$$

$$\Rightarrow \gamma_h = 12.$$

- Link proportional power allocation (LPPA):

$$\frac{p_{M,h}}{p_{\mu,h}} = \frac{L_{M,h}}{L_{\mu,h}} = \frac{1}{2},$$

$$p_{M,h}L_{M,h} + p_{\mu,h}L_{\mu,h} = 12.$$

$$p_{M,h} = 1.2, p_{\mu,h} = 2.4,$$

$$\Rightarrow \gamma_h = 12.$$

Note that EPA will ask the serving base stations to allocate the same power in the two active links, thereby making a “microcell” waste too much power to obtain higher received

signal quality. Thus, handoff users from a macrocell will be very likely to exhaust most of the power budget of the microcell. This is so called “*power exhausting problem*”. Based on the QBPA scheme, both base stations allocate total power 4.5 units for the user, whereas base station using the LPPA scheme only require the total power of 3.6 units to maintain the same signal quality before handoff. As for the SSDT scheme, we find that SSDT can allocate the least power to achieve the required signal quality for a handoff user. However, when considering measurement errors during the base station selection procedure, SSDT may select a wrong base station for transmission, thereby consuming more power to serve handoff users. The impact of measurement errors on SSDT and other soft handoff power allocation schemes will be compared in this chapter.

## 2.4 Downlink Power Resource Allocation Mechanisms

In this section, we discuss a downlink resource allocation mechanism, which incorporates the modified quality balancing power allocation scheme for non-handoff users, the soft handoff power allocation scheme, and the removal algorithm. In order to specialize radio resource management of handoff, we differentiate handoff users from all users, and propose a modified quality balancing power allocation only for non-handoff users. By doing so, the system can allocate resources more efficiently. All the existing downlink power allocation techniques for handoff, such as EPA, QBPA, SSDT, and LPPA, can be implemented in this downlink power resource allocation mechanism. Moreover, based on the concept of LPPA presented in last section, we detail the algorithm design of the LPPA scheme, and use it as an example of soft handoff power allocation in the downlink mechanism of power resource allocation. All kinds of handoff power allocation can be fitted into the mechanism.

Figure 2.5 shows the flowchart of the procedures for downlink power resource allocation mechanism. As mentioned, this mechanism includes four key algorithms. First, based on soft handoff algorithm, an active set of candidate handoff base stations is determined for each user. Second, the necessary allocated power to each user is pre-estimated according to different schemes, i.e. EPA, QBPA, SSDT, and LPPA. Third, based on quality balancing

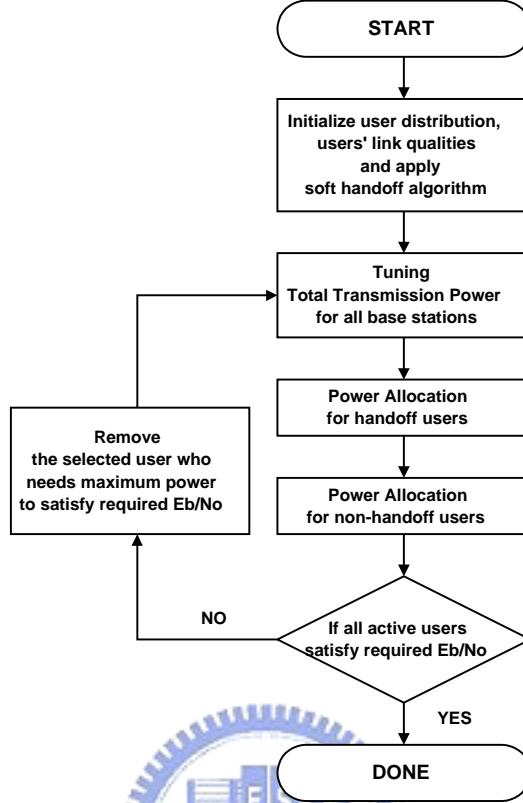


Figure 2.5: The flowchart of a downlink power resource allocation mechanism integrating four key techniques: 1) the soft handoff algorithm, 2) the downlink power allocation for handoff users, 3) the downlink power allocation for non-handoff users, and 4) the removal algorithm.

strategy for each cell, a modified quality balancing power allocation is adopted for non-handoff users. Four, if the balanced signal quality is lower than the required signal quality for all users in the system, removal algorithm is activated to release the system resources from users with poor link conditions. The iteration of power allocation stops when the signal quality meets the requirement. In the following, we detail the design for each algorithm.

### 2.4.1 Soft Handoff Algorithm

The soft handoff algorithm is used to determine the active set  $D_m$  for each user  $m$ . If the difference of the received signal strength of the pilot signal between the serving cell  $b$  and adjacent cell  $k$  is less than the soft handoff threshold  $\eta$ , i.e.

$$P_b^I \cdot L_{b,m} - P_k^I \cdot L_{k,m} \leq \eta, \text{ for } b \neq k, \quad (2.26)$$

then base station  $k$  should be added into the active set  $D_m$  of user  $m$ .

### 2.4.2 The Downlink Power Allocation Algorithm for Soft Handoff Users

In this subsection, we detail the design of the LPPA scheme, which can be implemented in an iterative manner, and prove its convergence characteristic.

The principle of LPPA is to distribute required power among active links in proportional to the link qualities of the connections. That is, LPPA allocates more power to a link with better link quality than to others in the active set of the soft handoff user. The followings describe the procedure of the power allocation by using LPPA. The LPPA scheme estimates the required power for soft handoff user  $h$ ,  $p_h^*$ ; then it distributes  $p_h^*$  to all serving base stations in  $D_h$  under the constraint of maximum link power to each user by base station  $b \in D_h$ ,  $\tilde{p}_b$ . And  $p_{b,h}$  is proportional to the link quality between the serving base station  $b$  and the soft handoff user  $h$ . If the required transmission power of one link reaches to the constraint of maximum link power, LPPA will compensate the required power through other active links.

The LPPA scheme is an iterative method to distribute  $p_h^*$  to all serving base stations so that the required signal quality can be satisfied. The design tries to accomplish *power balance* between cells in the CDMA cellular system with mixed-size cells. Besides, it is noteworthy that due to the constraint of the maximum link power, there exists a forced termination situation for the soft handoff because the soft handoff user cannot obtain required signal quality even though all active links are allocated with maximum link power. If the soft handoff is forced to terminate,  $p_{b,h}$  of each link  $b$  in the active set  $D_h$  are reset to zero, it means the transmission is ceased temporary. The LPPA scheme is stated in more details in the following.

#### [The LPPA Scheme]

**Step 0:** [Exam soft handoff feasibility]

- Allocate maximum link power  $\tilde{p}_b$  for each active links  $b$ .
- Calculate received signal quality  $\gamma_h$  based on (3.2) and (4.4).

- IF  $\gamma_h > \gamma^*$ , THEN Goto **Step 1**.  
 ELSEIF  $\gamma_h = \gamma^*$ , THEN Set  $p_{b,h} = \tilde{p}_b$ ,  $b \in D_h$ , DONE.  
 ELSE soft handoff user  $h$  is forced to terminate ( $p_{b,h} = 0$ ,  $b \in D_h$ ), DONE.

**Step 1:** [Initialize]

- Initialize required transmission power,  $p_h^*$ , for soft handoff user  $h$  to be the summation of maximum link power,  $\tilde{p}_b$ , of each serving base station  $b$  by

$$p_h^* = \sum_{b \in D_h} \tilde{p}_b. \quad (2.27)$$

**Step 2:** [Calculate weighting factor]

- Set weighting factor  $w_{b,h}$  of the transmission power from base station  $b$  in  $D_h$ , based on link quality  $L_{b,h}$  between cell  $b$  and soft handoff user  $h$ , by

$$w_{b,h} = \frac{L_{b,h}}{\sum_{b \in D_h} L_{b,h}}. \quad (2.28)$$

**Step 3:** [Calculate allocation power]

- Determine the power that base station  $b$  in  $D_h$  allocates to soft handoff user  $h$ ,  $p_{b,h}$ , by

$$p_{b,h} = \text{Min}\{p_h^* \times w_{b,h}, \tilde{p}_b\}, \forall b \in D_h. \quad (2.29)$$

**Step 4:** [Compute received  $E_b/N_o$  and tuning factor]

- Compute corresponding  $\gamma_h$  in (2.12), and set tuning factor  $\varphi_h$  by

$$\varphi_h = \frac{\gamma_h^*}{\gamma_h}. \quad (2.30)$$

Note that  $\gamma_h^*$  is the required signal quality of soft handoff user  $h$ .

**Step 5:** [Check Stop Criterion]

- IF  $\varphi_h \neq 1.0$ , THEN

– Let

$$p_h^* = \varphi_h \times p_h^* \quad (2.31)$$

– Goto **Step 3**.

ELSE DONE. ■



Next, we prove the convergence characteristic of the LPPA scheme that is in iterative manner. The required transmission power of each active link,  $p_{b,h}$ ,  $b \in D_h$ , for all soft handoff users can be obtained through the LPPA scheme. The LPPA scheme is proven to be convergent in the following.

**[Convergence Proof of the LPPA Scheme]**

**[Definition]:** A function  $F$  is “**standard**” if it satisfies the following conditions for all non-negative power vectors [50]:

- Positivity :  $F(y) > 0$ ,
- Monotonicity :  $y_1 \geq y_2 \Rightarrow F(y_1) \geq F(y_2)$ ,
- Scalability :  $\forall \alpha > 1, \alpha F(y) \geq F(\alpha y)$ . ■

**[Proposition]:** A “**standard**” power control algorithm will converge to a unique “**effective**” power vector that achieves  $\gamma_h^*$  for any initial power  $p_h^*$ . The standard power control algorithm means that the power allocation function is standard.

The LPPA scheme has an iterative process to obtain the required power allocation for soft handoff user  $h$ ,  $p_h^*$ , which is described by

$$p_h^{*n+1} = \Theta(p_h^{*n}), \tag{2.32}$$

where the superscript of  $p_h^{*n}$  denotes the number of iteration  $n$  and  $\Theta$  denotes the power allocation function. From (2.2), (2.12), (2.31), and (2.30),  $\Theta$  is given by

$$\Theta(p_h^{*n}) = \frac{\gamma_h^*}{\sum_{b \in D_h} \gamma_{b,h}} \times p_h^{*n}. \tag{2.33}$$

Based on (2.2),  $\gamma_{b,h}$  is the function of  $p_{b,h}$ ,  $b \in D_h$ , which should obey the constraint of maximum link power given in (2.10) and (2.11). In order to represent these relationship, we denote  $\gamma_{b,h}$  as  $\Gamma(p_{b,h})$ , instead of (2.2).

Since all the link qualities and background noise between soft handoff user  $h$  and serving base stations  $b$ ,  $b \in D_h$ , are positive, the power allocation function given in (2.32) has the positivity and monotonicity properties. As for the scalability property, there are two kinds

of cases in the resulting allocation power vector  $p_{b,h}$ ,  $b \in D_h$ , considering the effect of the maximum link power constraint:

**Case 1:**  $p_{b,h} = \min(p_h^* w_{b,h}, \tilde{p}_{b,h}) < \tilde{p}_{b,h}, \forall b$ .

Since  $\alpha p_h^* w_{b,h} > p_h^* w_{b,h}$ , for  $\alpha > 1$ ,

it can be found that  $\Gamma(\alpha p_h^* w_{b,h}) > \Gamma(p_h^* w_{b,h})$ ,

and  $\sum_{b \in D_h} \Gamma(\alpha p_h^* w_{b,h}) > \sum_{b \in D_h} \Gamma(p_h^* w_{b,h})$ .

Thus,

$$\Theta(\alpha p_h^*) = \frac{\gamma_h^*}{\sum_{b \in D_h} \Gamma(\alpha p_h^* w_{b,h})} \times (\alpha p_h^*) < \alpha \Theta(p_h^*).$$

**Case 2:**  $\exists k, k \in D_h$  s.t.  $p_{k,h} = \min(p_h^* w_{k,h}, \tilde{p}_k) = \tilde{p}_k$ .

It can be found that  $\sum_{b \in D_h} \Gamma(p_h^* w_{b,h}) = \sum_{\substack{b \neq k, \\ b \in D_h}} \Gamma(p_h^* w_{b,h}) + \sum_k \Gamma(\tilde{p}_k)$ ,

then  $\sum_{b \in D_h} \Gamma(\alpha p_h^* w_{b,h}) = \sum_{\substack{b \neq k, \\ b \in D_h}} \Gamma(\alpha p_h^* w_{b,h}) + \sum_k \Gamma(\tilde{p}_k) \geq \sum_{b \in D_h} \Gamma(p_h^* w_{b,h})$ .

Thus,

$$\Theta(\alpha p_h^*) = \frac{\gamma_h^*}{\sum_{b \in D_h} \Gamma(\alpha p_h^* w_{b,h})} \times (\alpha p_h^*) \leq \alpha \Theta(p_h^*).$$

■

The power allocation function also possesses the scalability property. Therefore the proposed LPPA scheme is a standard power control algorithm, and it always exists an effective solution  $p_h^*$  for soft handoff user  $h$ .

### 2.4.3 The Downlink Power Allocation Algorithm for Non-Handoff Users

In the preceding sections, we specialize radio resource management of handoff by differentiating handoff users from all users. In this subsection, we further propose a modified quality balancing power allocation only for non-handoff users based on the concept of quality balancing in [13], [25]. The major idea of quality balancing power allocation techniques is to offer all users in the same cell the same quality level by allocating power in reverse proportional to link qualities. According to balanced quality of each cell, Kim [13] further proposed a simple scheme to adjust base stations' total power so as to balance signal quality to the same required level for each user in each cell. In this subsection, we propose a modified

quality balancing power allocation (Modified-QBPA) algorithm with adjustable total power of base stations to serve non-handoff users.

The Modified-QBPA algorithm is to provide all non-handoff user the same required signal quality. Assume the required signal quality is  $\gamma^*$ ; denote  $A_b$  ( $B_b$ ) as the total transmission power for non-handoff (soft handoff) in cell  $b$  such that  $A_b + B_b = P_b^T$ . Consider single service only, the Modified-QBPA algorithm assigns the non-handoff user  $m$  in cell  $b$  an amount of power,  $p_{b,m}$ , by

$$p_{b,m} = \frac{w_{b,m}}{\sum_{m \in \mathbf{U}_b} w_{b,m}} \cdot A_b, \quad (2.34)$$

where  $\sum_{m \in \mathbf{U}_b} p_{b,m} = A_b$ ,  $\mathbf{U}_b$  is the set of non-handoff user in cell  $b$ , and  $w_{b,m}$  is defined as

$$w_{b,m} = \frac{I_{b,m}}{L_{b,m} \cdot G_P}. \quad (2.35)$$

Substituting (2.34) and (2.35) into (2.2), the received signal quality of the non-handoff user  $m$  in cell  $b$  can be yielded as

$$\tilde{\gamma}_b = \gamma_{b,m} = \frac{A_b}{\sum_{m \in \mathbf{U}_b} w_{b,m}}, \quad (2.36)$$

where  $\tilde{\gamma}_b$  is the balanced signal quality of cell  $b$ , in which all non-handoff users in cell  $b$  have exactly the same signal quality,  $\gamma_{b,m}$ . The balancing target is to achieve  $\tilde{\gamma}_b \geq \gamma^*$  so that every non-handoff user can have  $\gamma_{b,m} \geq \gamma^*$ . If  $\tilde{\gamma}_b$  is not equal to  $\gamma^*$ , the total transmission power  $A_b$  should be adjusted by tuning factor  $\psi_b$ , which is given by

$$\psi_b = \frac{\gamma^*}{\tilde{\gamma}_b}. \quad (2.37)$$

The Modified-QBPA algorithm is described in the following.

**[Modified-QBPA Algorithm for Non-Handoff Users]**

**Step 1:** [Initialize]

- Initialize the total transmission power  $P_b^T$  to the maximum total transmission power  $\tilde{P}_b$  for each cell  $b$ .
- Calculate the total allocation power  $B_b$  for handoff users in each cell  $b$  after executing soft handoff power allocation algorithm, i.e. EPA, QBPA, SSDT, LPPA.

**Step 2:** [Calculate  $w_{b,m}$ ]

- Calculate  $w_{b,m}$ , based on (2.35), for user  $m$  in cell  $b$ .

**Step 3:** [Calculate allocation power]

- Calculate the total transmission power  $A_b$  for non-handoff users in each cell  $b$ , which is equal to  $(P_b^T - B_b)$ .
- Calculate allocation power  $p_{b,m} = \min(p_{b,m}, \tilde{p}_b)$  for each non-handoff user  $m$  in cell  $b$  based on (2.34).

**Step 4:** [Calculate balanced signal quality]

- Calculate balanced signal quality  $\tilde{\gamma}_b$  for users in cell  $b$  based on (2.36).

**Step 5:** [Calculate tuning factor]

- Calculate tuning factor  $\psi_b$  for each cell  $b$  based on (2.37).

**Step 6:** [Check Stop Criterion for each cell  $b$ ]

- IF any  $\psi_b \neq 1.0$  and the convergence is not met, THEN
  - Adjust total transmission power as  $P_b^T = \min(\psi_b \times A_b + B_b, \tilde{P}_b)$ .
  - Goto **Step 2**.
- ELSE DONE. ■

The proposed Modified-QBPA algorithm is standard as described in [13]. It will converge to a desired solution if there exists an effective individual power allocation solution for all users such that they can obtain their required signal qualities. If an effective solution does not exist, the issue becomes how to find a subset of users that can obtain their required signal qualities. Then, the removal algorithm will be activated, which is stated in the next subsection.

#### 2.4.4 Removal Algorithm

To achieve convergent solution for downlink power allocation, [26], [27] proposed removal algorithms to remove some users who owns weaker link quality for transmission. In this subsection, we further design two removal schemes to provide priority for soft handoff users who need seamless transmission.

After allocating power to handoff and non-handoff users, if the signal quality of the serving users is still below the required threshold, this means power resource is insufficient to support all the serving users. Thus, removal algorithm is activated to remove the user with the weakest link quality. The system can thus utilize the extra power from this user to serve other users who can improve their link quality to a satisfactory level. The pilot power in mixed-size cellular systems is dependent on cell sizes as described in (2.6) and (2.7). The criterion for selecting a user to be removed is based on the removal index,  $J_m$ , which can simply choose the user with the largest ratio of allocating power to user  $m$  over the maximum allowable power for each user in cell  $b$ . Define the removal index of user  $m$  as

$$J_m = \max \left\{ \frac{p_{b,m}}{\tilde{p}_b} \right\}, \quad (2.38)$$

where the denominator  $\tilde{p}_b$  is dependent on the cell sizes, e.g. (2.10) and (2.11).

In this subsection, we develop two removal algorithms.

- Removal Algorithm 1 (RV1): The system will remove the selected user based on the removal index for all users no matter if the selected one is handoff user or not.
- Removal Algorithm 2 (RV2): The system will only remove non-handoff users based on the removal index and leave handoff users a higher priority to remain in the system.

Numerical results will be given in the next section to compare the performance of these two removal algorithms.

## 2.5 Simulation Results and Discussions

In this section, we compare the performance of LPPA, EPA, QBPA, and SSDT schemes in the CDMA system with various cell sizes under the situation with and without measurement

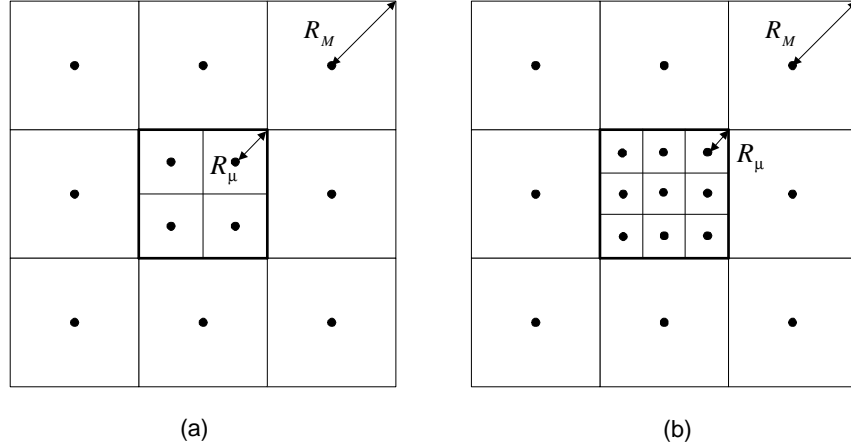


Figure 2.6: Simulation models of the CDMA mixed-size cellular network with (a)  $\rho = 1/2$ , (b)  $\rho = 1/3$ .

errors. Denote the cell radius size ratio between microcell and macrocell as  $\rho$ . Assume users are uniformly distributed in each square-shaped cell. Fig. 2.6(a) and (b) show the simulation model of mixed-size cellular structures with mixed-size cells, in which a central macrocell is split to four or nine microcells to represent the cases of the mixed-size cells  $\rho = 1/2$  and  $1/3$ . It is noteworthy that the mixed-size cellular model with square-shaped cells aids us to compare mixed-size cells model with different  $\rho$  values, while the cell coverage should still be in round shape because users choose their serving cells based on received signal strengths but not locations.

The simulation methodology and assumptions are summarized as follows:

- The snapshot simulation method is adopted in this work as [13], [16], [17], and [46]. Although the snapshot simulation methodology cannot capture the time correlation of a fading channel, it is actually a viable approach to observe qualitative performance results for the simulated wireless communication system without conflicting by other algorithms of radio resource management.
- Other related system parameters are listed in Table 2.1, in which the soft handoff threshold  $\eta = 2$  dB, the maximum active set size  $|D_h| = 3$ , and the values of the pilot power design and the maximum allocation power for each user are obtained according to (2.7), and (2.27), respectively.

Table 2.1: SYSTEM PARAMETERS OF THE SIMULATION MODEL FOR THE MIXED-SIZE CDMA CELLULAR SYSTEM

System parameters	value
macrocell's radius(km), $R_M$	3
microcell's radius(km), $R_\mu$	1.5
cell radius ratio( $R_\mu/R_M$ ), $\rho$	1/2
mobile's antenna height(m), $h_m$	1.5
macrocell antenna height(m), $h_M$	20
microcell antenna height(m), $h_\mu$	10
macrocell's max. transmission power(watt), $\tilde{P}_M$	20
macrocell's max. allocating power(watt), $\tilde{p}_M$	1
2 slope path loss exponent of base station $b$ , $\alpha_b, \beta_b$	2, 2
Standard deviation of 2-slope shadowing, $\sigma_1, \sigma_2$	4.0, 8.0
Soft handoff threshold(dB), $\eta$	2
Maximum active set size	3

- The system capacity is defined as the number of affordable users with outage probability less than 0.05. Because the outage event occurs when a base station has insufficient power to provide user's required signal quality, we can also define the outage probability as the ratio of the number of disconnected (removed) users to the total number of users. Thus the total capacity  $C_{tot}$  is defined as the sum of capacities of macrocells and microcells.

$$C_{tot} = \begin{cases} N_C \times C_C & , \rho = 1.0 \\ N_M \times C_M + N_\mu \times C_\mu & , \rho < 1.0 \end{cases}$$

where  $C_C$  is the system capacity per cell, and  $N_C$  is the number of cells in the same-size cellular systems, where  $N_C = 9$  in our same-size cellular model. For the mixed-size cellular systems,  $C_M$  and  $C_\mu$  represent macrocell and microcell capacity, respectively. Here, we consider two mixed-size cells as shown in Figure 2.6, where (a) is for  $\rho = 1/2$ ,  $N_M = 8$  and  $N_\mu = 4$ , and (b) is for  $\rho = 1/3$ ,  $N_M = 8$  and  $N_\mu = 9$ .

### 2.5.1 The Same-Size Cellular Case

Figure 2.7 compares system capacity versus average outage probability for different soft handoff power allocation schemes, including EPA, SSdT, QBPA, LPPA-RV1, and LPPA-RV2. In a same-size CDMA cellular system, we can observe that QBPA, SSdT and LPPA

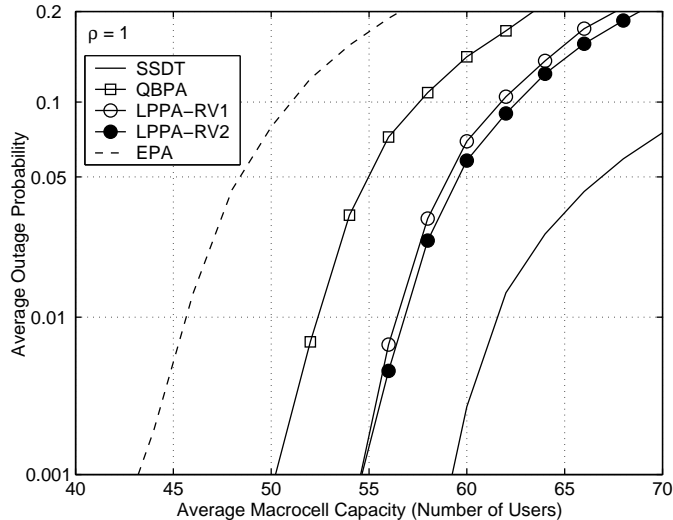


Figure 2.7: Averaged outage probability of the same-size cellular systems with  $\rho = 1.0$  for EPA, QBPA, SSDT, LPPA-RV1 and LPPA-RV2 schemes.

are better than EPA. The LPPA-RV2 scheme enhances 23.1 % and 8.5 % capacity over EPA and QBPA schemes, respectively. Furthermore, SSDT outperforms LPPA-RV1 and LPPA-RV2 up to 9.1 % and 10 %, respectively. Note that SSDT has been viewed as the optimal downlink transmission scheme in a same-size CDMA network.

In order to observe the impact of the measurement errors on the soft handoff power allocation scheme, we consider the case of 3 dB measurement errors during active set selection. Comparing Fig. 2.7 with Fig. 2.8, we observe that measurement errors degrade system capacity by 18.1 %, 13.7 %, 7.7 %, 2.2 %, and 1.3 % for SSDT, EPA, QBPA, LPPA-RV1, and LPPA-RV2, respectively. As shown in the figure, SSDT is the most sensitive to the measurement error since only one link is adopted for transmission. If the selected link is not the best link due to measurement errors, more transmission power may be wasted. On the other hand, subject to measurement errors case, LPPA-RV1 and LPPA-RV2 improve system capacity by 1.8 % and 3.8 % as compared to SSDT, respectively. Note that in a more stringent requirement on outage probability, the capacity gain of applying the LPPA scheme becomes more significant.



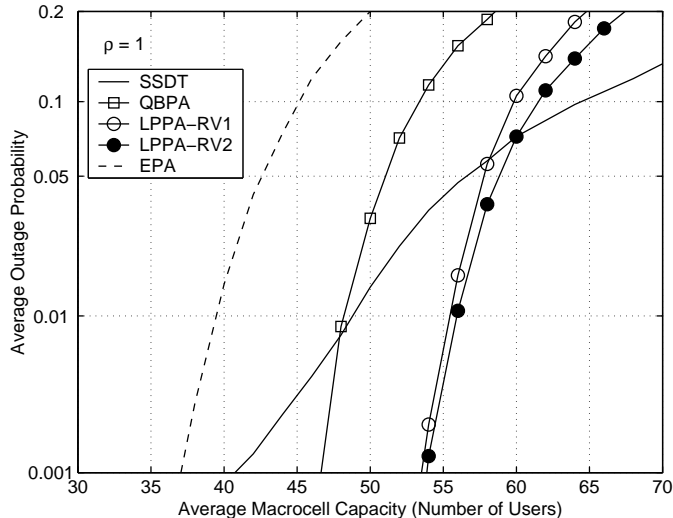


Figure 2.8: Averaged outage probability of the same-size cellular systems with  $\rho = 1.0$  subject to measurement errors for EPA, QBPA, SSDT, LPPA-RV1 and LPPA-RV2 schemes.

### 2.5.2 The Mixed-Size Cellular Case

Figure 2.9 compares the system capacity of all the aforementioned power allocation schemes for soft handoff under the mixed-size cellular systems with  $\rho = 1/2$ . Figures 2.9 (a) and (b) are the average outage probability of the macrocell and microcell, respectively. Because EPA wastes too much power in serving soft handoff users, the system with EPA encounters the “power exhausting problem”. This problem would become worse for the mixed-size cellular systems in which adjacent cells have different cell sizes. Thus, based on (2.39), all schemes have higher total capacity than EPA. The LPPA-RV2 scheme improves EPA and QBPA by 76.9 % and 19.3 %, respectively. Compared to SSDT, the capacity of LPPA-RV2 is 2.9 % less in the mixed-size cellular systems with  $\rho = 1/2$ .

Next we evaluate the impact of measurement errors on the performance of the mixed-size cellular system with  $\rho = 1/2$ . As shown in Fig. 2.10, measurement errors results in degrading system capacity by 23.4 %, 17.6 %, 8.4 %, % 2.2 %, and 1.0 % for EPA, SSDT, QBPA, LPPA-RV1, and LPPA-RV2, respectively. For the EPA scheme, the power exhausting problem occurs more easily , thereby having insufficient power to serve other non-handoff users, especially in the microcell. Clearly, the measurement errors may worsen the impact of the power exhausting problem. On the other hand, since LPPA can distribute

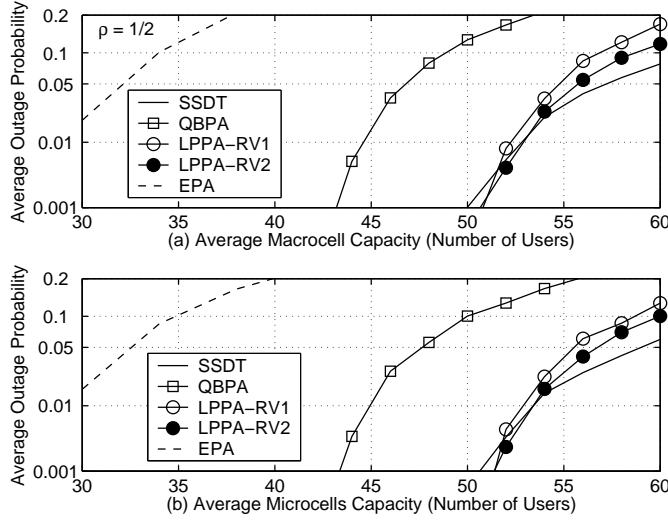


Figure 2.9: Averaged outage probability of the mixed-size cellular systems with  $\rho = 1/2$  for EPA, QBPA, SSDT, LPPA-RV1 and LPPA-RV2 schemes.

the required power among serving base stations, the sensitivity on measurement errors is relatively smaller than SSDT. Compare the case of measurement errors, both LPPA-RV1 and LPPA-RV2 improve the system capacity of the SSDT scheme by 9.6 % and 13.1 %, respectively.

Figure 2.11 shows average outage probability of different schemes in the case of  $\rho = 1/3$ . In the case without measurement errors, LPPA-RV2 and LPPA-RV1 improve the system capacity by 4.8 % and 1.7 % over SSDT. Furthermore, the capacity of LPPA-RV2 is 29.6 % and 124.8 % higher than QBPA and EPA schemes. Consider the case of measurement errors, Fig. 2.12 shows the same cellular environment as Fig. 2.11 but includes measurement errors. As shown in the figure, the measurement errors exacerbates the problem of the power exhausting for EPA, QBPA, and SSDT. We find that LPPA-RV2 improves system capacity by 22.8 %, 40.7 %, 181.4 % compared to SSDT, QBPA, and EPA schemes. Therefore, it is concluded that LPPA-RV1 and LPPA-RV2 can successfully ease the power exhausting problem in the mixed-size cellular systems, even when there occurs measurement errors.

Based on the previous discussions, we have three important observations.

- For mixed-size cellular systems with smaller  $\rho$ , the system capacity is increased because of cell splitting. However, serving soft handoff users may also easily cause the serious

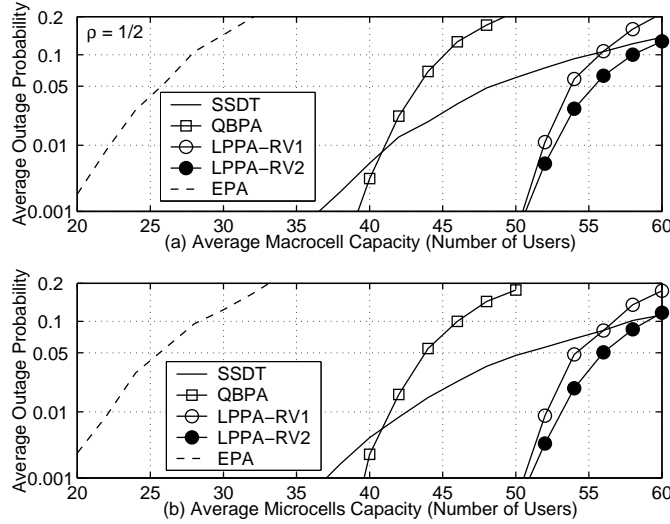


Figure 2.10: Averaged outage probability of the mixed-size cellular systems with  $\rho = 1/2$  subject to measurement errors for EPA, QBPA, SSDT, LPPA-RV1 and LPPA-RV2 schemes.

power exhausting problem.

- We find that measurement errors will result in degrading system capacity. Both EPA and SSDT are more sensitive to measurement errors than LPPA and QBPA. This is because the LPPA scheme can effectively distribute the required allocation power among the serving base stations.
- Measurement errors exacerbate the power exhausting problem in the mixed-size cellular systems. Therefore, the system capacity of EPA, QBPA, SSDT schemes are degraded even more seriously.

Figure 2.13 shows the total system capacity with considered schemes of soft handoff power allocation. For the case without measurement errors, SSDT outperforms other schemes except in the mixed-size cellular case, e.g.  $\rho = 1/3$ . For SSDT in the mixed-size cellular system, because the maximum allocation power constraint is more stringent, the required allocation power may easily exceed the power constraint when serving soft handoff users. When incorporating measurement errors, the SSDT performance is significantly degraded because only one single link is used to serve the soft handoff user. If the selected link is not the best link, SSDT may waste too much transmission power in serving a soft handoff

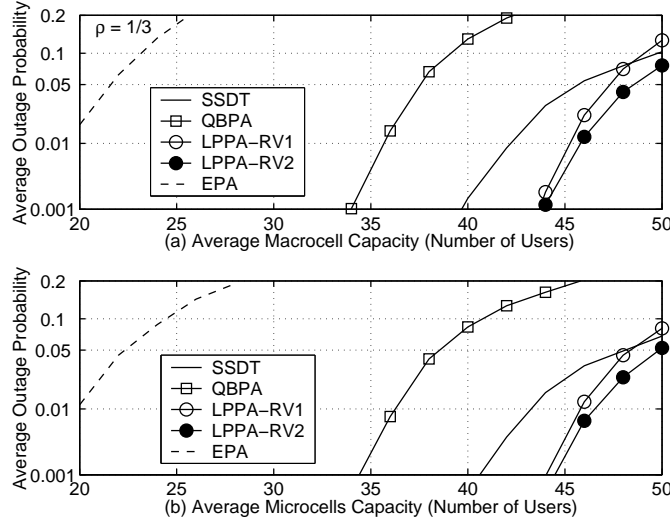


Figure 2.11: Averaged outage probability of the mixed-size cellular systems with  $\rho = 1/3$  for EPA, QBPA, SSDT, LPPA-RV1 and LPPA-RV2 schemes.

user, thereby more likely causing the power exhausting problem especially in the mixed-size cellular systems. From the figure, we have the following observations:

- Compared to the SSDT, QBPA and LPPA schemes, EPA is the least efficient one, and very sensitive to measurement errors. Thus, the system capacity using EPA is the lowest among all the considered soft handoff power allocation scheme.
- For QBPA, the basic idea is to allocate less (more) power via a better (weak) link. If using QBPA for both non-handoff and handoff users, it may waste too much power in serving soft handoff users. QBPA can slightly ease the power exhausting problem and result in higher system capacity than EPA.
- As for LPPA, the required power for the soft handoff user is distributed among all active links in its active set. If the required power of one active link is larger than its constraint of the maximum link power, the maximum link power will be allocated. And the rest of the required power will continuously be distributed by other active base stations. This is the reason why the LPPA scheme is less sensitive for the case of measurement errors.
- For same-size cellular systems, LPPA-RV2 improves capacity over EPA, QBPA, and

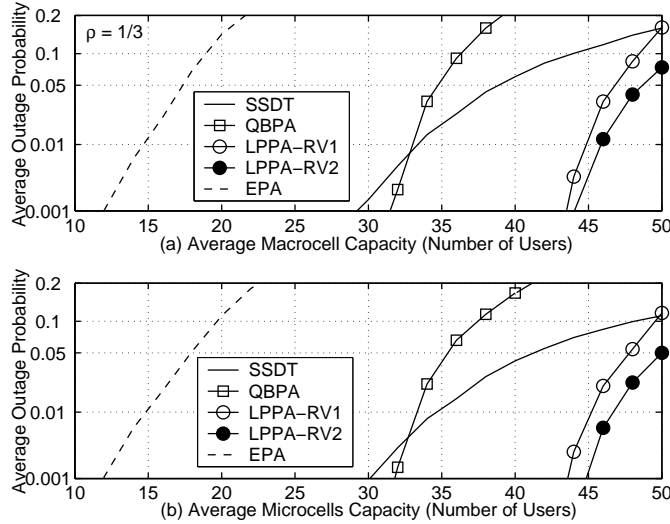


Figure 2.12: Averaged outage probability of the mixed-size cellular systems with  $\rho = 1/3$  subject to measurement errors for EPA, QBPA, SSDT, LPPA-RV1 and LPPA-RV2 schemes.

SSDT by 38.1%, 15.4 %, and 3.8 %. Meanwhile, for the mixed-size cellular systems with  $\rho = 1/3$ , LPPA-RV2 further improves the capacity by 181.4 %, 40.7 %, and 22.8 % as compared to EPA, QBPA, SSDT, respectively.

- LPPA outperforms other schemes in both the same-size and the mixed-size cellular systems even with measurement errors. Note that LPPA-RV2 is always slightly better than LPPA-RV1 because it provides protection for soft handoff in the removal algorithm. This kind of protection strategy for soft handoff is a useful strategy to enhance the efficiency of utilizing radio resource.

## 2.6 Concluding Remarks

In this chapter, we have studied impacts of the soft handoff in the mixed-size cellular system. We address a “power exhausting problem” and propose a novel LPPA scheme to ease the problem. By taking account of the effects of different cell sizes, simulation results show that LPPA can prevent a microcell base station from wasting too much transmission power in serving handoff users. Consequently, the simulation results show that LPPA can more effectively alleviate the power exhausting problem than others by outstanding the “power balance” characteristic. Also, the LPPA scheme can support higher system capacity than

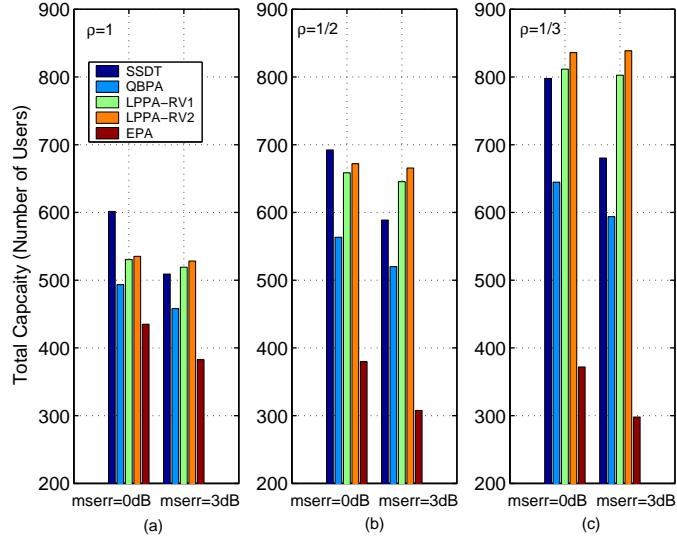


Figure 2.13: Total capacity with and without measurement errors for EPA, QBPA, SSdT, LPPA-RV1 and LPPA-RV2 schemes of (a) the same-size cellular system, (b) the mixed-size cellular system with  $\rho = 1/2$ , (c) the mixed-size cellular system with  $\rho = 1/3$ .

other schemes in both the same-size and mixed-size cellular systems even with measurement errors. In summary, we find that it is important to design a handoff mechanism from both power efficiency and link reliability perspectives. The concept and the methodology are useful to develop advanced radio resource algorithms for multirate CDMA systems in next chapter.

## Chapter 3

# A Joint Power And Rate Allocation mechanism for Multirate Soft Handoff in Mixed-Size WCDMA Cellular Systems

---

*The chapter proposes a joint power and rate assignment (JPRA) algorithm to deal with multirate soft handoffs in WCDMA mixed-size cellular systems. This JPRA algorithm, containing a link proportional power allocation (LPPA) scheme and an evolutionary computing rate assignment (ECRA) method, can determine an appropriate allocation of power and service rate for multirate soft handoffs, respectively. It can achieve power balance among cells through soft handoffs better than the conventional site-selection diversity transmission (SSDT) scheme with best-effort rate allocation. Simulation results show that the JPRA algorithm can reduce the handoff forced termination probability and improve the total throughput, which means better cell's service coverage and higher system capacity. Besides, it is shown that JPRA is less sensitive than SSDT to measurement errors occurring in the active set selection.*

### 3.1 Introduction

The tremendous growths of internet services drive multirate transmission becoming necessary in the third generation systems such as Universal Mobile Telecommunications Systems (UMTS). Because of abundance multimedia traffic in the downlink (from base station to mobile station), downlink transmission is generally the capacity-limited direction in the multirate wideband code division multiple access (WCDMA) systems. To utilize downlink radio resources efficiently, many previous studies focus on joint power and rate allocations for all users in the systems [18], [19], whereas the possible combinatorial numbers of the solutions are too large to be tractable for optimal allocations. This problem becomes more complicated when taking into account multi-site transmission mechanisms for soft handoff.

Soft handoff is one of the most important features in WCDMA cellular systems. When mobile users move from one cell to another cell, the soft handoff mechanism can provide seamless connections and better signal qualities for users near the cell boundaries. However, base stations often have to consume more power to serve soft handoff users than that to serve non-handoff users. The fact that the total power resource in each base station is confined and shared among non-handoff and soft handoff users raises the issue of the tradeoffs between coverage and capacity. For example, if a base station fails to serve multirate handoff users near the cell boundaries, the cell's service coverage is shrunk whereas there are more power applicable to non-handoff users for higher transmission rates. Therefore, joint power and rate allocations of multirate soft handoffs play an important role for downlink radio resource management. Instead of optimal power and rate allocations for all users in the system, the complexity can be greatly reduced by optimal radio resource management for multirate soft handoffs, which makes system implementation feasible.

Furthermore, consider a WCDMA cellular system with mixed-size cells due to non-uniform traffic load distribution, in which all cells utilize the same frequency so that the emitted power of different base stations interferes each other. Generally, congested micro-cells, which are with stringent power budget for maximum total transmission power and maximum link power, may easily exhaust their total transmission power because of serv-



ing soft handoff users in the downlink [8], and then there is no extra power resource to serve other users in the system. When taking into account multirate services, this power exhausting problem becomes more critical. Therefore, the ultimate goal of this chapter is to design an optimal scheme with *power balance* characteristics for radio resource management of soft handoffs. As long as power balance can be achieved among macrocells and microcells through the optimal scheme of soft handoffs, there are more power resources can be allocated for other users in the congested microcells. As a result, the system performance can be improved. References [5]-[7] considered capacity issues in mixed-size cellular systems with mixed-size cells. Both [5] and [6] only focused on the reverse link and only voice service is considered. On the other hand, Kishore, et al, [7] concluded that uplink and downlink directions are equivalent in mixed-size mixed-size cellular systems. However, it does not consider multirate services which are often regarded as highly resource-exhausting traffics and often have more volumes of traffic in the downlink than that in the uplink. Therefore, in this chapter, we specialize in the downlink transmission which is generally the capacity-limited direction in the multimedia WCDMA cellular systems.

Many literatures discussed the topic of joint power and rate assignment for *all users* in the cellular system in the sense of global optimization problem [18], [19]. However, they focused on the reverse link and did not concern about multirate soft handoffs. Kim [22] dealt with rate-regulated power control in the reverse link without concerning handoff. Reference [23] discussed radio resource management in multiple-chip-rate direct sequence CDMA systems supporting multiclass services. It arranged handoff in the same subsystem or execute inter-frequency handoff. Kim and Sung [24] proposed a handoff management scheme for multirate services using guard channels and reservation on demand queue control, but a hard handoff scheme was considered. References [20] and [21] proposed joint power and rate allocation algorithms in the downlink WCDMA same-size cellular systems. The former proposed two sub-optimal algorithms based on fairness consideration, and the latter adopted dynamic programming technique to optimize total throughput. However, both considered same-size cellular systems without soft handoff mechanisms. A conventional site selection diversity

transmission (SSDT) scheme was proposed for handoff power allocation in [14]. It provides transmission diversity by dynamically selecting one base station with best link quality in the active set. However, due to the maximum link power constraint, SSDT sometimes could not afford enough power required to multirate soft handoff users. Moreover, since SSDT is a single-site transmission mechanism at one time, it may select the wrong link resulting in wasting more power for handoffs when suffering measurement errors during active set selection. The advantage of the power saving characteristic for SSDT would disappear.

In this chapter, we propose a joint power and rate assignment (JPRA) algorithm for *downlink multirate soft handoff users* in WCDMA mixed-size cellular systems. The proposed JPRA algorithm is a two-phase process, which is composed of LPPA and ECRA. In the first phase, a link proportional power allocation (LPPA) scheme is designed for power allocation of soft handoffs. Unlike the SSDT scheme, LPPA is a multi-site transmission mechanism, which distributes the required power in proportion to the link qualities between a soft handoff user and all base stations in its active set. That is, the base station with better link quality will allocate more power than others with worse link qualities. In the second phase of JPRA algorithm, an evolutionary computing rate assignment (ECRA) method is proposed to formulate an integer and discrete optimization problem under a predefined total power constraint for soft handoffs in each cell. It is well known that conventional optimization methods can hardly cope with problems with integer and discrete variables, whereas evolutionary computing methods are very efficient for these problems to reduce the searching complexity [40]. In the meantime, a new multi-quality balancing power allocation (MQBPA) algorithm for non-handoff users with multiple service rates is also developed. Previous work for quality balancing power allocation technique were studied only for a single service rate with unique required signal quality [13], [25]. On the other hand, a multirate removal (MRV) algorithm is proposed to pick out a user who consumes system resource most and to reduce its service rate or even block it when the system resource is insufficient. Several removal algorithms had been proposed in [26]-[28]. Among these, the link-based and received signal-strength based removal algorithms were only suitable for single service [26],

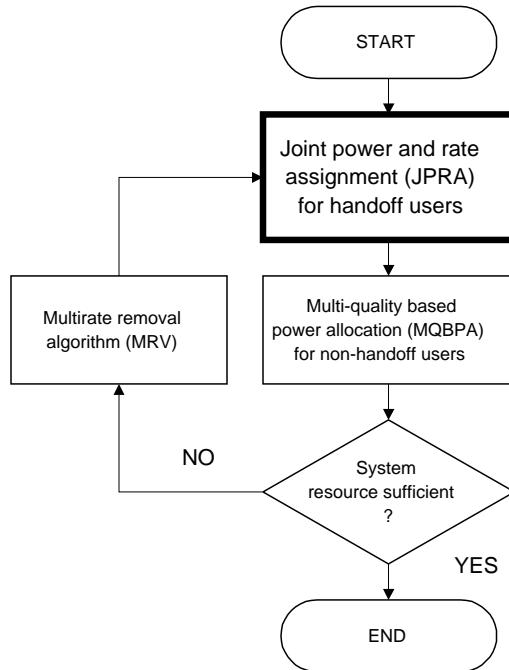


Figure 3.1: The system operation of downlink power and rate assignment

[27]. The prioritized removal algorithm in [28], based on predefined service priority, did not consider service rate tuning for users in the reverse link of a multiservice cellular system.

Compared to the conventional SSDT scheme with best-effort rate allocation, simulation results show that the service coverage of a cell and the system capacity can be improved significantly in terms of handoff forced termination probability and total system throughput. Besides, on the perspective of the users, JPRA can support excellent user satisfaction indexes for voice and data users. Moreover, it is shown that JPRA owns less sensitive than SSDT to the occurrence of the measurement errors during active set selection.

The remaining parts of this chapter are organized as follows. Section 3.2 details the flow of the system operation, and provides the design of the MQBPA and MRV algorithms. In section 3.3, the JPRA algorithm for multirate soft handoffs is proposed, including LPPA algorithm and ECRA algorithms. Also, the proof of LPPA convergence is provided. Simulation results are presented and discussed in section 3.4. Finally, section 3.5 provides conclusions of this chapter.

## 3.2 System Operation

The system operation for downlink power and rate assignments for mixed-size WCDMA cellular systems is shown in Fig. 3.1. The base station allocates power to handoff users based on the joint power and rate assignment (JPRA) algorithm firstly, then the non-handoff users based on the multi-quality balancing power allocation (MQBPA) algorithm. If the system resource is insufficient to support all the users with the allocated rates the required signal qualities, a multirate removal algorithm (MRV) is activated to release system resources by reducing users' service rate or even suspending users' transmission. The total transmission power of the base stations are adjusted based on the tuning factor obtained from MQBPA algorithm. The procedure of the radio resource allocation is done as soon as the stop criterion is satisfied.

### 3.2.1 System Model

In the multirate mixed-size WCDMA cellular system, the received interference of user  $m$  served by base station  $b$ , determined by  $I_{b,m}$ , is

$$I_{b,m} = (1 - f_\alpha)P_b^T L_{b,m} + \sum_{k \neq i} P_k^T L_{k,j} + \eta_o, \quad (3.1)$$

where  $f_\alpha$  is the orthogonality factor;  $L_{b,m}$  is the link quality from cell  $b$  to user  $m$ , which includes effects of both pathloss and shadowing;  $\eta_o$  is background noise. Note that the first and second terms in (4.1) denote the intra-cell and inter-cell interferences, respectively, in which the first term is caused by imperfect orthogonality of channel codes. Moreover, the received bit-energy-to-noise ratio ( $E_b/N_o$ ) of user  $m$  in base station  $b$  and with service rate  $r$ , denoted by  $\gamma_{b,m}(r)$ , must be larger than or equal to the required signal quality, denoted by  $\gamma^*(r)$ . For bandwidth  $W$ , the  $\gamma_{b,m}(r)$  can be expressed as

$$\gamma_{b,m}(r) = \frac{p_{b,m}(r) \cdot L_{b,m} \cdot G_P(r)}{I_{b,m}} \geq \gamma^*(r), \quad (3.2)$$

where  $p_{b,m}(r)$  is the transmission power from base station  $b$  to user  $m$ , and  $G_P(r) = W/r$  is the processing gain of service rate  $r$ . Furthermore, for a soft handoff user  $h$  with service

rate  $r$ , its received  $E_b/N_o$ ,  $\gamma_h(r)$ , can be obtained by using the maximum ratio combining (MRC) method to combine signals from all serving base stations in the active set  $D_h$ , i.e.,

$$\gamma_h(r) = \sum_{b \in D_h} \gamma_{b,h}(r). \quad (3.3)$$

### 3.2.2 The MQBPA algorithm

The multi-quality balancing power allocation (MQBPA) algorithm is to provide each non-handoff user the required signal quality of itself. Assume each service rate  $r$  has the required signal quality  $\gamma^*(r)$ ; denote  $A_b$  ( $B_b$ ) as the total transmission power for non-handoff (soft handoff) in cell  $b$  such that  $A_b + B_b = P_b^T$ . The MQBPA algorithm assigns the non-handoff user  $m$  in cell  $b$  with service rate  $r$  an amount of power,  $p_{b,m}(r)$ , by

$$p_{b,m}(r) = \frac{w_{b,m}}{\sum_{m \in \mathbf{U}_b} w_{b,m}} \cdot A_b, \quad (3.4)$$

where  $\sum_{m \in \mathbf{U}_b} p_{b,m}(r) = A_b$ ,  $\mathbf{U}_b$  is the set of non-handoff user in cell  $b$ , and  $w_{b,m}$  is defined as

$$w_{b,m} = \frac{I_{b,m}}{L_{b,m} \cdot G_P(r)} \cdot \gamma^*(r). \quad (3.5)$$

Substituting (3.4) and (3.5) into (3.2), the received signal quality of the non-handoff user  $m$  in cell  $b$  can be yielded as

$$\gamma_{b,m}(r) = \frac{A_b}{\sum_{m \in \mathbf{U}_b} w_{b,m}} \gamma^*(r). \quad (3.6)$$

The goal of the quality balancing power allocation is to make each user with service rate  $r$  have its required signal quality such that  $\gamma_{b,m}(r) \geq \gamma^*(r)$ . That is,  $A_b / \sum_{m \in \mathbf{U}_b} w_{b,m}$  should be larger or equal to 1. Otherwise, the total allocation power  $A_b$  of base station  $b$  for non-handoff users should be adjusted by tuning factor  $\psi_b$ , which is given by

$$\psi_b = \frac{\gamma^*(r)}{\gamma_{b,m}(r)}. \quad (3.7)$$

This is because, from (3.6), all non-handoff users in cell  $b$  have exactly the same value of  $\gamma_{b,m}(r) / \gamma^*(r)$ , no matter what kind of service rate  $r$  is allocated. The MQBPA algorithm is described in the following.

### [The MQBPA Algorithm]

#### Step 1: [Initialize]

- Initialize the total transmission power  $P_b^T$  of the traffic channel to the maximum total transmission power  $\tilde{P}_b$  for each cell  $b$ .
- Calculate the total allocation power  $B_b$  for handoff users in each cell  $b$  after executing JPRA algorithm.

#### Step 2: [Calculate $w_{b,m}$ ]

- Calculate  $w_{b,m}$ , based on (3.5), for user  $m$  in cell  $b$ .

#### Step 3: [Calculate allocation power]

- Calculate the total transmission power  $A_b$  for non-handoff users in each cell  $b$ , which is equal to  $(P_b^T - B_b)$ .
- Calculate allocation power  $p_{b,m}(r) = \min(p_{b,m}(r), \tilde{p}_b)$  for each non-handoff user  $m$  with service rate  $r$  in cell  $b$  based on (3.4).

#### Step 4: [Calculate tuning factor]

- Calculate tuning factor  $\psi_b$  for each cell  $b$  based on (3.6) and (3.7).

#### Step 5: [Check Stop Criterion for each cell $b$ ]

- IF any  $\psi_b \neq 1.0$  and the convergence is not met, THEN
  - Adjust total transmission power as  $P_b^T = \min(\psi_b \times A_b + B_b, \tilde{P}_b)$ .
  - Goto **Step 2**.

ELSE DONE. ■

The proposed MQBPA algorithm will converge to a desired solution if there exists an effective individual power allocation for all users and they can obtain their required signal qualities. If the solution does not exist, the MRV algorithm will be activated, which is stated in the next subsection.

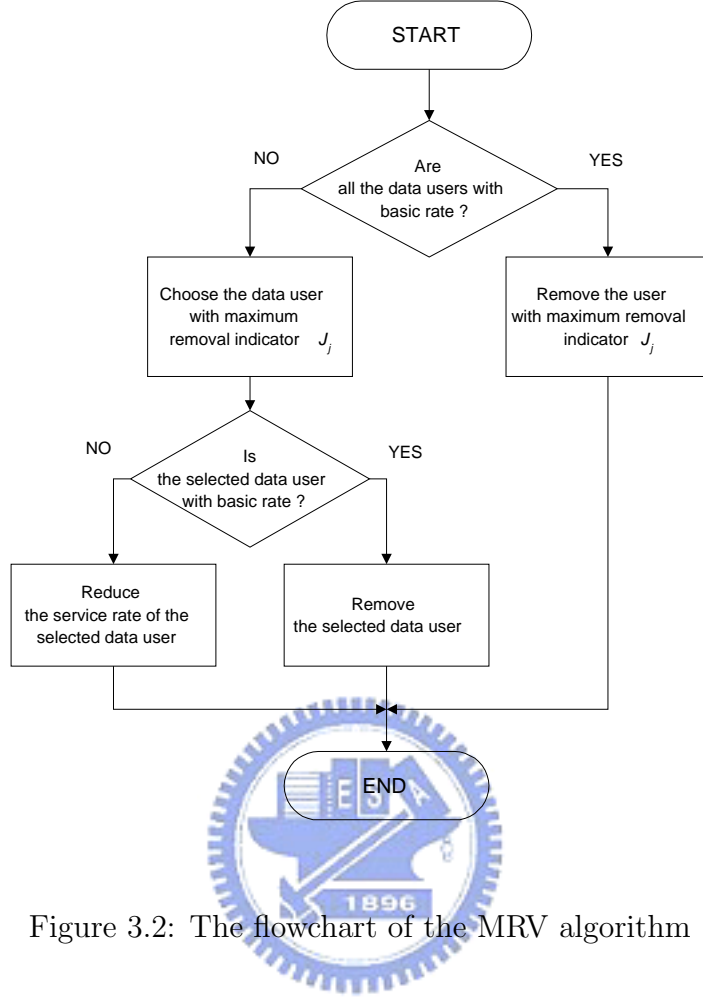


Figure 3.2: The flowchart of the MRV algorithm

### 3.2.3 The MRV algorithm

The multirate removal (MRV) algorithm defines a novel removal index for user  $m$  with service rate  $r$ , denoted by  $J_m(r)$ , as

$$J_m(r) = \frac{\gamma^*(r)}{\tilde{P}_b \cdot L_{b,m} \cdot G_P(r)}, \quad (3.8)$$

where  $\tilde{P}_b$  is pilot power of base station  $b$ , which is related to the cell size. The removal index shows how much the system resource is required to serve user  $m$ . The worse the received signal strength, the higher the service rate and the required signal quality are, and the larger the removal index value will be.

In order to provide higher priority for voice users, the proposed MRV algorithm removes system resource from data users first unless all the data users are reduced to basic service rate. The flowchart of MRV algorithm is shown in Fig. 3.2. At first, the MRV scheme will

check if all data users are with basic rate. If there exists at least one data user not with the basic rate, the MRV scheme will choose the data user with the maximum removal index. If the service rate of the selected user is with the basic rate, then the system will remove it directly, otherwise reduce its rate to the next lower service rate. If all data users are with basic rate, the system will remove the user which is with the maximum removal index.

### 3.3 The JPRA Algorithm

The JPRA algorithm is mainly composed of the link proportional power allocation (LPPA) scheme in the first phase and the evolutionary computing rate assignment (ECRA) method in the second phase.

#### 3.3.1 The LPPA Scheme

The link proportional power allocation (LPPA) scheme estimates the required transmission power for soft handoff user  $h$ ,  $p_h^*(r)$ ; then it distributes  $p_h^*(r)$  to all serving base stations in  $D_h$  under the constraint of maximum link power to each user by base station  $b \in D_h$ ,  $\tilde{p}_b$ . And  $p_{b,h}(r)$  is proportional to the link quality between the serving base station  $b$  and the soft handoff user  $h$  [8]. If the required transmission power of one link reaches to the constraint of maximum link power, LPPA will compensate the required power through other links. The LPPA scheme is an iterative method to distribute  $p_h^*(r)$  to all serving base stations so that the required signal quality can be satisfied. The design tries to accomplish power balance between cells in the CDMA cellular system with mixed-size cells. Besides, it is noteworthy that due to the constraint of the maximum link power, there exists a forced termination situation for the soft handoff because the soft handoff user cannot obtain required signal quality even though all active links are allocated with maximum link power. If the soft handoff is forced to terminate,  $p_{b,h}(r)$  of each link  $i$  in the active set  $D_h$  are reset to zero. The LPPA scheme and the proof of the convergence has detailed in the Chapter 2. The required transmission power of each active link,  $p_{b,h}(r)$ ,  $b \in D_h$ , for all soft handoff users with all kinds of service rates can be obtained through the LPPA scheme.



### 3.3.2 The ECRA Method

The ECRA method performs the rate assignment for multirate soft handoff users. It formulates the rate assignment issue as a constrained optimization problem with an objective to maximize the total throughput of multirate soft handoffs such that the total power allocated to soft handoffs in cell  $b$  would be constrained by a maximum value, denoted by  $\tilde{B}_b$ , and  $\tilde{B}_b < P_b^T$ . Note that the total power budget for each base station is limited. When there are a larger number of multirate soft handoff users being managed, the computation time would become a major concern for system operators. In this chapter an evolutionary computing algorithm [40], which is a promising intelligent technique to effectively search a global optimal solution, is adopted. Assume there is  $N_d$  soft handoff users with data services. If there are  $N_S$  kinds of data service rates, the searching complexity is  $(N_S + 1)^{N_d}$  by using exhaustive method, in which 1 means zero service rate for suspending transmission. For example, if  $N_d$  is 10 and  $N_S$  is 4, there are nearly  $10^7$  searching complexity. This is far beyond the reasonable computation time for the system's requirement. In order to reduce the complexity of exhaustive search, the evolutionary computing technique [40] is applied.

The evolutionary computing technique can represent the service rate of each user as a chromosome in a population, in which each population is the possible solution with a collection of chromosomes for all handoff data users. For  $N_S$  kinds of data service rates, each rate  $r$  is encoded into  $\lceil \log_2(N_S + 1) \rceil$  binary digits, denoted by  $x$ , and the decoder function for  $x$  is denoted by  $s(x)$ . Thus, for soft handoff data user  $h$  with service rate  $r$ , its corresponding required total transmission power is  $p_h^*(s(x_h))$ , in which the transmission power from active link  $h$  is  $p_{b,h}(s(x_h))$  by the LPPA scheme.

Assume there are  $N_v$  number of the voice users in each cell. Also,  $r_v$  is the service rate of soft handoff voice users, and  $p_{b,h}(r_v)$  is the corresponding allocation power from active link  $b$  to soft handoff user  $h$ . The ECRA method is to find an optimal rate assignment vector (decision vector) of  $N_d$  soft handoffs,  $\mathbf{x}^* = [x_1^*, x_2^*, \dots, x_{N_d}^*]$ , for maximizing the objective function  $O(\mathbf{x})$ , which is defined to be the total throughput of soft handoff data users, given

by

$$O(\mathbf{x}) = \max \left\{ \sum_{h=1}^{N_d} s(x_h) \right\}, \quad (3.9)$$

subject to constraints:

$$\sum_{h=1}^{N_v} p_{b,h}(r_v) + \sum_{h=1}^{N_d} p_{b,h}(x_h) \leq \tilde{B}_b, \forall b, \text{ where } 1 \leq b \leq N_b, \quad (3.10)$$

where  $N_b$  is the number of base stations in the system. And

$$\gamma_h(s(x_h)) \geq \gamma^*(s(x_h)), \forall h. \quad (3.11)$$

Because of these constraints, some decision vectors may be out of the feasible domain. A violation function, which is proportional to the square of violation, is used to rank violated constraints of the decision vector [40]. The values of the constraint violation function indicate how far the solutions deviate from the feasible region. This constrained violation function is defined as

$$X(\mathbf{x}) = \frac{\sum_{b=1}^{N_b} Z_b [B_b(\mathbf{x})]^2 + \sum_{h=1}^{N_d} H_h [\gamma_h(s(x_h))]^2}{2N_b + 2N_d}, \quad (3.12)$$

where  $Z_b$ , and  $H_h$  are the Heavieside operators [40], i.e.  $Z_b(\cdot) = 1$  whenever the constraint in (3.10) is violated, and  $Z_b(\cdot) = 0$  otherwise. The evolutionary computing method is a more advanced genetic algorithm, which uses stochastic searches through simulating natural genetic processes of living organisms, including selection, mutation, and crossover, to solve difficult optimization problem in real-world. Based on the formulation of constrained optimization problem, the optimal decision vector,  $\mathbf{x}^*$ , can be found by maximizing the objective function,  $O(\mathbf{x})$ . The ECRA method is described in the following. Noticeably, the allocation power for the soft handoffs are corresponding to the ones obtained by the LPPA scheme.

### [The ECRA method]

#### Step 1: [Initialize]

- Set crossover rate  $p_c$ , mutation rate  $p_u$ , and maximum number of generations  $T$ .
- Initialize generation  $t = 1$ , optimal objective value  $O^* = 0$ , and optimal decision vector  $\mathbf{x}^*$  to be a zero pattern.

- Generate  $K_P$  populations that are randomly selected decision vectors  $\mathbf{x}_k = [x_1^k, \dots, x_{N_d}^k]$ ,  $1 \leq k \leq K_P$ .

**Step 2:** [Constraint tournament selection]

- Choose  $K_P$  tournament pairs randomly among all populations.
- Calculate the violation function  $X(\mathbf{x})$  in (3.12) for each competitive pair, and determine one winner, which owns a smaller value of the violation function.
- Replace each population  $\mathbf{x}_k$  with the winner population of each competitive pair, thus form  $K_P$  new populations.

**Step 3:** [Variable point crossover]

- Choose  $K_P/2$  crossover pairs from adjacent population  $\mathbf{x}_k$  and  $\mathbf{x}_{k+1}$ , where  $k$  is odd.
- Generate a random number  $c$  in  $[0, 1]$  for each chromosome in each crossover pair.
- For the chromosome with  $c < p_c$ , generate the crossover point randomly in  $[1, \lfloor \log_2(N_S + 1) \rfloor]$ , and make the crossover operation within this crossover chromosome.

**Step 4:** [Uniform mutation]

- Generate a random number  $u$  in  $[0, 1]$  for every bit in each population, and mutate bits whenever  $u < p_u$ .

**Step 5:** [Calculate the objective function of resulting new population]

- Calculate the violation function value for each population.
- Find feasible population  $\{\mathbf{x}_f\}$  with zero violation among  $K_P$  populations.
- IF  $\{\mathbf{x}_f\}$  is not empty set, THEN Calculate objective function value  $\{O(\mathbf{x}_f)\}$ .
  - IF  $\max\{O(\mathbf{x}_f)\} > O^*$ , THEN
    - Set  $O^* = \max\{O(\mathbf{x}_f)\}$  and optimal decision vector  $\mathbf{x}^* = \arg_{\mathbf{x}_f} \max\{O(\mathbf{x}_f)\}$ .
  - ELSE Goto **Step 6**.
- ELSE Goto **Step 6**.

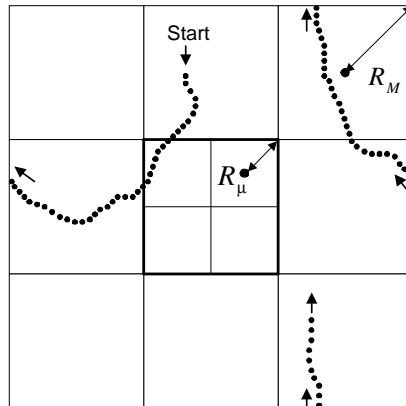


Figure 3.3: The mixed-size cellular model ( $\rho = 1/2$ ) with an example of mobility trajectory.

**Step 6:** [Check the stop criterion]

- IF  $t < T$ , THEN Set  $t = t + 1$ , and Goto **Step 2**.  
ELSE DONE. ■

## 3.4 Simulation Results and Discussion

### 3.4.1 Simulation Model

Consider a mixed-size cellular system with 12 wrap-around squared cells, including 4 microcells in the central congested region and 8 macrocells in the neighboring cells as shown in Fig. 3.3. The radii of macrocell and microcell are 1 km ( $R_M$ ) and 0.5 km ( $R_\mu$ ), respectively, thus the cell radius ratio ( $\rho$ ) between microcell and macrocell,  $R_\mu/R_M$ , is 0.5. Moreover, the antenna heights of macrocell and microcell are 20 meters and 10 meters, respectively, and the antenna height of mobile stations is 1.5 meters. For the propagation channel model, only pathloss and long-term shadowing are taken into account, in which two slope pathloss exponents are 2 dB and 4 dB, and standard deviations of two slope shadowing are 4 dB and 8 dB [43]. Furthermore, assume the bandwidth  $W$  is 4.096 MHz, and each cell utilizes the same frequency so the emitted power of different base stations interferes each other, in which the intra-cell interferences are caused by imperfect orthogonality of channel codes and the orthogonality factor is 0.5 in the simulation.

For the power budget design, the maximum transmission power,  $\tilde{P}_b$ , of the traffic channel for macrocell (microcell)  $b$  is 20 (10) watt, and the maximum link power of the macrocell (microcell) is 1 (0.5) watt. Each user determines its active set members based on received signal strength by the soft handoff algorithm which is based on the differences of the received signal strength between users and cells,  $P_b^I L_{b,m} - P_k^I L_{k,m} \leq \eta, b \neq k$ , where  $\eta$  is the soft handoff threshold and  $P_b^I$  is the transmission power of pilot signal for base station  $b$ , which is related to the cell size. Here,  $\eta$  is 2 dB and the maximum active set size is 3. In the simulations, two cases without and with measurement errors during the active set selection are concerned. For the model of measurement errors, the received signal strength of each user is added one Gaussian distributed random variable with zero mean and 1.5 dB standard deviation.

Assume users are uniformly distributed in each cell, and each user moves in a constant speed 36 km/hr. The change probability of moving direction for users is 0.2 and the update of the direction angle is among  $\pm 45$  degree [51]. During the mobility, the correlated shadowing effect is based on Gudmundson model [52], in which the normalized autocorrelation function between two correlated points, for user  $m$  in cell  $b$ , with distance  $d_{b,m}$  can be described accurately by an exponential function

$$\exp \left\{ -\frac{|d_{b,m}|}{d_{corr}} \ln 2 \right\}, \quad (3.13)$$

where  $d_{corr}$  is the decorrelation length equal to 20 meters in a vehicular environment. Fig. 3.3 shows an example of mobility trajectory. Assume the shadowing factor will not be changed when the moving distance is less than 4 meters and there are 5 averaging windows in each snapshot. For 36km/hr mobility speed, the correlated shadowing duration is 400 msec. Assume the power allocation duration is equal to one frame time (10 msec), the allowable iteration is 40 times. These performance measurements are averaging from 2000 independent instances of user location and shadowing, and each snapshot has 5 times correlated instances.

For parameters of the ECRA method in the JPRA algorithm, the total power constraint for soft handoffs,  $\tilde{B}_b$ , is assumed to be 0.3 times the maximum transmission power of each cell  $b$  [9] so as to confine maximum power resource for soft handoffs. On the contrary, non-

Table 3.1: SERVICE CLASSES

Service	$r$ (kbps)	$\gamma^*(r)$ (dB)	encoded $x$
Voice	12.2	5	
Data	0	N/A	(100)
Data	16	4	(001), (101)
Data	32	3	(011), (111)
Data	64	2	(010), (110)
Data	144	1.5	(000)

handoff still could share the power resource if all soft handoff users do not use up allowable power resource. The supportable service classes and the corresponding codes for ECRA method are listed in Table 3.1. The population size ( $K_P$ ) is 100, the crossover rate ( $p_c$ ) is 0.5, the mutation rate ( $p_m$ ) is 0.05, and the stop generation ( $T$ ) is 20. The computing time of ECRA method is much more than that of the exhaustive searching method. The ECRA method will search whole 2000 searching patterns to find optimal rate sets for multirate soft handoffs in the very first iteration. Since the system gradually approaches to convergent point, the optimal rate sets need less searching patterns afterward.

In the simulations, each cell has the same amount of voice and data users, thus the central four microcells form a highly traffic congested region. In each cell, assume the number of voice users is 30, and that of data users are ranging from 3 to 12. In simulations, there are two essential performance measures investigated. One is the handoff forced termination probability, which indicates the service continuity for soft handoffs and the effectiveness of the cell's service coverage. It is evaluated by counting the proportion of soft handoff users that are terminated by the system due to insufficient power resource for soft handoffs temporarily. The other is the total throughput of the system, which is obtained by summing all allocated transmission rates of users, which represents the system capacity. Because of limited power resources of one base station in the downlink, under various non-uniform traffic load situations, there exists the tradeoff between the cell's service coverage and the system capacity using different joint power and rate allocation schemes.

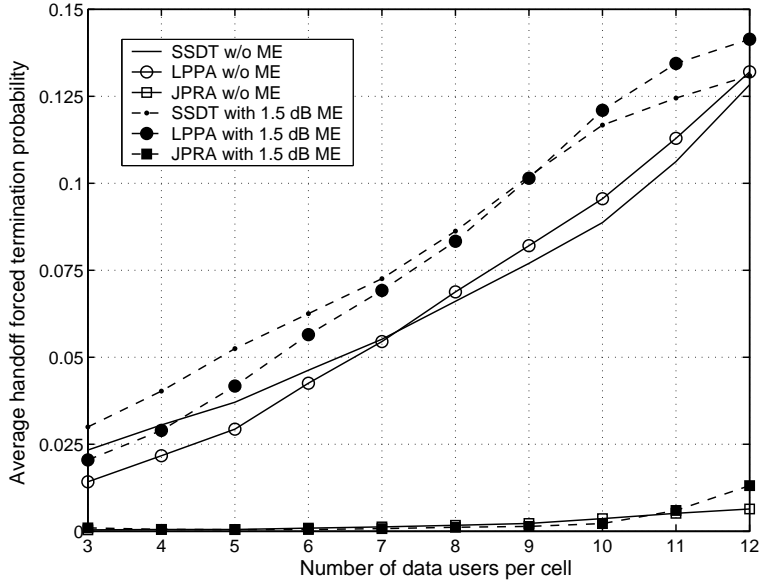


Figure 3.4: Averaged handoff forced termination probability without measurement errors (ME) and with 1.5 dB measurement errors (ME).

### 3.4.2 Results and Discussion

The proposed JPRA algorithm is compared with the SSDT [14] and the LPPA schemes with the best-effort rate allocation. The major idea of the conventional SSDT algorithm is to dynamically choose one base station with the best link quality in the active set for transmission in order to mitigate interference caused by multiple-site transmission. However, because of the maximum link power constraint, SSDT may not be able to offer enough required power for soft handoff users with high transmission rates. Also, under the constraint of maximum link power, best-effort rate allocation is to assign handoff users maximum allowable transmission rate which exists feasible solutions of power allocation to satisfy users' required quality of services. In order to achieve fair comparison for all schemes, the total power constraint of soft handoffs is confined to 0.3 times maximum transmission power of each base station. In the following, we take best-effort rate allocation as the benchmark for comparisons, and denote SSDT with best-effort rate allocation and LPPA with best-effort rate allocation by SSDT and LPPA, respectively

Figure 3.4 shows average handoff forced termination probability under different traffic load situations. It can be seen that, when the traffic load is light, the LPPA scheme improves

over the SSDT scheme. However, when there are more data users served in the system, the handoff forced termination probability of the LPPA scheme is worse than that of the SSDT scheme. The reason is that higher interferences are induced by the multi-site transmission mechanism than by the single-site transmission mechanism for handoffs. The results mean that power balance and power saving are important characteristics for the radio resource management of the handoff mechanisms, and both are impact factors on the system performance under different traffic load situations. Furthermore, it is found that the handoff forced termination probability of JPRA is superior to that of the SSDT schemes by over 300%. Besides, JPRA improves LPPA by around 200%, which can be inferred that the gain comes from the rate allocation by evolutionary computation method. The allowable transmission rates are highly coupled to the feasible solutions of power allocation, which can be formulated as a constraint optimization problem. The ECRA method is thus designed to find an optimal rate allocation for multirate soft handoff users, in which the goal is to accomplish maximum throughput of all soft handoff users such that the total power constraints of soft handoffs for all base stations should be satisfied. Besides, because the rate allocation of each soft handoff user directly affects the management of power resource in at least two base stations, an optimal rate allocation for soft handoff users can further enhance the effect of power balance among cells.

Moreover, consider the case with measurement errors during the active set selection, it is observed that measurement errors incur higher handoff forced termination probabilities for all schemes because base stations waste more power on multirate handoff users. The improvement of JPRA is by around 500% over SSDT. Besides, because of link power constraint and the single-site transmission mechanism, SSDT is more sensitive than JPRA and LPPA to the occurrences of measurement errors. In this case, it is found that the effects of measurement errors can be relieved by the multi-site transmission mechanisms and their power balance characteristic. With the superb power balance characteristic, not only can JPRA provides better service continuity performance but also possess the capability of the resistance to measurement errors. It is particularly noteworthy that the performance of the



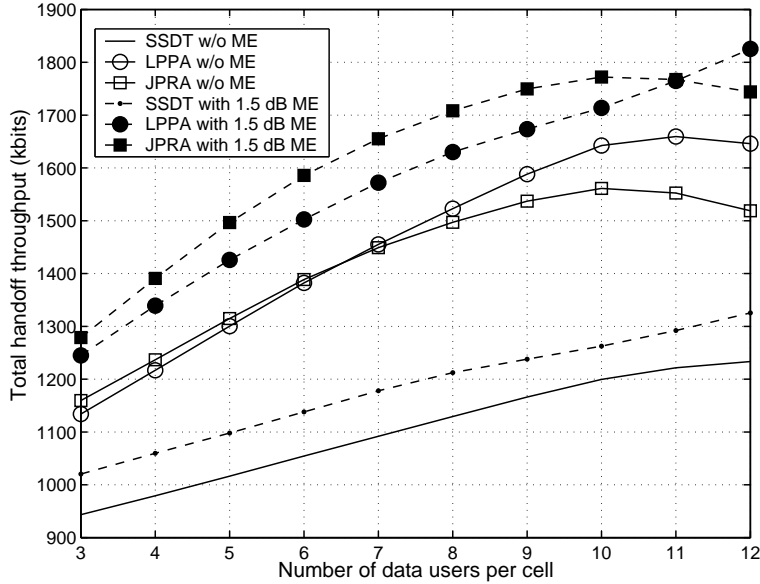


Figure 3.5: Total handoff throughput versus the number of data users per cell without measurement errors (ME) and with 1.5 dB measurement errors (ME).

handoff forced termination probability can also be regarded as the performance index of the cell's service coverage, in which smaller handoff forced termination probability means better cell coverage. Thus, Fig. 3.4 also shows that JPRA achieves better cell's service coverage than SSDT and LPPA.

Based on the viewpoint of the capacity, Fig. 3.5 shows the results of the total handoff throughput versus different number of data users. It is found that both LPPA and JPRA have higher throughput than SSDT, because of the multi-site transmission mechanism. Besides, due to total power constraint of soft handoffs, there exists the tradeoff between coverage and capacity for the LPPA and JPRA schemes. From Fig. 3.4 and Fig. 3.5, the results show that the ECRA method in the JPRA reduces average transmission rate of the multirate soft handoffs so as to accomplish better cell coverage while LPPA leads to more terminated handoff users but achieves higher handoff throughput than JPRA. The similar results could be observed for the case of measurement errors. Since more power is wasted by measurement errors, higher handoff forced termination probability makes more power left for the survived handoff users to transmit with higher average transmission rates. In addition, we can see that the ECRA method in JPRA plays an important role to reduce performance degradation

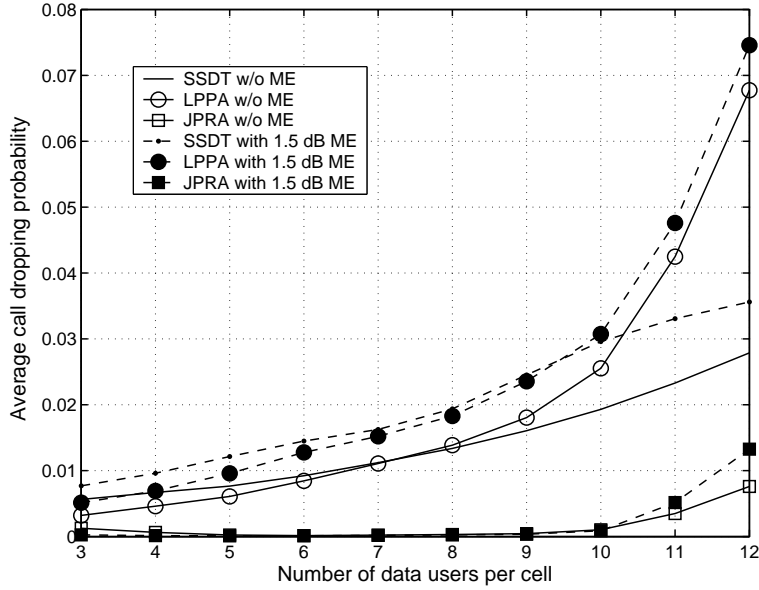


Figure 3.6: The average call dropping probability versus the number of data users per cell without measurement errors (ME) and with 1.5 dB measurement errors (ME).

by measurement errors. This is because the ECRA method allocates optimal transmission rates for multirate soft handoffs to further balance power loads among cells. Therefore, JPRA successfully enhances cell's service coverage and handoff throughput.

In the following, we show that joint power and rate allocation strategies for multirate soft handoff have significant impacts on system performance in terms of average total throughput and average call dropping probability. Fig. 3.6 shows that JPRA can improve the average call dropping probability of all users by 71% and 200% without and with measurement errors compared to the SSDT scheme, in which the call dropping occurs when there is no feasible solution of power allocation to support users with their required service qualities for a period of time. From the preceding results of the handoff performance, the superiority of JPRA over SSDT is mainly because JPRA owns the power balance characteristic resulting from LPPA and ECRA methods. Since proper power balance can prevent one base station from wasting too much power resources to serve multirate soft handoffs, the power resource can be preserved to serve non-handoff users with higher transmission rates by optimally managing radio resource of multirate soft handoffs.

Fig. 3.7 shows the system performance of the total throughput gain referred to the SSDT

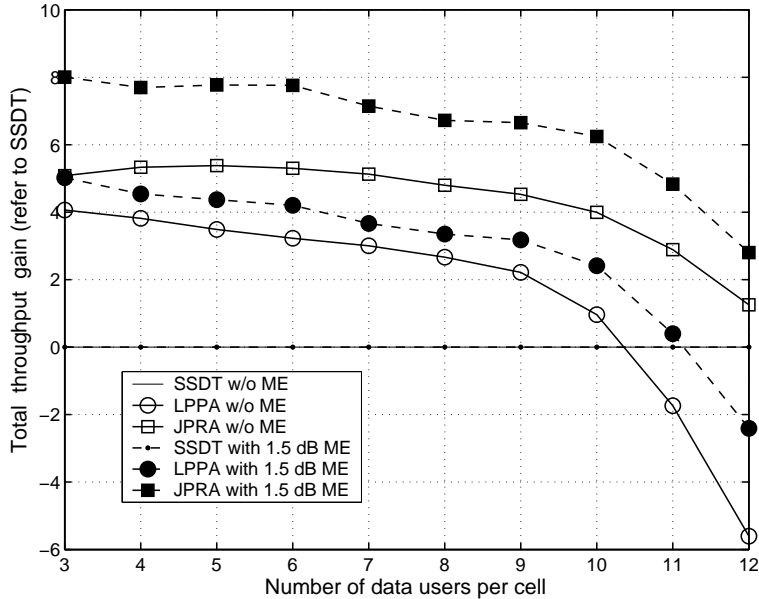


Figure 3.7: The total throughput gain, which is referred to SSDT, versus the number of data users per cell without measurement errors (ME) and with 1.5 dB measurement errors (ME).

scheme. We can see that JPRA can enhance the average total throughput than SSDT by 5% and 8% in the case of measurement error free and 1.5 dB measurement errors, respectively. From above results of system performance, it is found that JPRA makes great improvements of cell's service coverage and system capacity because it can optimally allocate radio resource of soft handoffs.

In the meantime, on the perspective of the user satisfaction, voice and data users should have different service requirements. Denote the call dropping probabilities of voice and data users as  $P_v$  and  $P_d$ , respectively. Also, the summation of the allocated and required transmission rates of all data users are represented as  $R_d$  and  $R_d^*$ , respectively. We then define two satisfaction indexes for voice and data users, denoted by  $USI_v$  and  $USI_d$ , respectively, as

$$\begin{cases} USI_v = (P_v^* - P_v)/P_v^*, \\ USI_d = \kappa_d \times R_d/R_d^* + (1 - \kappa_d) \times (P_d^* - P_d)/P_d^*, \end{cases} \quad (3.14)$$

where  $\kappa_d$  and  $1 - \kappa_d$  are the weighting factors for the total throughput and call dropping probability of data users, respectively. Here, both  $P_v^*$  and  $P_d^*$  are set as 0.05. For voice users, because of constant transmission rate, the satisfaction comes from call dropping probability.

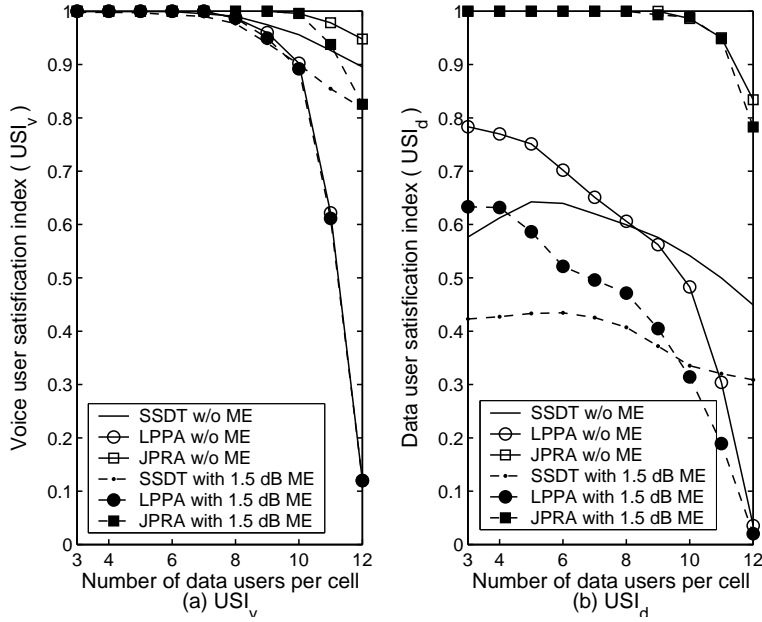


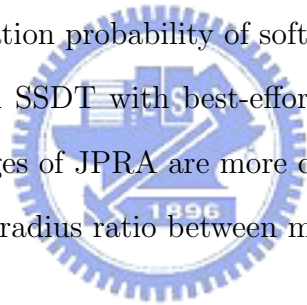
Figure 3.8: The user satisfaction index (USI) versus the number of data users per cell for (a) USI of voice users ( $USI_v$ ) and (b) USI of data users ( $USI_d$ ), respectively.

Also, for data users, assume  $\kappa_d$  is 0.7 because data users usually are satisfied with higher transmission rate and can tolerate longer transmission delay because of call dropping events and retransmission mechanisms. In Fig. 3.8, it is shown that the proposed JPRA scheme can provide outstanding user satisfaction indexes for voice and data users even when there exists measurement errors during active set selection.

For the mixed-size cellular system with mix-sized cells, microcells are normally congested cells and with stringent power budget of link power and maximum transmission power. It is useful to adopt multi-site transmission mechanisms for soft handoffs to balance some power loads into neighboring cells. Besides, because the constraint of maximum link power is tight for microcells, the single-site handoff mechanism, like SSDT, may fail to support soft handoff user enough required power for high rate services by the best link to microcells. Therefore, a reasonable inference is that when the cell radius ratio between macrocell and microcell gets smaller ( $\rho < 1/2$ ), the larger gain could be obtained from the JPRA algorithm because of the outstanding power balance characteristic.

### 3.5 *Conclusions*

In this Chapter, a joint power and rate assignment (JPRA) algorithm is proposed to deal with multirate soft handoffs in WCDMA mixed-size cellular systems. It contains link proportional power allocation (LPPA) scheme and the evolutionary computing rate assignment (ECRA) method. Compared to SSDT and LPPA schemes with best-effort based rate assignments, simulation results show that JPRA accomplishes superior power balance among cells so that the JPRA algorithm can improve the forced termination probability of soft handoffs by over 300% and the total throughput by around 5.0%. It means JPRA can achieve better cell's service coverage and higher system capacity. Also, JPRA can offer great user satisfaction for voice and data users. Furthermore, JPRA is less sensitive to the measurement error for active set selection than SSDT with best-effort rate allocation. In such a situation, JPRA can obtain less the forced termination probability of soft handoffs by 500% and higher total throughput by around 8.0% than SSDT with best-effort rate allocation. It is noteworthy that the aforementioned advantages of JPRA are more conspicuous in WCDMA mixed-size cellular systems with smaller cell radius ratio between microcell and macrocells.



## Chapter 4

# Dynamic Cell Configuration with Radio Resource Management in Next-Generation Situation-Aware Mobile Networks

---

*In next-generation CDMA networks, due to random user mobility and time-varying multimedia traffic activity, the system design of coverage and capacity is a challenging issue. To utilize radio resources efficiently, it is crucial for future cellular networks to be aware of the system situation and configures cell coverage and capacity dynamically to balance traffic loads over all cells. Most of previous study concentrates on pilot power allocation for dynamic cell configuration. In this chapter, we show that pilot power allocation and other radio resource management algorithms are highly coupled. Dynamically adjusting pilot power alone while not changing other radio resource management algorithms can result in performance degradation. We then propose a novel dynamic cell configuration scheme in multimedia CDMA networks via reinforcement-learning, which takes into account pilot, soft handoff, and maximum link power allocations as well as call admission control mechanisms. Simulation results demonstrate the effectiveness of the proposed scheme in situation-aware CDMA networks.*

## 4.1 Introduction

Soft handover is one of the most important merits of In recent years, wireless mobile communication systems have experienced tremendous growth. To utilize the radio spectrum efficiently, the cellular architecture is used in wireless mobile networks. In such networks, the cell coverage and capacity of a network are planned in the pre-deployment stage according to pre-defined traffic patterns. In practice, however, traffic patterns are changing with time due to random user mobility and versatile service activity. Therefore, the planned cellular mobile networks may not utilize radio resources optimally under the varying traffic patterns. In next-generation code division multiple access (CDMA) cellular networks, this problem becomes more severe especially for the downlink (from base station to mobile station) capacity-limited scenario because of the necessity for abundance downlink multimedia traffic and the interdependence of coverage and capacity in CDMA systems [1], [4], [29], [53].

In response to the variation of traffic patterns, tradeoffs between coverage and capacity should be considered carefully in CDMA cellular systems [1], [29], [30], [54]. For example, to guarantee the coverage of a cell, more power is used for mobile users near cell boundaries under power control. However, this will generate higher inter-cell interference to other cells, which reduces the system capacity significantly. Moreover, power control may not be effective if a large traffic variation occurs [1], [29], [30], [54], [55]. It is found in [54] that uniform network layout with equal-sized cells is optimal for uniform distributed users, and the capacity degrades significantly if traffic loads are not balanced over all cells. Therefore, to utilize radio resources efficiently, it is crucial for next-generation CDMA cellular networks to be aware of system situations and configures cell coverage and capacity dynamically to balance traffic loads over all cells [29], [30].

Several schemes have recently been proposed for dynamic cell configuration in cellular networks [31]–[37]. In [31], the optimization of pilot power and the planning procedures of downlink capacity and cell coverage were proposed. In [32], authors used analytical methods to study the competitive characteristics of network coverage and capacity in a simple network. Only one class of service was considered in [31] and [32], and it may be difficult to extend

these schemes to a network with multi-classes of services. There are also some heuristic-rule-based techniques in the literature for dynamic pilot control to balance downlink traffic load while assuring service coverage [33]–[35]. However, these schemes may cause some “coverage failure regions” between cells where all the received pilot signals are too weak to serve a mobile station [36], [37]. Moreover, the common shortcomings of the previous work [31]–[37] are that only pilot power is adjusted and other radio resource management schemes are not taken into account in the time-varying environment.

In fact, pilot power allocation and other radio resource management schemes, such as soft handoff power and maximum link power allocations as well as call admission control mechanisms, are highly coupled in CDMA systems. For example, it was showed that signal quality degradation can be prevented by configuring cell areas adaptively and setting transmission power levels appropriately [4]. Also, authors in [38] and [39] showed that soft handoff has significant impacts on the system capacity and cell coverage. Moreover, we have presented an effective link proportional power allocation (LPPA) for soft handoffs in chapter 2, 3 and [8], which can enhance system capacity in mixed-size cellular systems compared to the conventional site-selection diversity transmission (SSDT) scheme [14].

In this chapter, we show that dynamically adjusting pilot power alone while not changing other radio resource management algorithms accordingly can result in performance degradation. We then propose a novel reinforcement-learning approach to solve the dynamic cell configuration problem in multimedia mobile CDMA networks. The novelties of the proposed scheme are as follows.

1. The proposed scheme takes into account pilot, soft handoff, and maximum link power allocations as well as call admission control mechanisms, enabling it to dynamically adapt to changes in traffic situations and improve the system performance [56].
2. It can efficiently tackle problems with large state spaces and action sets by applying reinforcement-learning algorithms [57]. Since there will be several service classes in future CDMA networks, the state spaces and action sets are very large in the dynamic cell configuration problem. It was shown that reinforcement-learning algorithms make



it feasible for the first time to solve optimization problems for large-scale realistic networks, which were previously deemed intractable [58].

3. The proposed scheme can be implemented in a distributed manner in each base station, which monitors the variation of its power load that can implicitly reveal the load information about all other cells in the whole network. Therefore, the coverage and capacity can be coordinated between cells accordingly. The system can thus be fully self-organized for dynamic cell configuration.
4. The distributed algorithm can avoid overloaded signaling between base stations and radio network controllers, which is necessary for the centralized algorithm, in the systems with dynamic cell configuration. Besides, the modelling of the centralized algorithm needs volumes of system states, which results in high computation complexity to obtain an optimal solution that may be outdated. Therefore, the efficiency of the distributed algorithm makes the system be adaptive to the situations with greatly traffic variation.
5. It does not require a priori knowledge of the state transition probabilities associated with the cellular networks, which are very difficult to estimate in practice due to the different propagation environment, diverse multimedia services, and random user mobility. Therefore, the assumptions behind the underlying system model can be made more realistic than those in previous schemes.

We compare our scheme with the fixed scheme and the scheme in which only pilot power is adjusted dynamically but other radio resource management algorithms are not changed accordingly. Extensive simulation results show that the proposed dynamic scheme outperforms the others by increasing the total throughput, decreasing the frame error probabilities, blocking probability, and handoff forced termination probability with the price of increasing the size of active set slightly.

The rest parts of this chapter are arranged as follows. In section 4.2, the issues of dynamic radio resource management are discussed. Also, the preliminary simulation results are presented. In section 4.3, the system model and the problem of dynamic cell configuration

are described. In section 4.4, the proposed dynamic cell configuration scheme is presented. Simulation results are presented and discussed in section 4.5. Finally, section 4.6 concludes this chapter.

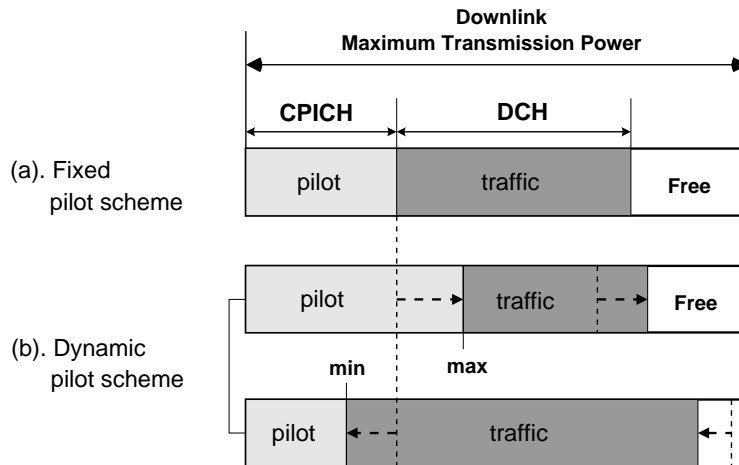


Figure 4.1: Diagram of total power allocation of the base station in downlink CDMA systems with (a) fixed pilot and (b) dynamic pilot schemes.

## 4.2 Dynamic Cell Configuration (DCC) Issues

Several mechanisms of radio resource management have effects on the system capacity and cell coverage of CDMA networks. In this section, we discuss the effects of pilot and soft handoff power allocation schemes. Some preliminary simulation results are also presented.

### 4.2.1 Effects of Pilot Power Allocation Schemes

Since each base station has finite power resource, the pilot channel and traffic channels have to share the total power resource. This explains the interdependence of coverage and capacity in CDMA systems. Pilot power allocation can be either fixed or dynamic. In fixed pilot power allocation scheme, which is used by current CDMA systems, about 10-15% of the total power is allocated to the common pilot channel and is not changed after the deployment of a cellular network, as shown in Fig. 4.1(a). Fig. 4.1(b) shows the dynamic pilot power allocation scheme. With the maximum and minimum constraints, the pilot power can be

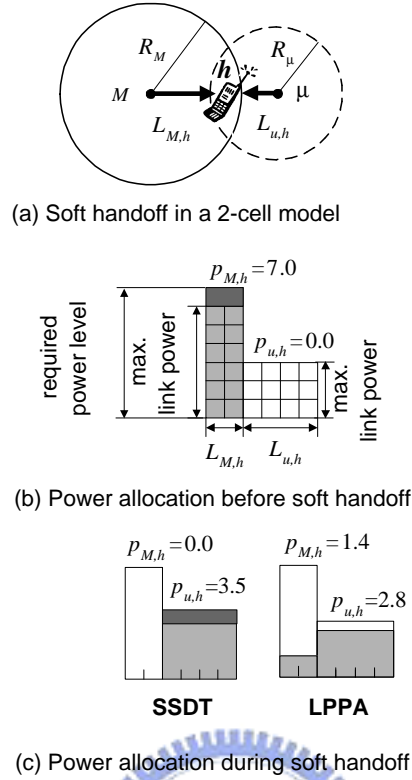


Figure 4.2: Diagram of the soft handoff power allocation in downlink CDMA systems with (a) soft handoff in two mixed-size cell model, (b) before soft handoff, and (c) during soft handoff.

adjusted between them based on various traffic situations. When the required traffic is low, the pilot power can be increased to extend cell coverage so as to accommodate more users around the adjacent cells. On the other hand, when the required traffic power is too high to have risks of degrading system performance, the pilot power can be decreased to shrink cell coverage.

#### 4.2.2 Effects of Soft Handoff Power Allocation Schemes

In this subsection, we illustrate the effects of soft handoff power allocation on system capacity and cell coverage by a simple example. Consider a handoff user  $h$  located around the boundaries of cell  $M$  and cell  $\mu$ , which have different sizes ( $R_M \neq R_\mu$ ), as shown in Fig. 4.2(a). The power allocated to the user before soft handoff is shown in Fig. 4.2(b). Fig. 4.2(c) shows the allocated power during soft handoff in the SSdT and LPPA schemes. The height of each block is the constraint of maximum link power for each cell, and the width is

the link quality,  $L_{M,h}$  ( $L_{\mu,h}$ ), from cell  $M$  ( $\mu$ ) to the mobile station  $h$ . Assume  $L_{\mu,h} = 2L_{M,h}$  in the example. Moreover, let  $p_{M,h}$  ( $p_{\mu,h}$ ) denote the allocated link power from cell  $M$  ( $\mu$ ). By multiplying the allocated link power with the link quality, we can obtain the received signal quality of the user, which is the area of the shadowed blocks in Fig. 2. Assume that the received signal quality is 14 ( $7 \times 2$ ) before soft handoff. During soft handoff, the SSDT scheme, defined in 3GPP [14], [46], allocates power level 3.5 units to the user to guarantee the same requested signal quality ( $3.5 \times 4 = 14$ ). Because power level 3.5 units exceeds the constraint of maximum link power 3.0 units, the user cannot be served. Consequently, the user is dropped and the coverage of cell  $\mu$  is shrunk. In the LPPA scheme of Chapter 2, 3 and [8], transmission power is allocated to all links in the active set distributively, in which the power level is proportional to the link quality. In Fig. 4.2(c),  $p_{M,h} = 1.4$  units and  $p_{\mu,h} = 2.8$  units. The received signal quality in LPPA is 14 ( $1.4 \times 2 + 2.8 \times 4$ ). Therefore, the allocated power in each link does not exceed the constraint of maximum link power. LPPA can still obtain the same requested signal quality. Thus, LPPA achieves larger service coverage and capacity than SSDT. This example can explain the possible impacts of soft handoff power allocation schemes on cell coverage and capacity.

### 4.2.3 Simulation Examples of Adjusting Pilot Power Only

The above discussions reveal that other radio resource management algorithms besides pilot power allocation have great impacts on dynamic cell configuration. In this subsection, we show by simulation examples that pilot power allocation and other radio resource management algorithms are highly coupled. Dynamically adjusting pilot power alone while not changing other radio resource management algorithms accordingly can result in performance degradation. Detailed simulation environment and parameters will be given in Section 4.5. Fig. 4.3 shows the system throughput with different pilot power levels are considered under uniform ( $\rho = 1$ ) and (b) non-uniform ( $\rho = 4$ ) cell load cases for both SSDT and LPPA soft handoff schemes. For the non-uniform cell load cases, the traffic load in the hotspot cell is 4 times that of the surrounding cells. Note that only pilot power is adjusted, and all other radio resource management algorithms are not changed accordingly in the simulations. In

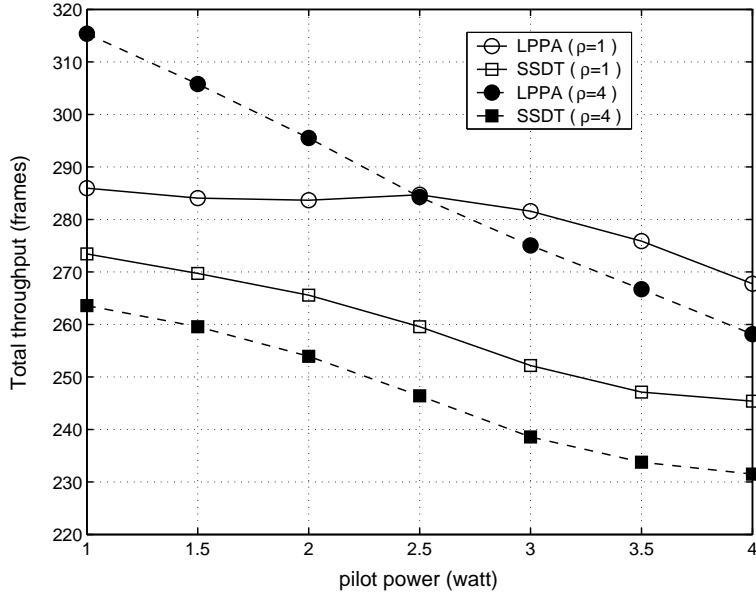


Figure 4.3: Capacity results of the fixed pilot power design by applying SSDT and LPPA schemes under cases with (a) uniform ( $\rho = 1$ ) and (b) non-uniform ( $\rho = 4$ ) cell loads.

the simulations, 1 watt power is allocated to the pilot channel in the fixed pilot power allocation scheme, and all other radio resource management algorithms are optimized according to this pilot power setting and pre-defined link budget design. We further adjust the pilot power level manually but not changing all other radio resource management algorithms.

We can see from Fig. 4.3 that the system throughput degrades whenever a pilot power other than 1 watt (used in the fixed scheme) is used in dynamic pilot power allocation schemes. This result is not surprising, because pilot power can also cause interference to users. We can observe that the larger the pilot power, the larger the interference, and the lower the throughput. Another reason is that the call admission control criterion and the constraint of maximum link power remain the same when the pilot power changes cell coverage. For example, when new or handoff calls issue requests to cells with light (heavy) traffic load, the tight (loose) criteria of CAC may result in new call blockings or handoff forced terminations. The uncoordinated design of pilot power and other radio resource management strategies can degrade the system performance severely. It is also observed in Fig. 4.3 that soft handoff power allocation and pilot power allocation are highly coupled, both of which have effects on the system throughput. LPPA has larger throughput than

SSDT with different pilot power and traffic load distributions. The throughput difference between SSDT and LPPA is larger when the traffic load is non-uniformly distributed ( $\rho = 4$ ).

#### 4.2.4 Our Approach

This chapter proposes a novel dynamic cell configuration in next-generation CDMA networks via reinforcement-learning technique, which takes into account pilot, soft handoff power and maximum link power allocations as well as call admission control mechanisms [56]. Fig. 4.4 shows the system block diagram of our proposed approach. Each base station is equipped with our proposed scheme. A base station adjusts its pilot power periodically to adapt to the variations of system situations through the dynamic pilot power controller. Based on the determined pilot power level, the maximum link power constraint and call admission control criterion are adjusted accordingly. Then, the traffic channel power allocator adjusts its constraint of maximum link power that is obtained from the maximum link power estimator. After applying all updates for radio resource management, the reinforcement signal is input to the dynamic pilot power controller to aid its decision for the next pilot power level. The detailed design will be illustrated in the following sections.

### 4.3 System Model

In this section, we describe the signal model and the link budget model in CDMA systems. Then, we introduce the problem of dynamic cell configuration.

#### 4.3.1 Signal Model

Assume the total allocated power of a base station  $b$  is  $P_b$ , including pilot channel power  $P_b^I$  and traffic channel power  $P_b^T$ , where  $P_b^T$  is smaller than the base station's maximum transmission power  $\tilde{P}_b$ . Furthermore, for the pilot power of base station  $b$ ,  $P_b^I = f_b \times \tilde{P}_b$ , where  $f_b$  is the fraction of the pilot power to base station  $b$ 's maximum transmission power, in which  $f_b \in [f_{min}, f_{max}]$ ;  $f_{min}$  and  $f_{max}$  are the minimum and maximum constraints of the pilot fraction. On the other hand, for the traffic channel power of base station  $b$ , assume  $\phi_m$  is the allocated power ratio of the traffic channel power for mobile station  $m$ , so the allocated

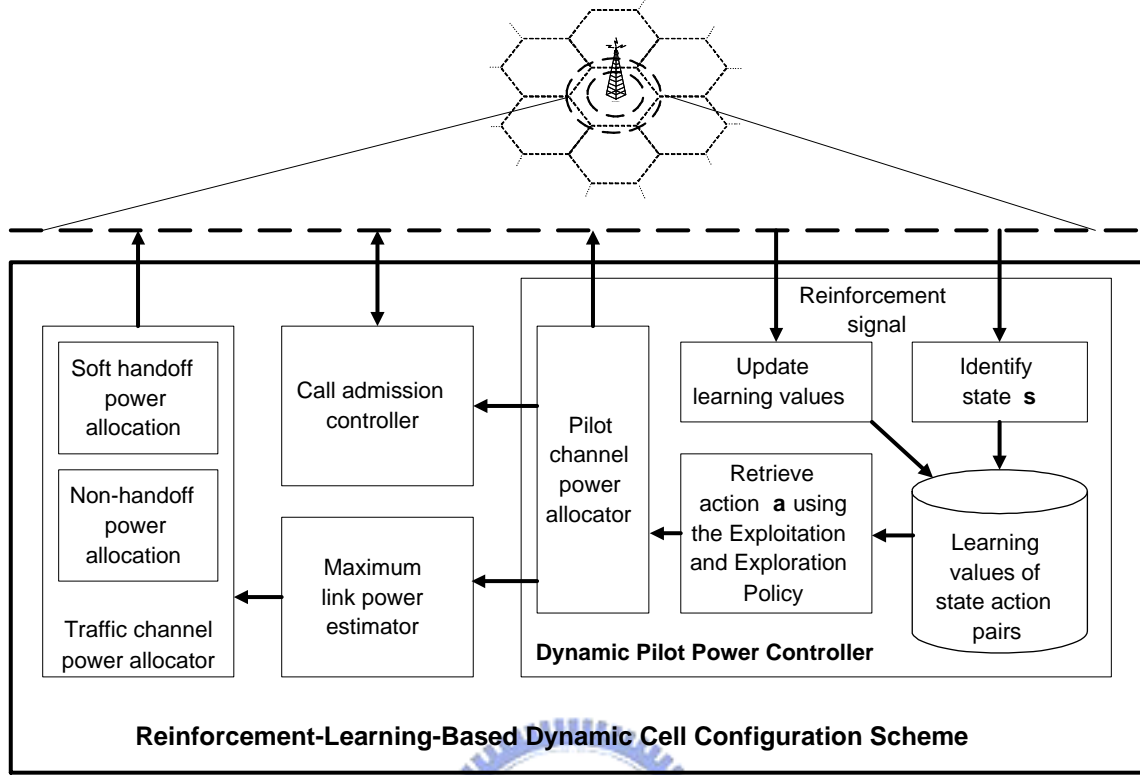


Figure 4.4: System block diagram of the proposed dynamic cell configuration (DCC) scheme with radio resource management.

power  $p_{b,m}$  for mobile station  $m$  from base station  $b$  is  $p_{b,m} = \phi_m P_b^T \leq \tilde{p}_b$ , where  $\tilde{p}_b$  is the maximum link power constraint. Thus,  $\sum_{m \in U_b} \phi_m = 1$ , where the  $U_b$  represents the set of all mobile stations served by base station  $b$ .

Define  $L_{b,m}$  as the link quality between base station  $b$  and mobile station  $m$ , and  $\eta_o$  is the thermal noise. Note that the link quality depends on effects of both path loss and shadowing. The total received interference of the mobile station  $m$  served by the base station  $b$ ,  $I_{b,m}$ , is

$$I_{b,m} = (1 - f_\alpha) P_b^T L_{b,m} + \sum_{k \neq b} P_k^T L_{k,m} + \eta_o, \quad (4.1)$$

where  $f_\alpha$  is the orthogonality factor. Note that the first and second terms in (4.1) mean intra-cell and inter-cell interferences, respectively, in which the first term is caused by imperfect orthogonality of channel codes.

The received chip-energy-to-interference ratio ( $E_c/I_o$ ), denoted by  $v_{b,m}$ , for mobile station

$m$  with service rate  $r$  served by base station  $b$  is

$$v_{b,m} = \frac{P_b^I L_{b,m} G_P^I}{I_{b,m}} \geq \Upsilon, \quad (4.2)$$

where  $G_P^I$  is the processing gain of pilot signal,  $\Upsilon$  is the minimum  $E_c/I_o$  constraint of the system. In order to maintain good connection with at least one base station in the system, the mobile station's  $E_c/I_o$  should exceed  $\Upsilon$  at all the time. In subsection 4.3.3, detailed designs of pilot power  $P_b^I$  and maximum link power constraint for service rate  $r$ ,  $\tilde{p}_b(r)$ , in CDMA systems are discussed using link budget analysis.

Moreover, in CDMA cellular systems, for mobile station  $m$  with service rate  $r$  served by base station  $b$ , the received bit-energy-to-interference ratio ( $E_b/I_o$ ), denoted as  $\gamma_{b,m}(r)$ , must be larger than or equal to the required service quality, denoted as  $\gamma^*(r)$ . For bandwidth  $W$ ,  $\gamma_{b,m}(r)$  of mobile station  $m$  can be expressed as

$$\gamma_{b,m}(r) = \frac{\phi_m P_b^T L_{b,m} G_P(r)}{I_{b,m}} \geq \gamma^*(r), \quad (4.3)$$

where  $G_P(r) = W/r$  is the processing gain for service rate  $r$ . Furthermore, for a soft handoff user  $h$  with service rate  $r$ , the maximum ratio combining (MRC) method is used to combine signals from all serving base stations in its active set  $D_h$ . Thus, its received  $E_b/N_o$ ,  $\gamma_h(r)$ , can be obtained by

$$\gamma_h(r) = \sum_{b \in D_h} \gamma_{b,h}(r). \quad (4.4)$$

### 4.3.2 Handoff Power Allocation Schemes

Soft handoff is one of the important features in CDMA cellular mobile communication systems. When mobile users move from one cell to another cell, the soft handoff technique can provide seamless connections and better signal qualities for users in the cell boundary. Because of multiple links transmission, power balance can be achieved between cells by executing soft handoffs. As a matter of fact, the service coverage can thus be extended. In the following, two techniques of handoff power allocation are discussed.



## A. The Site Selection Diversity Transmission (SSDT) Scheme

The main concept of site selective transmit diversity (SSDT) scheme [14] is to dynamically choose one base station with the best link quality in the active set for transmission in order to mitigate interference caused by multiple site transmission. Assume there is one handoff mobile station  $h$  with service rate  $r$ . Let  $p_{b,h}(r)$ , where  $b \in D_h = \{1, \dots, |D_h|\}$ , be the required transmission power from base station  $b$  for satisfying the required service quality of handoff user  $h$  with service rate  $r$  such that  $\gamma_h(r) \geq \gamma^*(r)$ , which can be calculated from (4.3). According to the SSDT scheme, the transmission power is allocated as follows

- [STEP1]: Select the best link  $\kappa_s$  among the links in the active set so that the base station can allocate the least transmission power:

$$\kappa_s = \arg_b \min \{p_{1,h}, p_{2,h}, \dots, p_{|D_h|,h}\}. \quad (4.5)$$

- [STEP2]: The required transmission power,  $p_h^*(r)$ , for mobile station  $h$  from serving base station  $b$  is

$$p_h^*(r) = \begin{cases} p_{b,h}, & \text{if } b = \kappa_s \\ 0, & \text{if } b \neq \kappa_s \end{cases} \quad (4.6)$$

- [STEP3]: The allocated power from base station  $b$  should be confined by the constraint of maximum transmission power for each link

$$p_{b,h}(r) = \min \{ p_h^*(r), \tilde{p}_b \}. \quad (4.7)$$

It is noteworthy that because of the maximum link power constraint, the SSDT scheme sometimes cannot offer enough required power for soft handoff users.

## B. The Link Proportional Power Allocation (LPPA) Scheme

The link proportional power allocation (LPPA) scheme was suggested in Chapter 2, 3 and [8]. The main idea of the LPPA scheme is based on the link proportional strategy to distribute required transmission power of the handoff user among all the links in the active set. That is, the base station with better (weak) link connection provides more (less) power. In other

words, the LPPA finds a set of  $p_{b,h}$ , where  $b \in D_h = \{1, \dots, |D_h|\}$ , such that  $\sum_{b \in D_h} \gamma_{b,h}(r) \geq \gamma^*(r)$  and

$$p_{1,h} : p_{2,h} : \dots : p_{|D_h|,h} = L_{1,h} : L_{2,h} : \dots : L_{|D_h|,h} , \quad (4.8)$$

where  $L_{b,h}$  is the link quality from base station  $b$  to handoff user  $h$ . According to the LPPA scheme, the transmission power is allocated as follows

- [STEP1]: Calculate weighting factor of the required power from base station  $b$ ,  $b \in D_h$ , for user  $h$  as

$$w_{b,h} = \frac{L_{b,h}}{\sum_{b \in D_h} L_{b,h}} . \quad (4.9)$$

- [STEP2]: Calculate the required transmission power,  $p_{b,h}(r)$ , from base station  $b$  to the soft handoff user  $h$  by

$$p_{b,h}(r) = \min\{w_{b,h} \cdot p_h^*(r), \tilde{p}_b\}, \forall b \in D_h, \quad (4.10)$$

where  $p_h^*(r)$  is the required total power that can be obtained using iterative method by the tuning ratio of required service quality to the resultant service quality,  $\gamma^*(r)/\gamma_h(r)$ .

The LPPA scheme estimates the required power for soft handoff user  $h$ ,  $p_h^*(r)$ ; then it distributes  $p_h^*(r)$  to all serving base stations in  $D_h$  under the maximum link power constraint in base station  $b \in D_h$ ,  $\tilde{p}_b$ . If the required power of one link over the constraint of maximum transmission power, the LPPA compensates the required power through other links. The detailed design and the prove of convergent can be found in [8].

### 4.3.3 Link Budget Analysis

From the perspective of the base station's transmitter, there exists antenna gain  $G_B$  and cable loss  $L_C$  of the base station, the equivalent isotropic radiated power (EIRP),  $E_P$ , of the traffic channel can be calculated by:

$$E_P[\text{dBm}] = \tilde{p}_b [\text{dBm}] + G_B[\text{dBi}] - L_C[\text{dB}]. \quad (4.11)$$

Note that units of parameters are denoted by the bracket in the following descriptions <sup>1</sup>. On the other hand, from the perspective of mobile station's receiver, taking soft gain  $G_S$ ,

<sup>1</sup>In this chapter, if the unit of a variable is not specified, the variables is linear.

antenna gain  $G_M$ , and body loss  $L_D$  of the mobile station into account, the total EIRP,  $E_T$ , is

$$E_T[\text{dBm}] = E_P[\text{dBm}] + G_M[\text{dB}] - L_D[\text{dB}] + G_S[\text{dB}]. \quad (4.12)$$

Moreover, consider the budget of interference margin  $\Omega_I$  and received noise power  $\eta_o$ , the receiver sensitivities of the mobile station with different service rates is

$$H_R(r)[\text{dB}] = H_S(r)[\text{dB}] + (\Omega_I + \eta_o)[\text{dBm}], \quad (4.13)$$

where  $H_S(r)[\text{dB}]$  is the required signal to interference and noise value for different service rate  $r$ , which is equal to required bit-energy-to-noise ratio,  $\gamma^*(r)[\text{dB}]$ , minus processing gain  $G(r)[\text{dB}]$ . From the preceding link budget, leaving a margin for log-normal fading  $\Omega_L$ , the resultant allowable maximum pathloss for different service rates is

$$PL(r)[\text{dB}] = E_T[\text{dBm}] - H_R(r)[\text{dB}] - \Omega_L[\text{dB}]. \quad (4.14)$$

Based on the allowable maximum pathloss and the applied channel model, the resultant cell radius  $R(r)$  is different to service rates  $r$ . For  $r \in [r_{min}, r_{max}]$ , from (4.13) and (4.14), since  $H_S(r_{min}) > H_S(r_{max})$ , then  $PL(r_{min}) < PL(r_{max})$ . We can thus find that  $R(r_{min}) > R(r_{max})$  as shown in Fig. 4.5 such that different service rates have different service coverage. Apparently, this phenomenon arises the issue of fairness for different service rates since it's unfair for the mobile station with higher service rates to be served near cell boundary. In order to take fairness of service coverage into account for the mobile station with different service rates near the cell boundary, it is necessary to choose a suitable reference service rate for the cell radius design. Assume the default cell radius is reference to service rate  $r^*$ , where  $r^* \in [r_{min}, r_{max}]$ .

In general, pilot power  $P_b^I$  is around 1 watt to 4 watt, which is about 5% – 20% of the maximum transmission power of base station  $b$ ,  $\tilde{P}_b$ . When a mobile station at the cell boundary, the received chip-energy-to-interference ratio,  $E_c/I_o$ , should be equal to or larger than the required  $E_c/I_o$ ,  $\Upsilon$ , which can be calculated as

$$\Upsilon[\text{dB}] = P_b^I[\text{dBm}] - PL(r^*)[\text{dB}] - (\Omega_I + \eta_o)[\text{dBm}]. \quad (4.15)$$

Normally,  $\Upsilon$  is within the range from  $-16$  [dB] to  $-20$  [dB].

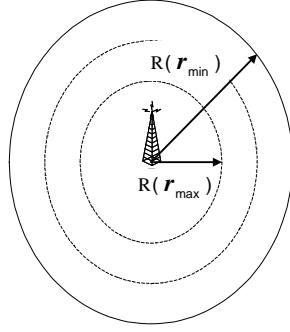


Figure 4.5: Service coverage with different service rates.

#### 4.3.4 DCC Problems

In future WCDMA networks, diverse multimedia traffics and random user mobility make cell coverage and capacity difficult to design. This is because each base station has finite power resource to be shared among users, the allocated pilot and traffic channel power are directly related to the coverage and capacity of the cell. Conventionally, fixed pilot power scheme is adopted. However, when the traffic load is too high to allocate enough required power for users, the system performance will be degraded severely. Some strategies of radio resource management have to be employed to release power or balance power among cells. The dynamic pilot power scheme is one possible approach to balance power load among cells. Therefore, in order to achieve load balance whenever traffic congestion occurs, dynamic cell configuration by adjusting pilot power is necessary. When the required traffic power is low (high), the base station could increase (decrease) its pilot power level to extend (shrink) cell coverage so as to accommodate (release) more users around the adjacent cells. However, dynamic cell configuration may induce some side effects on the system performance as described in the followings.

- For new arriving mobile stations near cell boundaries, their initial access cells will be determined by the received signal strength, which directly relate to the pilot power level of the base stations. Therefore, reducing the pilot power of the congested cell causes them to request traffic channels from other adjacent cells. If an initial new call fails to detect any base station with enough  $E_c/I_o$ , it cannot make a call request to

the system. This is the so-called *coverage failure*. As a consequence, although the new call blocking probability of the congested cell could be decreased, the coverage failure probability might be increased.

- For existing mobile stations near cell boundaries, decreasing (increasing) the pilot power of a base station may force some of them to handoff into other (its) cell(s). Therefore, the average size of the active set and handoff rates would be increased. In addition, if a mobile station suffers bad link quality and fails to pass handoff call admission to execute handoff in time before its received  $E_c/I_o$  dropping off the requirement,  $\Upsilon$ , a handoff forced termination occurs.

From the the above discussion, in order to design an effective dynamic cell configuration scheme that improves the system performance and minimizes the undesirable effects, it is necessary to consider the pilot power allocation and other radio resource management strategies jointly.

#### 4.3.5 Solving DCC Problems by Reinforcement-Learning

In this chapter, we design a dynamic cell configuration (DCC) scheme that takes into account pilot, soft handoff, and maximum link power allocations as well as call admission control jointly as shown in Fig. 4.4. This scheme can be implemented in each base station being aware of the system load variation in next-generation CDMA systems. Using the proposed DCC scheme, each base station can adjust its pilot power and maximum link power constraint as well as new/handoff call admission threshold periodically. The dynamic cell configuration problem is formulated as a Markov decision process (MDP) [59]. However, traditional model-based solutions to MDP, such as policy iteration and linear programming, require a prior knowledge of the state transition probabilities and hence suffer from two “curses”: the *curse of dimensionality* and the *curse of modelling*. The curse of dimensionality is that the complexity in these algorithms increases exponentially as the number of state increases. Dynamic cell configuration involves very large state space that makes model-based solutions infeasible. The curse of modelling is that in order to apply model-based

methods, it is first necessary to express state transition probabilities explicitly. In practice, this is a very difficult proposition for next-generation CDMA cellular networks due to the diverse multimedia traffic and random user mobility.

Q-learning technique was broadly adopted to solve these thorny problems in the wireless communication systems, e.g. [60] and [61]. In general, the Q-values of state-action pair are usually stored in a look-up table, but it's impossible for the problems with continuous state spaces. Authors in [62], [63] shown that fuzzy Q-learning is an efficient technique for the approximation of continuous system states. It is an adaptation of Watkins's Q-learning [64] for fuzzy inference systems (FIS) where both the actions and Q-functions are inferred from fuzzy rules. Taking advantage of the Q-learning technique, the universal approximation property of the FIS makes the representation of Q-values with large state-action space possible. Moreover, a priori knowledge can be integrated in the learning procedure.

This chapter proposes a reinforcement-learning-based DCC scheme by fuzzy-Q-learning to find an optimal policy for pilot power, maximum link power constraint, soft handoff power allocation, and call admission control criterion in CDMA multimedia networks. It uses power load variations as the system states, which implicitly reveal the information about load variations of all other cells in the whole network . Therefore, the cell coverage and capacity can be coordinated between cells accordingly. In the next section, we detail the design for the DCC scheme.

## 4.4 DCC Design

In this section, the cell configuration problem in CDMA networks is formulated as a Markov decision process (MDP) [59]. The pilot power of a base station is periodically adjusted to adapt to the variations of system situations. These time instants are called *decision epochs* and the adjustments of pilot power are called *actions*. The chosen action is based on the current *state* of the system, in which the state information includes the mean and variance of the power load. We then present a fuzzy Q-learning solution to the problem. In order to apply the fuzzy Q-learning algorithm, it is necessary to identify the decision

epochs, states, actions and rewards in the system.

#### 4.4.1 Problem Formulation as a Markov Decision Process (MDP)

The dynamic cell configuration problem is formulated as a MDP as follows:

- [Decision epochs]: In CDMA systems, the pilot signal is broadcasted from each base station periodically [51], and the state of the system changes accordingly. Therefore, we adjust the pilot power every  $M$  frames, where  $M$  is a design parameter.
- [State]: Define the state vector of the system as  $s = (\varpi_M, \varpi_V) \in S$ , where  $\varpi_M$  denotes the mean power of the base station and  $\varpi_V$  denotes the variance of the power load. Assume each sample denotes  $n$ , and there are  $N$  samples for the measurements, in which  $N$  is also a design parameter. For convenience, each sample is indicated by the brackets for power load  $P_b^T$  of base station  $b$ . Thus,  $\varpi_M$  and  $\varpi_V$  can be calculated by sample mean and variance, respectively, as follows.

$$\varpi_M = \frac{1}{N} \sum_{n=1}^N P_b^T(n) \quad (4.16)$$

$$\varpi_V = \frac{1}{N-1} \sum_{n=1}^N (P_b^T(n) - \varpi_M)^2. \quad (4.17)$$

The decision process can be implemented in each base station in distributed manner. This is because the variation of the base station's power load can implicitly reveal the load information about all other cells from (4.1) and (4.3). Therefore, the system can be self-organized for cell configuration so that the coverage and capacity can be coordinated between cells accordingly.

- [Action]: At each decision epoch, the base station makes a decision to choose a suitable fraction of the pilot power based on the system state  $s$ . The action  $a(s) \in A$  is defined as  $f_b \in [f_{min}, f_{max}]$ , where  $A$  is the action set;  $f_{min}$  and  $f_{max}$  are the minimum and maximum fraction of the pilot power, respectively.

- [Rewards function]: Based on the action  $a(s)$  in a state  $s$ , a reward  $\mu(s, a(s))$  occurs in the system. We choose the system throughput as the reward:

$$\mu(s, a(s)) = \sum_m r_m, \quad (4.18)$$

where  $r_m \in r = [r_{min}, r_{max}]$  is the transmission rate of mobile station  $m$ .

#### 4.4.2 Reinforcement-Learning-Based Solutions

The objective of the decision process is to find an optimal policy  $\pi^*$  for each state  $s$ , which minimizes the cumulative measure of the reward  $\mu_t = \mu(s_t, a(s_t))$  that is received over time. Note that the subscript  $t$  is indicated to represent time instant  $t$ . The total expected discounted reward over an infinite time horizon can be represented by the value function with policy  $\pi$ ,  $V^\pi(s)$ , and is given by

$$V^\pi(s) = \mathbf{E} \left\{ \sum_{t=0}^{\infty} \gamma_d^t \cdot \mu(s_t, \pi(s_t)) \mid s_0 = s \right\}, \quad (4.19)$$

where  $\gamma_d$  is a discount factor, and  $0 \leq \gamma_d < 1$ . By taking action  $a(s)$ , assume the state transition from  $s$  to  $s'$  with transition probability  $P(s'|s, a(s))$ , the equation (4.19) can be rewritten as

$$V^\pi(s) = U(s, \pi(s)) + \gamma_d \sum_{s' \in S} \Pr(s'|s, \pi(s)) V^\pi(s'), \quad (4.20)$$

where  $U(s, \pi(s)) = E \{ \mu(s, \pi(s)) \}$  is the mean value of  $\mu(s, \pi(s))$ . Define a Q-function of state-action pair with policy  $\pi$  as

$$Q^\pi(s, a(s)) = U(s, a(s)) + \gamma_d \sum_{s' \in S} \Pr(s'|s, \pi(s)) V^\pi(s'). \quad (4.21)$$

The optimal value function  $V^{\pi^*}$  with the optimal policy  $\pi^*$  satisfies Bellman's optimality criterion [65]

$$\begin{aligned} Q^*(s, a(s)) = V^{\pi^*} &= \max_{b(s) \in A} \left\{ U(s, b(s)) + \gamma_d \sum_{s' \in S} \Pr(s'|s, \pi(s)) V^{\pi^*}(s') \right\} \\ &= \max_{b(s) \in A} Q^{\pi^*}(s, b(s)). \end{aligned} \quad (4.22)$$



Thus, the optimal Q-function  $Q^*(s, a(s))$  can be obtained from finding an optimal policy of Q-function  $Q^{\pi^*}(s, a(s))$ . Without knowing  $U(s, a(s))$  and  $\Pr(s'|s, a(s))$ , Q-learning process can still find an optimal policy  $\pi^*$  through updating  $Q(s, a(s))$  to find  $Q^*(s, a(s))$  in a recursive manner using the information of current state  $s_t$ , action  $a_t(s_t)$ , reward  $\mu_t$ , and next state  $s'_t$ . Thus, at time instant  $t$ , the Q-learning rule is

$$Q_{t+1}(s, a(s)) = \begin{cases} Q_t(s, a(s)) + \lambda_L \Delta Q_t(s, a(s)), & \text{if } s = s_t \text{ and } a(s) = a_t(s_t) \\ Q_t(s, a(s)), & \text{otherwise} \end{cases} \quad (4.23)$$

where  $\lambda_L$  is the learning rate, and based on (4.22),

$$\Delta Q_t(s, a(s)) = \mu_t + \gamma_d Q_t^*(s', a(s)) - Q_t(s, a(s)). \quad (4.24)$$

Watkins [64] has shown that if the Q-value of each feasible state-action pair  $\{s, a(s)\}$  is visited infinitely often, and if the learning rate is decreased to zero in a suitable way, then as  $t \rightarrow \infty$ .  $Q(s, a(s))$  can converge to  $Q^*(s, a(s))$  with probability 1. Considering huge continuous state space in the CDMA multimedia system, the curse of dimensionality is hard to tackle. Therefore, fuzzy inference system (FIS) [66] is implemented into reinforcement-learning method which is based on value iteration method [59], [62] and [63] to generalize Q-learning with FIS.

### 4.4.3 FQ-DCC Scheme

In this section, the detailed design of fuzzy-Q-learning based SOC (FQ-SOC) is provided. As shown in Fig. 4.6, the interaction between FQ-SOC and the system at each time instant consists of the following procedures. Based on the information imported from the environment, FQ-SOC identifies the state  $s$ . On the current state, takagi-sugeno FIS calculates the truth value of each rule for the input vector [66]. Also, feasible action set are approximated based on the current state. For each rule, an action is selected by using the exploitation and exploitation policies (EEP), and then eligibility factor for each rule can be calculated. The resultant action is converted to the pilot power level of the base station. The reward signal can be measured from the system, and fed back to FQ-SOC to update the Q-function and q-value for each rule.

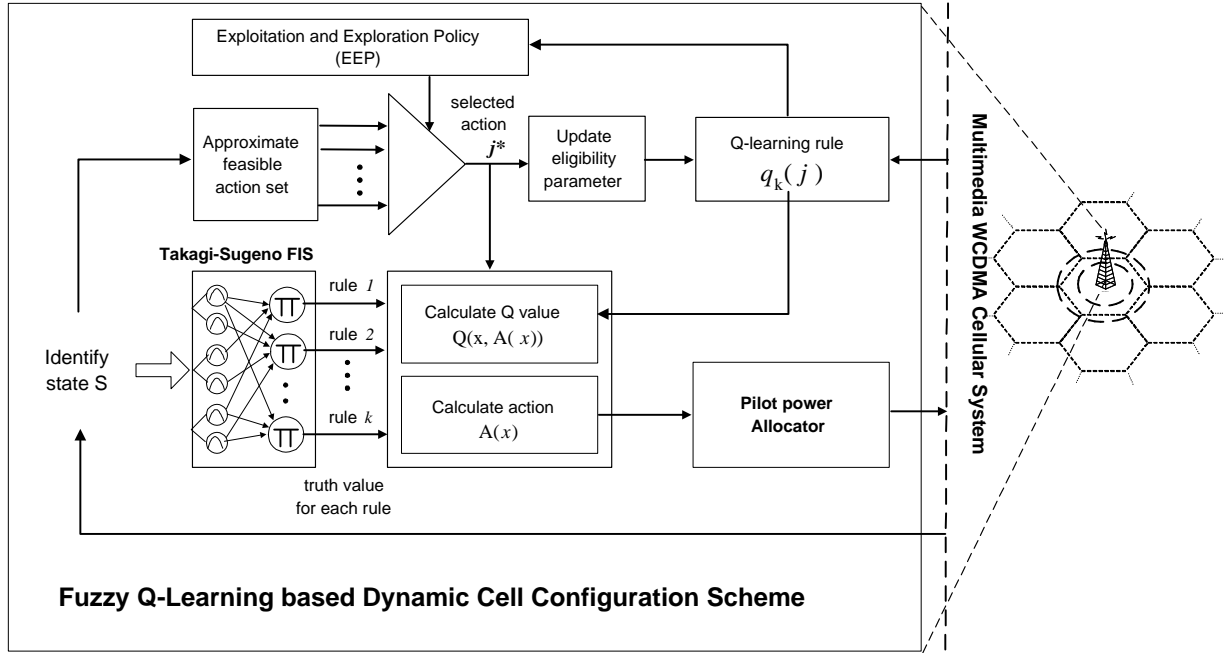


Figure 4.6: Fuzzy Q-learning-based dynamic cell configuration (FQ-DCC) scheme.

### A. Representation of Q-function by a FIS

FIS is based on the concept of fuzzy set theory, fuzzy IF-THEN rules, and fuzzy reasoning as shown in Fig. 4.7. The *fuzzifier* performs a mapping function from observed input  $\mathbf{x}$  to a fuzzy set  $T(\mathbf{x})$ . The *fuzzy rule-base* is characterized by a set of linguistic statements based on designer's knowledge and experiences in a form of "IF-THEN" rules that describe a fuzzy logic relationship between the input  $\mathbf{x}$  and the output  $\mathbf{y}$ . According to the fuzzy rules and the input linguistic terms  $T(\mathbf{x})$ , the *inference engine* performs an implication function, which is a decision making logic using an inference method to obtain the output linguistic terms  $T(\mathbf{y})$ . The *defuzzifier* adopts a defuzzification function to convert  $T(\mathbf{y})$  into a crisp value  $\mathbf{y}$ . Consider Sugeno fuzzy model [67], which is the most widely applied model due to its transparency and high interpretation of the fuzzy rule and the systematic approach. It can build up the fuzzy rule base by a crisp linear function,  $\mathbf{y} = g(T(\mathbf{y}))$ , where  $g(\cdot)$  is a weighting sum in a polynomial form.

Assume the state of rule  $k$  is  $S_k = \{S_{k,1}, \dots, S_{k,Z}\}$ , where  $S_{k,z}$  is the fuzzy label for  $z$ -th input variable in rule  $k$ . For input variable  $\mathbf{x}$ , the FIS function can be defined by the

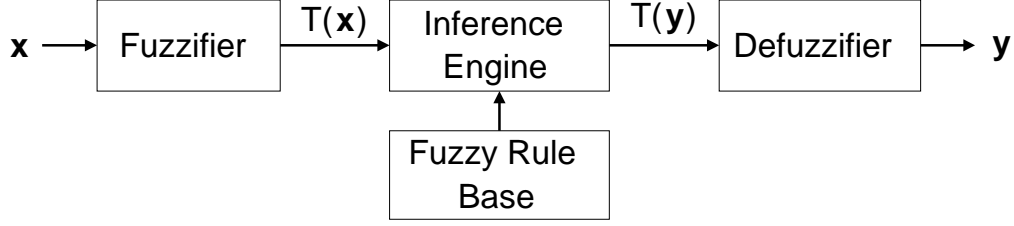


Figure 4.7: The structure of the fuzzy inference system (FIS).

elementary rules  $k = 1 \cdots , K$  with format

$$\text{IF } \mathbf{x} \text{ is } S_k \text{ THEN } \mathbf{y} = a_k \text{ WITH } q_k,$$

where  $a_k$  and  $q_k$  are the action and q-value for each rule  $k$ . Thus, the representation of  $Q(\mathbf{x}, a(\mathbf{x}))$  by a FIS is equivalent to determining  $q_k$ . Assume the input and output variables are represented by  $\mathbf{x}$  and  $\mathbf{y}$ , respectively, we can associate the Q value of input  $\mathbf{x}$  and action  $a(\mathbf{x})$  by the FIS function as

$$\mathbf{x} \rightarrow \mathbf{y} = Q(\mathbf{x}, a(\mathbf{x})) = FIS(\mathbf{x}), \quad (4.25)$$

where input vector is  $\mathbf{x} = (x_1, x_2, \cdots, x_Z)$ , which represents system state  $s$ , where  $Z$  is the size of the vector.

In FQ-SOC, there are two input linguistic variables are considered for input variable  $\mathbf{x}$ . Moreover, the fuzzy term sets of  $(\varpi_M, \varpi_V)$  are defined as  $T(\varpi_M) = \{\text{Extremely Low, Medium Low, Low, Medium, High, Extremely High}\} = \{\text{EL, ML, LO, ME, HI, EH}\}$ . Also,  $T(\varpi_V) = \{\text{Extremely Low, Low, Medium, High, Extremely High}\} = \{\text{EL, LO, ME, HI, EH}\}$ . The fuzzy rules have dimension  $|T(\varpi_M)| \times |T(\varpi_V)|$ . In FQ-SOC, there are 30 ( $6 \times 5$ ) rules. As for the output linguistic variable, it represents possible actions for the allocation of pilot power fraction  $f_b$ . Thus, the pilot power of base station  $b$ ,  $P_b^I$ , is equal to  $f_b \times \tilde{P}_b$ . Here, output dimension is designed as 13.

Assume  $J$  is the overall action set. For every rule  $k$ , assume  $j$  is possible solution of action  $a_k$  and the q-value  $q_k$ , denoted as  $a_k(j)$  and  $q_k(j)$ ,  $j \in J$ , respectively. Moreover, since greedy policy easily dragging system to approach local optimal solutions, it is necessary

for FQ-SOC scheme to visit all the set of possible actions for all states. This is so-called exploration/exploitation dilemma. Here, pseudo-exhaustive policy is applied, in which rule action  $j$  with the best q-value has a selection probability to be chosen, which is  $\Pr(j|q_k(j))$  based on Boltzmann distribution, otherwise an action which is the least lately chosen in the given rule will be chosen. Through exploration/exploitation policy (EEP), action  $a_k(j^*)$  is selected from action set  $a_k(j)$ , where  $j^* \in J$ .

$$\mathbf{x} \rightarrow a_k(j^*) = EEP(\mathbf{x}). \quad (4.26)$$

Therefore, in the context of fuzzy Sugeno model for FIS [66], the output of the FIS function, including inferred action  $A(\mathbf{x})$  and its associated Q value  $Q(\mathbf{x}, A(\mathbf{x}))$ , become:

$$A(\mathbf{x}) = \frac{\sum_{k=1}^K \alpha_k(\mathbf{x}) \times a_k(j^*)}{\sum_{k=1}^K \alpha_k(\mathbf{x})}, \quad (4.27)$$

$$Q(\mathbf{x}, A(\mathbf{x})) = \frac{\sum_{k=1}^R \alpha_k(\mathbf{x}) \times q_k(j^*)}{\sum_{k=1}^K \alpha_k(\mathbf{x})}, \quad (4.28)$$

where  $\alpha_k(\mathbf{x})$  is the truth value of each rule for the input vector  $\mathbf{x}$ ,  $\alpha_k(\mathbf{x}) = \prod_i \varphi_{S_{k,i}}(x_i)$ , in which  $\varphi_{S_{k,i}}(x_i)$  is the membership degree to the different fuzzy sets [62], and [63]. Note that the output inferred action represents the estimated optimal level of the pilot power, denoted as  $\hat{P}_b^I$ .

## B. Fuzzy Q-Learning Strategies

In the following, to clarify the time series during learning process, subscripts of time index  $t$  are added to some symbols. To update the Q-value, the optimal Q-value,  $Q^*(\mathbf{x}_{t+1}, A(\mathbf{x}_{t+1}))$ , of the next state  $\mathbf{x}_{t+1}$  in (4.22) then becomes:

$$Q^*(\mathbf{x}_{t+1}, A(\mathbf{x}_{t+1})) = \frac{\sum_{k=1}^K \alpha_k(\mathbf{x}_{t+1}) \times q_k(j^\dagger)}{\sum_{k=1}^K \alpha_k(\mathbf{x}_{t+1})}, \quad (4.29)$$

where  $j^\dagger = \arg \max_j q_k(j)$ ,  $j \in J$ . The temporal difference error:

$$\Delta Q = \beta_d \{U_t + \gamma_d Q^*(\mathbf{x}_{t+1}, A(\mathbf{x}_{t+1})) - Q(\mathbf{x}_t, \mathbf{A}(\mathbf{x}_t))\}, \quad (4.30)$$

where  $U_t = E \{\mu(s_t, \pi(s_t))\}$ . Sutton and Barto [57] spreads the evaluation for all states according to *eligibility*, the degree of visit of a state in the recent past. The trace of eligibility constitutes a short-term memory of the frequency of visit of a state. It decreases

exponentially in the time, unless to be reactivated by a new visit. Let  $e_k(j)$  be the replace eligibility of possible action  $a_k(j)$  in rule  $k$ . The eligibility factor is updated after the choice of the conclusions action  $a_k(j^*)$  by the EEP:

$$e_k(j) = \begin{cases} \gamma_d \lambda_L e_k(j) + \frac{\alpha_k(\mathbf{x}_t)}{\sum_{k=1}^K \alpha_k(\mathbf{x}_t)}, & \text{if } j = j^* \\ \gamma_d \lambda_L e_k(j), & \text{otherwise.} \end{cases} \quad (4.31)$$

Also, the elementary quality can be immediately updated by:

$$\Delta q_k(j) = \epsilon \times \Delta Q \times e_k(j). \quad (4.32)$$

Thus,

$$q_k(j) = q_k(j) + \Delta q_k(j). \quad (4.33)$$

### C. Feasible Action Selection and Exploitation and Exploration Policy

Feasible action set  $\mathbf{A}_s \subset \mathbf{A}$  can be obtained based on the current state  $s$ . In our proposed FQ-DCC scheme, a simple strategy for feasible action selection is applied. State  $\omega_M$  can be adopted as an indicator to classify the feasible action sets. For example,

$$\mathbf{A}_s = \begin{cases} \{f_{min}, \dots, f_{\Theta}\}, & \text{if } \varpi_M \geq \Theta \\ \{f_{\Theta}, \dots, f_{max}\}, & \text{otherwise} \end{cases} \quad (4.34)$$

where  $f_{\Theta}$  is the cutting value of the action set,  $f_{\Theta} \in [f_{min}, f_{max}]$ , and  $\Theta$  is the threshold of the mean power as the quality-of-service constraint. Since greedy policy can easily drag the system to approach local optimal solutions, it is necessary to visit all the set of possible actions for all states. This is so-called exploration/exploitation dilemma. An action of state  $s$ ,  $a(s)$ , is selected from feasible action set  $\mathbf{A}_s$  using a exploitation and exploitation policies. Here, pseudo-exhaustive policy is applied, in which the action with the best Q-value has a selection probability to be chosen based on Boltzmann distribution. Otherwise an action which is the least lately visit will be chosen. The resultant action is converted to the pilot power of the base station. The reward signal can be measured from the system, and feed back to update the Q-function.

#### 4.4.4 Dynamic Maximum Link Power Constraint Design

The main idea for the adjustment of maximum link power constraint is to couple with the pilot power into design. This is because pilot power adjustment affects cell coverage but not service coverage. The maximum link power determines the service coverage for users with different service rates near the cell boundary. When the cell is shrink by reducing the pilot power, the pathloss to the cell boundary is decreased so that the mobile station needs small transmission power to obtain required signal quality. On the other hand, when cell is expended by increasing pilot power, the base station needs larger power to compensate increased pathloss for users near the cell boundary.

In order to match cell coverage and service coverage, based on the maximum pathloss and the receiver sensitivity in terms of referenced service rate  $r^*$ , from (4.14), the total EIRP of transmitted pilot power  $E_T^I$  should be

$$E_T^I[\text{dBm}] = PL(r^*)[\text{dB}] + H_R^I[\text{dB}] + \Omega_L[\text{dB}], \quad (4.35)$$

where  $H_R^I$  is the receiver sensitivity of the pilot signal such that

$$H_R^I[\text{dB}] = H_S^I[\text{dB}] + (\Omega_I + \eta_o)[\text{dBm}], \quad (4.36)$$

where  $H_S^I$  is the required signal to interference and noise value of the pilot signal, which is equal to the required bit-energy-to-noise ratio of the pilot signal,  $\gamma_I^*[\text{dB}]$ , minus the processing gain of the pilot signal  $G_P^I[\text{dB}]$ . Then, substitute (4.14) into (4.35), we can obtain

$$E_T^I[\text{dBm}] = E_T[\text{dBm}] - H_R(r^*) + H_R^I[\text{dB}]. \quad (4.37)$$

Hence, as soon as the pilot power of base station  $b$ ,  $P_b^I$ , has been adjusted dynamically, the maximum link power of cell  $b$  should be

$$\tilde{p}_b[\text{dBm}] = P_b^I[\text{dBm}] + H_R(r^*)[\text{dB}] - H_R^I[\text{dB}]. \quad (4.38)$$

The maximum link power constraint is thus coupled with pilot power adjustments accordingly.

#### 4.4.5 Call Admission Controller

In FQ-DCC scheme, the output action represents the estimated level of the pilot power  $\widehat{P}_b^I$ . Since the maximum link power is the function of the pilot power in (4.38), as soon as the optimal pilot power has been calculated, the corresponding maximum link power  $\widehat{p}_b$  can be updated by

$$\widehat{p}_b[\text{dBm}] = \widehat{P}_b^I[\text{dBm}] + H_R(r^*)[\text{dB}] - H_R^I[\text{dB}], \quad (4.39)$$

where  $\widehat{H}_R^I$  is the estimated receiver sensitivity of the pilot signal received at cell boundary with referenced service rate  $r^*$ . Moreover, from (4.36) and (4.39), estimated call admission threshold  $\Lambda_b$  of signal-to-interference-ratio (SIR) for cell  $b$  becomes

$$\begin{aligned} \Lambda_b[\text{dB}] &= \widehat{H}_R^I[\text{dB}] - (\Omega_I + \eta_o)[\text{dBm}], \\ &= \widehat{P}_b^I[\text{dBm}] - \widehat{p}_b[\text{dBm}] + H_R(r^*)[\text{dBm}] - (\Omega_I + \eta_o)[\text{dBm}]. \end{aligned} \quad (4.40)$$

- New Call Admission Control Algorithm:** A new call user  $m$  measures and reports the received signal  $E_b/I_o$ ,  $\gamma_{b,m}(r)$ , to base station  $b$  to request traffic channel for transmitting service rate  $r$ . The received SIR of the mobile station,  $\widehat{H}_S[\text{dB}]$ , can thus be estimated as:  $\gamma_{b,m}(r)[\text{dB}] - G_P(r)[\text{dB}]$ . The base station will accept the request with  $\widehat{H}_S[\text{dB}]$  being larger than  $\Lambda_b[\text{dB}]$ , otherwise the new call will be blocked.
- Handoff Call Admission Control Algorithm:** The soft handoff algorithm is implemented based on [51]. The MRC method (4.4) is used to combine received  $E_b/I_o$ ,  $\gamma_h(r)$ , from all serving base stations in the active set  $D_h$ . Thus, the mobile station  $h$ 's received SIR,  $\widehat{H}_S$ , can thus be estimated as:  $\gamma_h(r)[\text{dB}] - G_P(r)[\text{dB}]$ . The handoff request will be issued to base station  $b$  whenever an add event occurs. The base station will accept a user with  $\widehat{H}_S[\text{dB}]$  being larger than  $\Lambda_b[\text{dB}]$ , otherwise the handoff call request will be blocked. The admitted handoff call will add new member of the base station into active set  $D_h$ . On the other hand, if the blocked handoff call doesn't exceed handoff delay time, it can make handoff request again as long as its  $E_c/I_o$  does not fall off the  $E_c/I_o$  requirement,  $\Upsilon[\text{dB}]$ .

## 4.5 Simulation Results and Discussions

### 4.5.1 Simulation Model

Consider a hexagon cellular system with 19 wrap-around cells, in which the central cell is a hotspot cell with high traffic load. Define the load ratio  $\rho$  as the ratio between the arrival rate of the hotspot cell and that of each other cell. Geographically, the cellular deployment is homogenous, and the default cell radii can be determined by the link budget design in subsection 4.3.3. Assume mobile stations are uniformly distributed in each cell, and the initial speeds of mobile stations are uniformly distributed. The maximum speeds for users in the hotspot cell, 1st-tier cells, and 2nd-tier cells are assumed to be 30, 60, and 60 km/hr, respectively. Whenever one mobile station moves into different cell tiers, the speed will be changed. Moreover, the probability of moving direction change for mobile stations is 0.2 and the direction update is among  $\pm 45$  degrees [51]. During the mobility, the correlated shadowing effect is based on Gudmundson model [51], [52], in which the decorrelation length is 20 meters in a vehicular environment. Also, for the channel model [51], the pathloss is obtained by

$$40 \times (1 - 0.004h_b) \times \log_{10}(d) - 18 \times \log_{10}(h_b) + 21 \times \log_{10}(f_d) + 80, \quad (4.41)$$

where  $d$  is the distance between a base station and a mobile station;  $h_b$  and  $f_d$  are the antenna height of the base station and the downlink frequency, respectively. In our simulations, the downlink frequency is 2.4 GHz and the antenna height is 20 meters. The link budget design of this simulation is provided in Table 4.1 [4], [53].



Table 4.1: LINK BUDGET IN THE MULTIMEDIA WCDMA SYSTEM

<b>System Parameters</b>	
Chip rate [Mchips]	3.84
Orthogonality Factor, $f_\alpha$	0.5
Referenced service rate $r = r^*$ (kbps)	144
Processing Gain of service rate $r$ , $G_P(r)$ [dB]	14.26
Required $E_b/N_o$ of service rate $r$ , $\gamma^*(r)$ [dB]	3
Required SIR of service rate $r$ , $H_S(r)$ [dB]	-11.26
Receiver Sensitivity of service rate $r$ , $H_R(r)$ [dBm]	-105.35
<b>Transmitter (Base station)</b>	
Maximum transmission power of base station $b$ , $\tilde{P}_b$ [dBm]	43.01
Maximum link power constraint, $\tilde{p}_b$ [dBm]	30
Cable loss of the base station, $G_c$ [dB]	3
Antenna gain of the base station, $G_B$ [dBi]	2
EIRP, $E_P$ [dBm]	29
<b>Receiver (Mobile station)</b>	
Antenna gain of the mobile station, $G_M$ [dBi]	2.0
Body loss of the mobile station, $L_D$ [dB]	3.0
Soft handoff Gain, $G_S$ [dB]	3.0
Thermal noise density [dBm/Hz]	-173.93
Noise figure [dB]	9.0
Noise power [dBm]	-99.09
Margin of interference [dB]	5.0
Margin of log-normal fade [dB]	5.0
Total EIRP, $E_T$ [dBm]	31.0
Maximum allowable pathloss of service rate $r$ , $PL(r)$ [dB]	131.35
<b>Pilot channel</b>	
Processing Gain of the pilot signal, $G_P^I$ [dB]	0.28
Required $E_c/I_o$ [dB]	-20
Receiver Sensitivity of the pilot signal, $H_R^I$ [dBm]	-114.37
Maximum allowable pathloss of pilot signal, $PL(r)$ [dB]	144.35
Minimum allowable $E_c/I_o$ , $\Upsilon$ [dB]	-19.28

We assume that the call arrival process is Poisson. There are three service classes in the system, real-time voice, data, and non-real-time data services. The call holding times of voice and data traffic are exponentially distributed with means 60 and 30 seconds, respectively. For the real-time services, a two-level Markov modulated Poisson process (MMPP) is used to model voice traffic while a 5-level MMPP is used to model the data traffic. The mean duration of each state in the 5-level MMPP is 1 second. The transmission rate (required bit-energy-to-noise ratio) of the voice traffic is 12.2 kbps (5 dB), and the service rates (required

bit-energy-to-noise ratio) of the data traffic are 16, 32, 64, and 144 kbps (5, 4, 3, and 2 dB). Note that adaptive rate transmission is applied whenever the power resources are not enough to support the existing users. For the non-real-time services, the variable length data bursts are assumed to be geometrically distributed with mean data burst size of 200 frames. Moreover, there are 6 different service rates (required bit-energy-to-noise ratio), 16, 32, 64, 144, 384, and 512 kbps (5, 4, 3, 2, 1.5, and 1 dB). The transmission is on burst-by-burst basis. That is, each burst should request for a traffic channel and release the channel as soon as it completes the burst transmission. In simulations, the traffic percentages of voice, real-time data, and non-real-time data are 60%, 35%, and 5%, respectively.

Because of different processing gain and required signal quality, different service classes have different service coverage. Apparently, higher rate services can be supported in smaller cell coverage, as shown in Fig. 4.5. In simulations, we consider seven service rates such that  $r_0 < r_1 < \dots < r_6$ . Based on the link budget, the cell radius is calculated in terms of different referenced service rates, represented as  $\text{ref} = \{0, 1, \dots, 6\}$ . Consider the fixed pilot power design, 1 watt power is allocated to the pilot channel. Fig. 4.8 shows the capacity results by applying SSdT and LPPA schemes in terms of different referenced service coverage under uniform ( $\rho = 1$ ) and non-uniform ( $\rho = 4$ ) cell load cases. Because of less propagation loss of small cell coverage, smaller cell can provide better signal quality for mobile stations. In all cases, the system capacity can be increased for smaller cell coverage. We can also see that the slope of throughput increments to the difference of referenced service coverage becomes flatter when reference service rate is larger than 4. This means the system reaches the capacity-limited situation. Hence, in this chapter, cell radius is referred to service rate 144 kbps, which is the maximum service rate of real-time data service.

#### 4.5.2 Performance Measurements and Discussions

We compare the performance of four schemes, including fixed pilot with SSdT (FIX-SSdT), LPPA (FIX-LPPA) schemes, and dynamic cell configuration with SSdT (DCC-SSdT), LPPA (DCC-LPPA) schemes. For the fixed pilot scheme, the default pilot power,  $P_b^I$ , is fixed and set as 2.5 watt for each cell (12.5% of maximum transmission power).

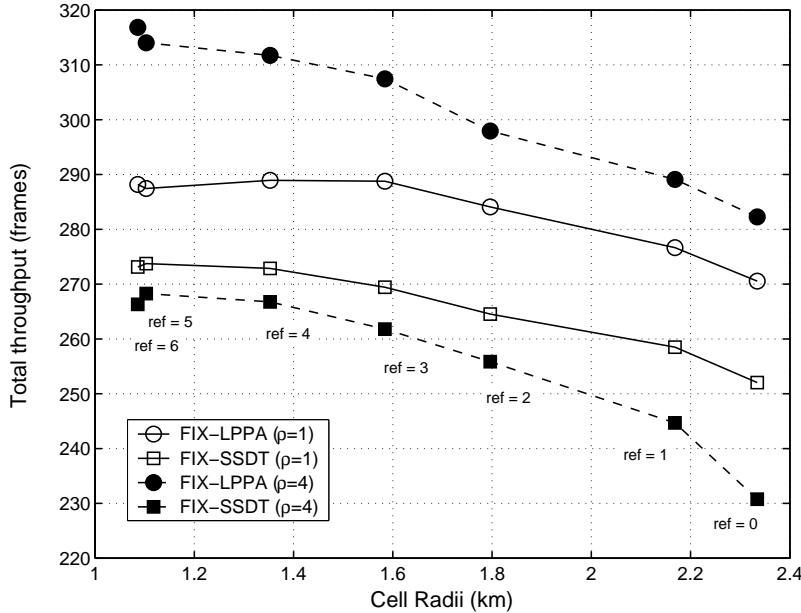


Figure 4.8: For fixed pilot power design, capacity results by applying SSDT and LPPA schemes in terms of different referenced service coverage under uniform ( $\rho = 1$ ) and non-uniform ( $\rho = 4$ ) cell load cases.

The maximum link power,  $\tilde{p}_b$ , and the threshold of the call admission control,  $H_S$ , are fixed and calculated from (4.38) and (4.40), respectively. The DCC scheme is the proposed reinforcement-learning-based dynamic cell configuration scheme. For the DCC scheme,  $P_b^I$ ,  $\tilde{p}_b$ , and  $\hat{H}_S$  are adjusted dynamically as described in section 4.4. Assume the arrival rate is 1.6, and the traffic load ratio,  $\rho$ , is changing from 1 to 5. For the design parameters of the DCC scheme, maximum and minimum fractions of pilot power are  $f_{min} = 0.05$  and  $f_{max} = 0.2$ , respectively; decision period  $N$  is 10 frames (100 msec); total number of measurement samples  $M$  is 10 frames; total simulation time is  $10^6$  frames ( $10^5$  learning times).

The comparison between FIX-LPPA and FIX-SSDT in terms of capacity and coverage is shown in Fig. 4.8. We see that the FIX-LPPA scheme achieves higher total throughput than the FIX-SSDT scheme for both uniform and non-uniform cell load cases. This is because FIX-LPPA successfully releases congested cell's load through power balance strategy so that it can support higher throughput than the FIX-SSDT scheme around 20% in the non-uniform cell load case. On the other hand, the FIX-SSDT scheme lacks of flexibility to adapt to non-uniform cell load situations so that the throughput is decreased compared to the uniform

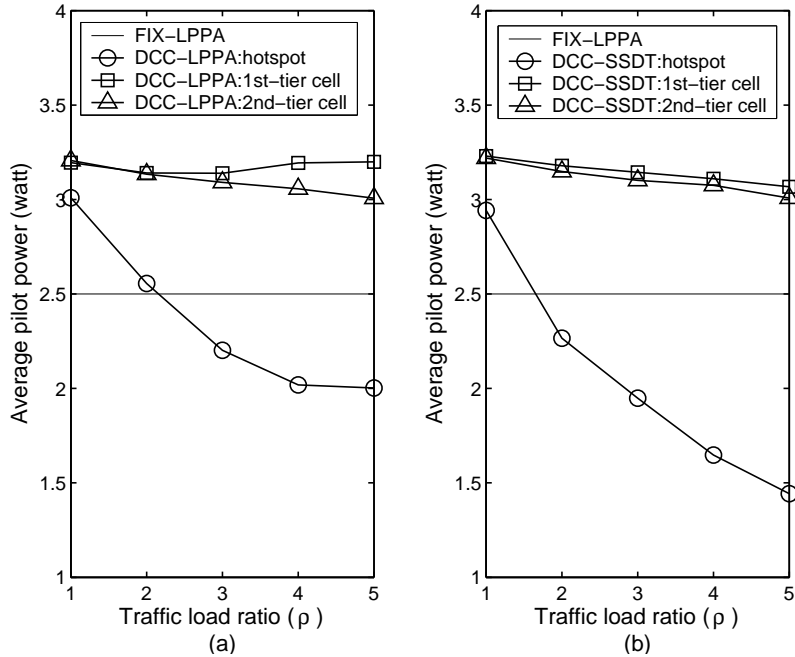


Figure 4.9: The average pilot power of hotspot, 1st-tier, and 2nd-tier cells for the fixed pilot (FIX) with SSDDT (FIX-SSDDT) and LPPA (FIX-LPPA), and pilot power allocation for dynamic cell configuration (DCC) with SSDDT (DCC-SSDDT) and LPPA (DCC-LPPA) schemes.

cell load case. It is noteworthy that the ripple occurs when the simulation result of reference rate equals 6. This is because the simulation time is not enough for accommodating high rate services which are interfere by many algorithms of radio resource management, i.e. call and handoff admission control, handoff algorithm, etc.

Figure 4.9(a) and (b) show the average pilot power distribution of the hotspot, 1st-tier, and 2nd-tier cells using DCC-LPPA and DCC-SSDDT schemes, respectively. We can see that the DCC scheme adjusts the pilot power in each cell according to various system situations. When the traffic load ratio is getting heavier, the pilot power of the hotspot cell is reduced aggressively so as to balance traffic load to adjacent cells, but the coverage is shrunk accordingly. In this way, the base station of hotspot can save more transmission power for traffic channels to serve new call arrivals. Besides, adjustments of the pilot power can make the existing mobile stations near the cell boundary enter soft handoff mode so as to balance traffic load. Furthermore, for hotspot cell, the slope of the pilot power level of different traffic load ratio for DCC-SSDDT is sharper than that for DCC-LPPA. This is

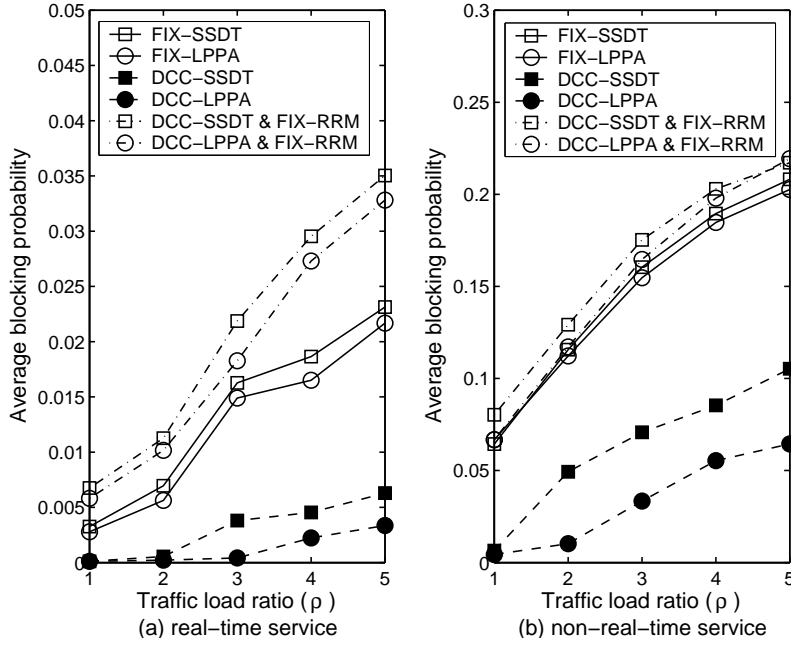


Figure 4.10: The average blocking probability of (a) real-time and (b) non-real-time services for FIX-SSDT, FIX-LPPA, DCC-SSDT, and DCC-LPPA schemes, respectively.

because both DCC and LPPA strategies are helpful for power balance; the pilot power of DCC-LPPA does not have to be adjusted as aggressive as DCC-SSDT.

Figure 4.10(a) and (b) show the new call blocking probabilities of real-time and non-real-time services, respectively. We can see that the DCC scheme improves the blocking probabilities of the FIX scheme for both real-time and non-real-time services. Because the base station has limited transmission power resources, it is important to achieve power balance between cells in downlink transmission. In order to achieve power balance between cells, our proposed DCC scheme adjusts pilot power and coordinates other radio resource mechanisms dynamically. This is the reason why the DCC scheme can save more power resource to accommodate new call requests. It is noteworthy that DCC-LPPA and DCC-SSDT schemes without changing the other radio resource management criteria are also presented for comparison. We can see that the DCC scheme without coordinating other radio resource management criteria has worse new call blocking probability performance than the FIX scheme. This is because when new or handoff calls issue requests to cells with light (heavy) traffic load, the tight (loose) criteria of call admission control may result in

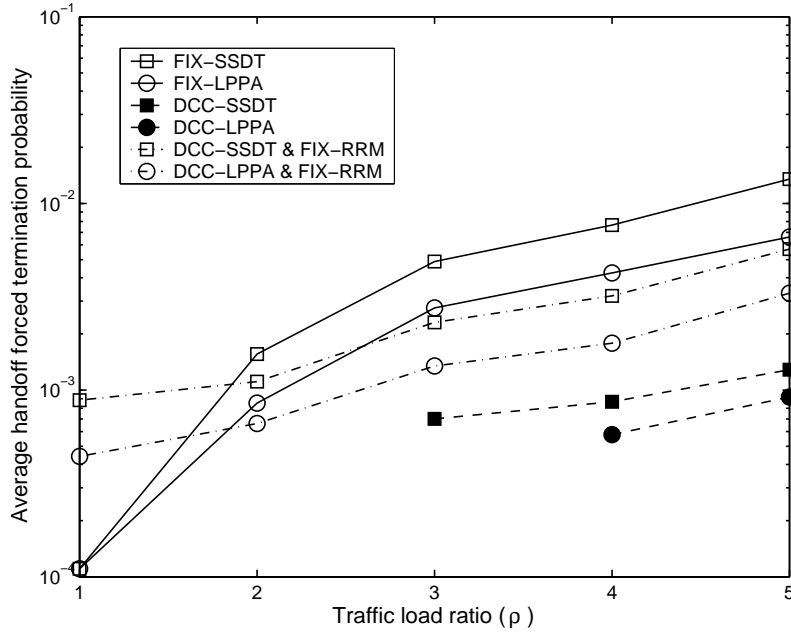


Figure 4.11: The average handoff forced termination probability for FIX-SSDT, FIX-LPPA, DCC-SSDT, and DCC-LPPA schemes.

new call blocks.

The similar impaired results occur when a mobile station fails to add new base stations into its active set and suffers worse channel quality, as shown in Fig. 4.11. This is so-called handoff forced termination. On the other hand, compared to the FIX scheme, our proposed DCC scheme can improve handoff forced termination probabilities greatly. This is because existing mobile stations near the cell boundaries often suffer bad transmission quality, and they may be dropped when power resource is not enough for admitting handoff requests.

Figure 4.12 shows the total throughput of the system. In the FIX case, FIX-LPPA outperforms FIX-SSDT. When the traffic load ratio is getting higher, the throughput of FIX-SSDT degrades sharply because of the inefficient handoff power allocation strategy. As for FIX-LPPA, it can even keep the average throughput when traffic load ratio is less than 4. Furthermore, through the cooperation of DCC and LPPA schemes for power balance between cells, DCC-LPPA can further enhance FIX-LPPA. Compared to the FIX scheme, the DCC scheme can improve the average throughput when the traffic load ratio is getting larger for both DCC-SSDT and DCC-LPPA schemes. This is because the DCC scheme can

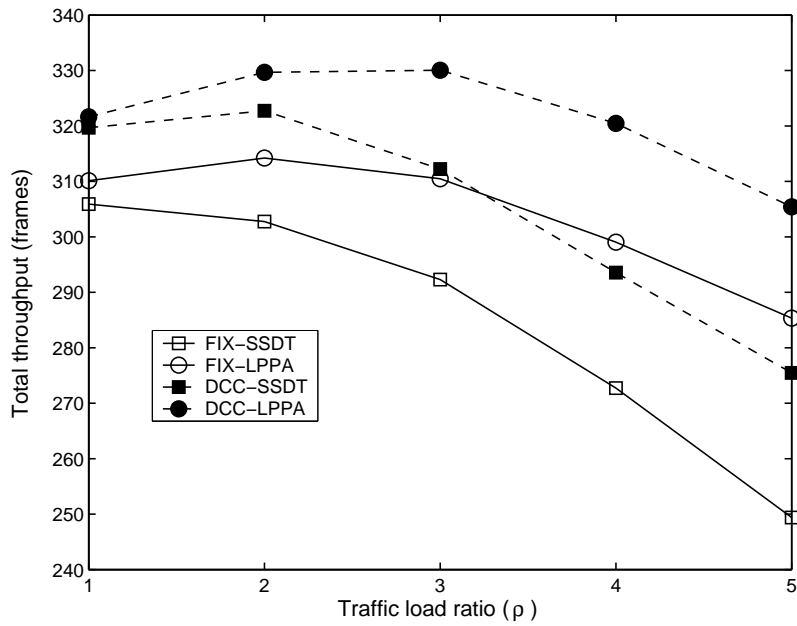


Figure 4.12: The average total throughput of systems for FIX-SSDT, FIX-LPPA, DCC-SSDT, and DCC-LPPA schemes.

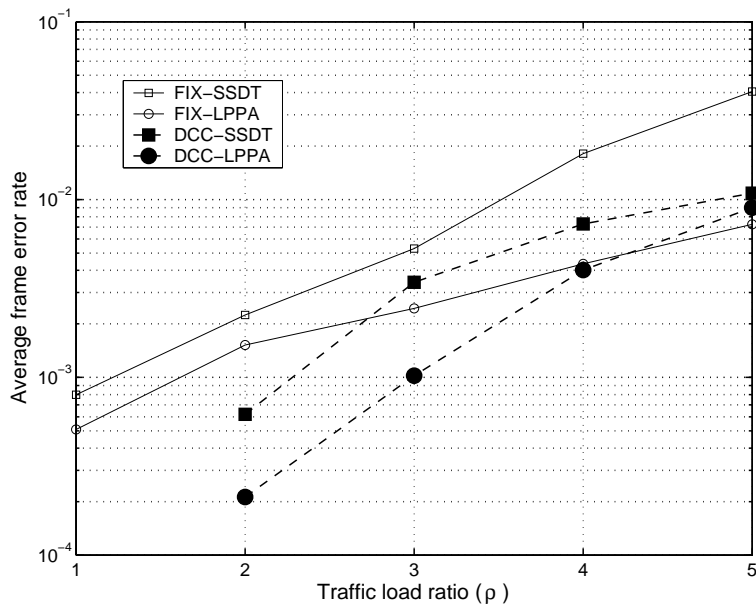


Figure 4.13: The average frame error probability for FIX-SSDT, FIX-LPPA, DCC-SSDT, and DCC-LPPA schemes.

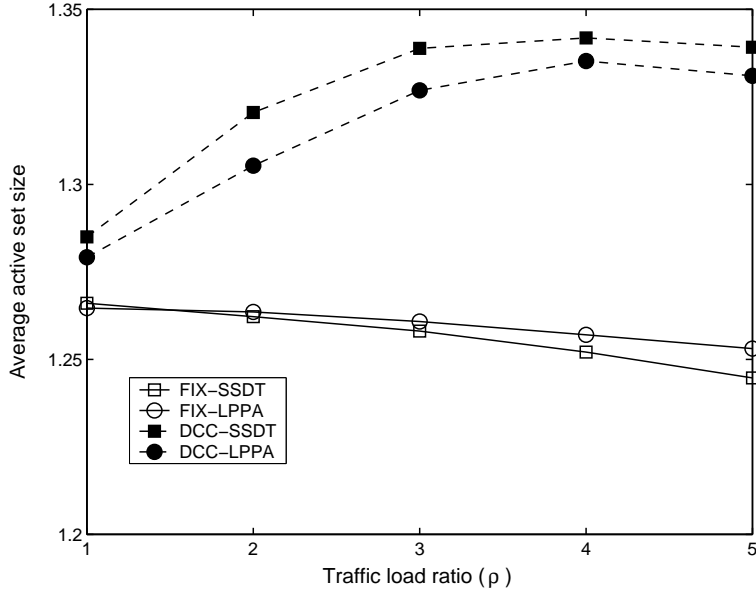


Figure 4.14: The average size of the active set for FIX-SSDT, FIX-LPPA, DCC-SSDT, and DCC-LPPA schemes.

dynamically balance traffic load between cells through pilot power adjustments based on system situations as well as call admission control criterion and the maximum link power constraint.

Furthermore, Fig. 4.13 presents the results of frame error probabilities. We observe that frame error probability can be improved by DCC schemes, and the requirement of frame error probability 0.01 can be satisfied through an effective feature abstraction design.

In order to balance traffic loads between cells, the DCC scheme can reduce or increase pilot power aggressively. The power balance can be achieved by forcing mobile stations near the cell boundary into handoff mode. Therefore, the average size of the active set and handoff rates can be increased, which is shown in Fig. 4.14. It is found that the DCC scheme results in more soft handoff events slightly.

Furthermore, Table 4.2 shows the results of coverage failure probabilities. A coverage failure occurs when a new call fails to detect good enough signal from a base station for requesting a traffic channel. From equation (4.15), we can see that there are two situations that could cause a coverage failure. One is when the mobile station suffers high interferences (the increment of the denominator in (4.15)), and another is when the mobile station has



weak signal strength (the reduction of the nominator in (4.15)). The DCC-SSDT and DCC-LPPA schemes cause slightly higher coverage failure probabilities than the FIX schemes. This is because even DCC devotes to balance traffic load through the pilot power adjustments so as to reduce interference of the hotspot cell, mobile stations near the cell boundary may suffer bad signal strength from any base station in the active set. This is the possible disadvantage for the DCC schemes in the distributed manner.

Table 4.2: AVERAGE COVERAGE FAILURE PROBABILITY

Scheme/Traffic load ratio	1.0	2.0	3.0	4.0	5.0
FIX-SSDT	0.0	0.0	0.0	0.0	0.0
FIX-LPPA	0.0	0.0	0.0	0.0	0.0
DCC-SSDT	0.0	0.0	4.2e-05	1.0e-04	4.6e-04
DCC-LPPA	0.0	0.0	0.0	3.2e-05	9.2e-05

## 4.6 Concluding Remarks

In this chapter, we have studied dynamic cell configuration problem in next generation CDMA networks. The large number of states and the difficulty to estimate the state transition probabilities in realistic networks motivate us to choose a model-free reinforcement-learning solution to solve the problem. The proposed scheme can dynamically configure cell coverage and capacity based on the varying situation of the systems. Simulation results have been shown the effectiveness of the proposed schemes. It was found that pilot and soft handoff power allocations, maximum power constraint design, and the admission control criterion are highly coupled and should be considered jointly. The system throughput can be increased significantly in the proposed dynamic cell configuration scheme compared to the conventional fixed scheme. Furthermore, both dynamic cell configuration and link proportional power allocation schemes have the advantage of power balance for soft handoffs so that the system capacity of the DCC-LPPA scheme outperforms conventional FIX-SSDT scheme significantly.

The proposed dynamic cell configuration scheme is the initiative framework for the next-generation CDMA networks. The dynamic cell configuration concept is applicable to future

cellular systems with whatever embedded multiple access techniques. Advanced study is in progress to apply the DCC scheme to the possible mechanisms of the next-generation systems.



# Chapter 5

## Conclusions and Future Works

---

In this dissertation, we specialize in the downlink soft handoff mechanisms and cell re-configuration planning in terms of *power balance characteristics* to tackle tradeoffs between service coverage and system capacity in CDMA mixed-size cellular systems. We first consider a CDMA mixed-size cellular system with mixed-size cells in Chapter 2 and 3, in which the cell configuration is determined by fixed pilot power allocation. Radio resource management of soft handoff for the narrowband CDMA supporting voice only system and the multirate WCDMA system are considered in Chapter 2 and 3, in which we propose a novel soft handoff power allocation scheme and joint power and rate allocation schemes, respectively. The snapshot simulations are adopted to evaluate the qualitative characteristics for the CDMA heterogeneous cellular system. Next, in Chapter 4, consider the cellular system with time-varying non-uniform cell loads distribution, we further design a reinforcement-learning-based dynamic cell configuration scheme with radio resource management to be aware of system situation and to adjust pilot power, maximum link power as well as call admission criterion dynamically. A practical wireless mobile cellular environment has been set up to simulate the dynamic cellular system with random mobility and versatile services activity. The conclusions of this dissertation are highlight as follows.

In Chapter 2, we propose a novel link proportional power allocation (LPPA) scheme and compare it with many existing soft handoff power allocation schemes, including EPA, SSDDT, and QBPA schemes. In the simulations, we show that LPPA can effectively relax the *power exhausting problem*. Specifically, by taking into account effects of different cell sizes, LPPA can prevent a microcell's base station from wasting too much transmission power in serving

handoff users. Consequently, the LPPA scheme can deliver higher system capacity and service coverage than other soft handoff power allocation schemes in both the homogeneous and mixed-size cellular systems even with measurement errors. All in all, we find that it is important to design a handoff mechanism from perspectives of power efficiency and link reliability in the CDMA mixed-size cellular system with mixed-size cells.

In Chapter 3, a joint power and rate assignment (JPRA) algorithm has been proposed to deal with multirate soft handoffs in WCDMA mixed-size cellular systems, containing the LPPA scheme and the evolutionary computing rate assignment (ECRA) method. Compared to SSDT and LPPA schemes with best-effort based rate assignments, simulation results show that JPRA accomplishes superior power balance among cells so that the system performance can be improved significantly, including better cell coverage, higher system throughput, and great user satisfaction for voice and data users. Furthermore, JPRA is less sensitive to the measurement errors during active set selection than SSDT with best-effort rate allocation, so JPRA also owns better link reliability. It is noteworthy that the aforementioned advantages of JPRA are more conspicuous in WCDMA mixed-size cellular systems with smaller cell radius ratio between microcell and macrocells.

In Chapter 4, we have studied dynamic cell configuration problem in next generation CDMA networks. The large number of states and the difficulty to estimate the state transition probabilities in realistic networks motivate us to choose a model-free reinforcement-learning solution to solve the problem. The proposed scheme can dynamically configure service coverage and system capacity based on the varying situation of the systems. It is found that pilot and soft handoff power allocations, maximum link power constraint as well as the admission control criterion are highly coupled and should be considered jointly. Simulation results have been shown the effectiveness of the proposed schemes. The system throughput can be increased significantly in the proposed dynamic cell configuration scheme with radio resource management compared to the conventional fixed scheme. Furthermore, the system capacity of the dynamic cell configuration with LPPA (DCC-LPPA) scheme outperforms conventional fixed cell configuration with SSDT (FIX-SSDT) scheme significantly.

It means that the DCC-LPPA scheme owns the excellent advantage of power balance. Therefore, for future multimedia and personal communications, cell area will be further reduced, and traffic variation and unevenness will be expanded. Dynamic cell configuration and soft handoff mechanism to balance cell loads are crucial to enhance the system efficiency for all types of cellular systems.

The proposed dynamic cell configuration scheme with radio resource manage is the initiative framework for the next-generation CDMA networks. The dynamic cell configuration concept is applicable to future cellular systems with whatever embedded multiple access techniques. Advanced study is to apply it to the possible mechanisms of the next-generation systems. Furthermore, in order to provide more flexible plan of cell reconfiguration, future works can take into account uplink and downlink capacity-limited scenarios together. Since the volumes of multimedia traffic loads are greatly asymmetrical, the dynamic cell configuration scheme with radio resource management affects both links of their service coverage and system capacity differently. The possible challenge of applying reinforcement-learning-based techniques distributively to the bidirectional dynamic cell configuration would be that there may induce some problems of the interaction between uplink and downlink transmissions for different cells. The optimal decisions of the pilot power level for the bidirectional dynamic cell configuration would face convergent problem. Some advanced multi-agent reinforcement-learning techniques would be useful to tackle the interaction problems.

# Bibliography

- [1] J. Laiho, A. wacker, and T. Novosad, Eds, *Radio Network Planning and Optimization for UMTS*, Wiley & Sons, pp. 280-290, 2002.
- [2] K. S. Gilhousen, et al., "On the capacity of a cellular CDMA system," *IEEE Trans. Veh. Technol.*, vol. 40, no. 2, pp. 303-312, May 1991.
- [3] W. C. Y. Lee, "Overview of cellular CDMA," *IEEE Trans. Veh. Technol.*, vol. 40, no. 2, pp. 291-302, May 1991.
- [4] W. W. Lu, *Broadband wireless mobile: 3G and beyond*, John Wiley & Sons Ltd, pp. 307-315, 2002.
- [5] H. G. Jeon, S. M. Shin, T. Hwang, and C. E. Kang, "Reverse link capacity analysis of a CDMA cellular system with mixed cell sizes," *IEEE Trans. Veh. Technol.*, vol. 49, no. 6, pp. 2158-2163, Nov. 2000.
- [6] S. Kishore, L. J. Greenstein, H. V. Poor, and S. C. Schwartz, "Uplink user capacity in a CDMA macrocell with a hotspot microcell: exact and approximate analyses," *IEEE Trans. Wireless Commun.*, vol.2, no.2, pp. 364-374, Mar. 2003.
- [7] S. Kishore, L. J. Greenstein, H. V. Poor, and S. C. Schwartz, "Downlink user capacity in a CDMA macrocell with a hotspot microcell," in *Proc. IEEE GLOBECOM'03*, San Francisco, CA, pp. 1573-1577, Dec. 2003.
- [8] C. Y. Liao, L. C. Wang, C. J. Chang, "Power allocation mechanisms for downlink hand-off in WCDMA systems with heterogeneous cell structures," ACM/Kluwer WINET, Jun. 2005.



- [9] A. J. Viterbi, *CDMA: principles of spread spectrum communication*, Addison-Wesley, pp. 218-224, June 1995.
- [10] H. Holma, and A. Toskala, "WCDMA for UMTS: radio access for third generation mobile communications," *John Wiley and Sons*, ltd., pp. 208-210, 2000.
- [11] O. Salonaho, and R. Padovani, "Flexible power allocation for physical control channel in wideband CDMA," *IEEE VTC'99 Spring*, Houston, TX USA, pp. 1455-1458, May 1999.
- [12] L. Dai, S. D. Zhou, and Y. Yao, "Effect of macrodiversity on CDMA forward-link capacity," *IEEE VTC'01 Fall*, Atlantic, NJ USA, pp. 2452-2456, 2001.
- [13] D. Kim, "A simple algorithm for adjusting cell-site transmitter power in CDMA cellular systems," *IEEE Trans. on Veh. Technol.*, vol. 48, no. 4, pp.1092-1098, July 1999.
- [14] H. Furukawa, K. Hamabe, and A. Ushirokawa, "SSDT – Site Selection Diversity Transmission Power Control for CDMA Forward Link," *IEEE J. Selected Areas in Commun.*, vol. 18, no. 8, pp. 1546-1554, Aug. 2000.
- [15] N. Takano, and K. Hamabe, "Enhancement of site selection diversity transmit power control in CDMA cellular systems," *IEEE VTC'01 Fall*, Atlantic, NJ USA, pp. 635 - 639, Oct. 2001.
- [16] F. Blaise, L. Elicegui, F. Goeusse, G. Vivier, "Power control algorithms for soft handoff users in UMTS," *IEEE VTC'02 Fall*, Vancouver, BC Canada, pp. 1110-1114, 2002.
- [17] D. Staehle, K. Leibnitz, and K. Heck, "Effects of soft handoff on the UMTS downlink performance," *IEEE VTC'02 Fall*, Vancouver, BC Canada, pp. 960-964, 2002.
- [18] S. L. Kim, Z. Rosberg, and J. Zander, "Combined power control and transmission rate selection in cellular networks," in *Proc. IEEE VTC'99 Fall*, Amsterdam, Netherlands, pp. 1653-1657, Sept. 1999.

- [19] C. W. Sung, W. S. Wong, "Power control and rate management for wireless multimedia CDMA systems," *IEEE Trans. Commun.* vol. 49, no. 7, pp. 1215-1226, July 2001.
- [20] D. I. Kim, E. Hossain, and V. K. Bhargava, "Downlink joint rate and power allocation in cellular multirate WCDMA systems," *IEEE Trans. Wireless Commun.*, vol. 2, no. 1, pp. 69-80, Jan. 2003.
- [21] S. Kahn, M. K. Gurcan, and O. O. Oyefuga, "Downlink throughput optimization for wideband CDMA systems," *IEEE Commun. Lett.*, vol. 7, no. 5, pp. 251-253, May 2003.
- [22] D. Kim, "Rate-regulated power control for supporting flexible transmission in future CDMA mobile networks," *IEEE J. Selected Areas in Commun.*, vol. 17, no. 5, pp. 968-977, May 1999.
- [23] Y. W. Kim, D. K. Kim, J. H. Kim, S. M. Shin, and D. K. Sung "Radio resource management in multiple-chip-rate DS/CDMA systems supporting multiclass services," *IEEE Trans. Veh. Technol.*, vol. 50, no. 3, pp. 723-736, May 2001.
- [24] D. K. Kim, and D. K. Sung, "Handoff management in CDMA systems with a mixture of low rate and high rate traffics," in *Proc. IEEE VTC'98 Spring*, Ottawa, ON, pp. 1346-1350, May 1998.
- [25] S. A. Grandhi, J. Zander, and R. D. Yates, "Constrained power control," *Wireless Personal Commun.*, vol. 1, no. 4, pp. 257-270, 1995.
- [26] M. Andersin, Z. Rosberg, and J. Zander, "Gradual removals in cellular PCS with constrained power control and noise," *ACM/Baltzer Wireless Networks J.*, vol. 2, no. 1, pp. 27-43, 1996.
- [27] F. Berggren, R. Jantti, and S. L. Kim, "A generalized algorithm for constrained power control with capability of temporary removal," *IEEE Trans. Veh. Technol.*, vol. 50, no. 6, pp. 1604-1612, Nov. 2001.



- [28] S. L. Kim, "Optimization approach to prioritized transmitter removal in a multiservice cellular PCS," in *Proc. IEEE PIMRC'98*, Boston, MA, pp. 1565-1569, Sept. 1998.
- [29] S. Sharma, A. R. Nix, and S. Olafsson, "Situation-aware wireless networks," *IEEE Commun. Mag.*, pp. 44-50, July 2003.
- [30] S. Sharma, and A. R. Nix, "Situation Awareness based automatic basestation detection and coverage reconfiguration in 3G systems," in *Proc. IEEE PIMRC'02*, Lisbon, Portugal, pp. 16-20, Sept. 2002.
- [31] Y. Ishikawa, T. Hayashi, and S. Onoe, "W-CDMA downlink transmit power and cell coverage planning," *IEICE Trans. Commn.*, vol. E85-B, no. 11, pp. 2416-2426, Nov. 2002.
- [32] G. Hampel, K. L. Clarkson, J. D. Hobby, and P. A. Polakos, "The tradeoff between coverage and capacity in dynamic optimization of 3G cellular networks," in *Proc. IEEE VTC'03 Fall*, Orlando, FL, pp. 927-932, Sept. 2003.
- [33] R. T. Love, K. A. Beshir, D. Schaeffer, and R. S. Nikides, "A pilot optimization technique for CDMA cellular systems," in *Proc. IEEE VTC'99 Fall*, Amsterdam, Netherlands, pp. 2238-2242, Sept. 1999.
- [34] K. Valkealahti, A. Hoglund, J. Parkkinen, and A. Flanagan, "CDMA common pilot power control with cost function minimization," in *Proc. IEEE VTC'02 Fall*, Vancouver, BC, pp. 2244-2247, Sept. 2002.
- [35] K. Valkealahti, A. Hoglund, J. Parkkinen, and A. Flanagan, "CDMA common pilot power control for load and converge balancing," in *Proc. IEEE PIMRC'02*, Lisbon, Portugal, pp. 1412-1416, Sept. 2002.
- [36] D. Kim, Y. Chang, and J. W. Lee, "Pilot power control and service coverage support in CDMA mobile systems," in *Proc. IEEE VTC'99 Spring*, vol. 2, pp. 1464-1468, May 1999.

- [37] A. D. Smith, "Designing for coverage availability with different data rates - an improved methodology," in *Proc. IEEE VTC'02 Fall*, pp. 1821-1824, Sept. 2002.
- [38] B. Hashem, and E. L. Strat, "On the balancing of the base stations transmitted powers during soft handoff in cellular CDMA systems," in *Proc. IEEE ICC'00*, New Orleans, LA, pp. 1497 - 1501, June 2000.
- [39] J. A. Flanagan, and T. Novosad, "CDMA network cost function minimization for soft handover optimization with variable user load," in *Proc. IEEE VTC'02 Fall*, Vancouver, BC, pp. 2224-2228, Sept. 2002.
- [40] A. Osyczka, *Evolutionary algorithms for single and multicriteria design optimization*, Physica-Verlag, 2002.
- [41] J. S. Wu, J. K. Chung, and Y. C. Yang, "Performance study for a microcell hot spot embedded in CDMA macrocell systems," *IEEE Trans. on Veh. Technol.*, vol. 48, no.1, pp. 47-59, Jan. 1999.
- [42] J. Y. Kim, G. L. Stuber, I. F. Akyildiz, "Macrodiversity power control in hierarchical CDMA cellular systems," *IEEE J. Select. Areas Commun.*, vol. 19, no. 2, pp. 266-276, Feb. 2001.
- [43] V. Erceg, S. Ghassemzadeh, M. Taylor, D. Li, and D. L. Schilling, "Urban/suburban out-of-sight propagation modeling," *IEEE Commun. Mag.*, vol 30. , no. 6, pp. 56-61, June 1992.
- [44] J. Shapira, "Microcell engineering in CDMA cellular networks," *IEEE Trans. Veh. Technol.*, vol. 43, no. 4, pp. 817-825, Nov. 1994.
- [45] S. Min, and H. L. Bertoni, "Effect of path loss model on CDMA system design for highway microcells," *IEEE VTC98*, Ottawa, Ont. Canada, pp. 1009-1013, 1998.
- [46] 3GPP Technical Specification 25.942, RF System Scenarios, page 26, December, 1999.

- [47] S. Schwartz, and Y. S. Yeh, "On the distribution function and moments of power sums with log-normal components," *Bell System Tech. Journal*, vol. 61, pp. 1441-1462, Sep. 1982.
- [48] L. C. Wang, C. Y. Liao, and C. J. Chang, "Performance study of soft handover with WCDMA heterogeneous cellular architectures," *Multiaccess, Mobility and Teletraffic for Wireless Comm., MMT'02*, Kluwer, pp. 87-102, June 2002.
- [49] L. C. Wang, C. Y. Liao, and C. J. Chang, "Downlink Soft Handover and Power Allocation for CDMA Heterogeneous Cellular Networks," *Proc. IEEE GLOBECOM'02.*, vol. 2, pp. 1830-1834, Nov. 2002.
- [50] R. Yates, "A Framework for uplink power control in cellular radio systems," *IEEE J. Selected Areas in Commun.*, vol. 13, no. 7, pp. 1341-1347, Sept. 1995.
- [51] 3GPP, Universal Mobile Telecommunication System (UMTS); "Selection procedures for the choice of radio transmission technologies of the UMTS," *UMTS 30.03*, version 3.2.0, TR 101 112, pp. 54-55, 1998.
- [52] M. Gudmundson, "Correlation model for shadow fading in mobile radio systems," *Electron. Lett.*, vol. 27, no. 23, pp. 2145-2146, Nov. 1991.
- [53] J. S. Lee, and L. E. Miller, *CDMA systems engineering handbook*, Artech House, pp. 1111-1186, 1998.
- [54] R. G. Akl, M. V. Hegde, M. Naraghi-Pour, and P. S. Min, "Multicell CDMA network design," *IEEE Trans. Veh. Technol.*, vol.50, no.3, May 2001.
- [55] V. V. Veeravalli and A. Sendonaris, "The coverage-capacity tradeoff in cellular CDMA systems," *IEEE Trans. Veh. Technol.*, vol. 48, no. 5, pp. 1443-1450, Sept. 1999.
- [56] C. Y. Liao, F. Yu, V. C. M. Leung, and C. J. Chang, "Reinforcement-learning-based self-organization for cell configuration in multimedia mobile networks," to be appeared

in European Trans. on Telecomm. with special issues on self-organization in mobile networking, 2005.

- [57] R. S. Sutton, and A. G. Barto, *Introduction to reinforcement learning*, MIT Press/Bradford Boos, Cambridge, MA. 1998.
- [58] D. Bertsekas and J.N. Tsitsiklis, *Neuro-Dynamic Programming*, Athena Scientific, 1996.
- [59] M. L. Putterman, *Markov decision processes: discrete stochastic dynamic programming*, John Wiley & Sons, inc., 1994.
- [60] J. Nie, and S. Haykin, "A Q-learning-based dynamic channel assignment technique for mobile communication systems," *IEEE Trans. Veh. Technol.*, vol. 48, no. 5, pp. 1676-1687, Sept. 1999.
- [61] Y. S. Chen, C. J. Chang, and F. C. Ren, "Q-learning-based multirate transmission control scheme for RRM in multimedia CDMA systems," *IEEE Trans. Veh. Technol.*, vol. 53, no. 1, Jan. 2004.
- [62] P. Y. Glorennec, "Fuzzy Q-learning and dynamic fuzzy Q-learning," in *Proc. IEEE FUZZ'94*, Orlando, FL, pp. 474 - 479, June 1994.
- [63] L. Jouffe, "Fuzzy inference system learning by reinforcement methods," *IEEE Trans. SMC*, Part C, vol. 8, no. 3, pp. 338-355, Aug. 1998.
- [64] C. J. C. H. Watkins, and P. Dayan, "Q-learning," *Machine Learning*, vol. 8, pp. 279-292, 1992.
- [65] R. E. Bellman, *Dynamic Programming*, Princeton, New Jersey: Princeton University Press, 1957.
- [66] J. S. R. Jang, C. T. Sun, and E. Mizutani, *Neuro-Fuzzy and soft computing: A computational approach to learning and machine intelligence*, Prentic Hall, pp. 81-85, 1997.

- [67] T. Takagi T, and M. Sugeno, “Fuzzy identification of systems and its application to modeling and control,” *IEEE Trans. Syst., Man, and Cybern.*, vol 15, no. 1, pp. 116-132, 1985.



# Vita

**Ching-Yu Liao** was born in Taipei, Taiwan. She received the B.S. and M.S. degrees in electrical engineering from Huafan Institute of Technology and National Central University (NCU), Taiwan, in 1995 and 1997, respectively. She is currently toward the Ph.D degree in communication engineering at National Chiao Tung University (NCTU), Hsinchu, Taiwan. In 2004, she joined the program of Graduate Student Study Abroad (GSSA), which is sponsored by National Science Council (NSC), Taiwan, ROC, being a visiting graduate student in Dept. of Electrical and Computer Engineering at University of British Columbia (UBC), Vancouver, Canada. She is a student member in IEEE association since 2002. Her research interests include handoff techniques, statistical optimization, radio resource management, heterogeneous cellular networks, etc.

